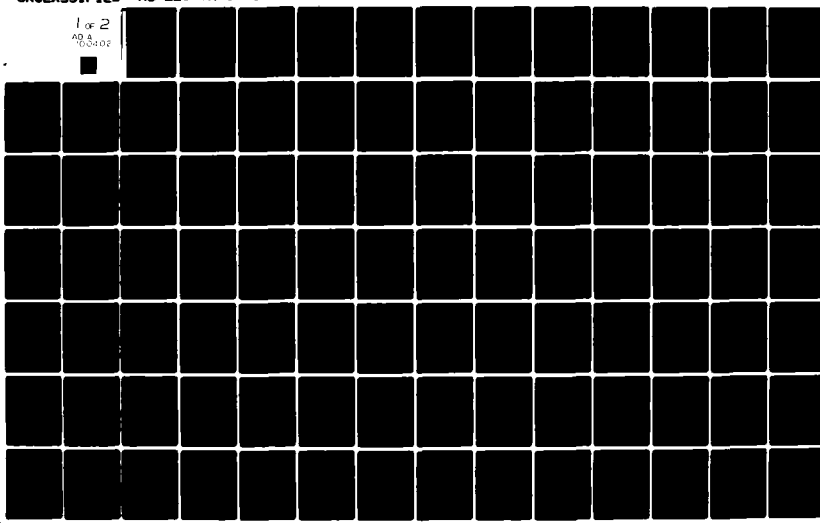


AD-A180 402 MOORE SCHOOL OF ELECTRICAL ENGINEERING PHILADELPHIA P--ETC F/6 20/3  
METHODOLOGY FOR EMC EVALUATION.(U)  
DEC 80 N00140-79-C-6628  
UNCLASSIFIED MS-EES-TR-80-1 NL

1 of 2  
AD-A180 402



(2) LEVEL II

MS-EES-TR-80-1

AD A100402

TECHNICAL REPORT

METHODOLOGY FOR EMC EVALUATION

by

R. M. Showers

Contract N00140-79-C-6628

with

Naval Underwater Systems Center  
New London Laboratory  
New London, CT 06320



University of Pennsylvania  
The Moore School of Electrical Engineering  
Department of Electrical Engineering and Science  
Philadelphia, Pennsylvania 19104

DMC FILE SUPPLY

December 1980

DISTRIBUTION STATEMENT A

Approved for public release;  
Distribution Unlimited

815 26 043

MS-EES-TR-80-1

TECHNICAL REPORT

METHODOLOGY FOR EMC EVALUATION

by

R. M. Showers

Contract N00140-79-C-6628

with

Naval Underwater Systems Center  
New London Laboratory  
New London, CT 06320

University of Pennsylvania  
The Moore School of Electrical Engineering  
Department of Electrical Engineering and Science  
Philadelphia, Pennsylvania 19104

December 1980

Unclassified

SECURITY CLASSIFICATION OF THIS PAGE (When Data Entered)

9 T h, / / Rept. 1979-1980,

REPORT DOCUMENTATION PAGE		READ INSTRUCTIONS BEFORE COMPLETING FORM
1. REPORT NUMBER MS-EES-TR-80-1	2. GOVT ACCESSION NO. AD-A100 402	3. RECIPIENT'S CATALOG NUMBER
4. TITLE (and Subtitle) <u>METHODOLOGY FOR EMC EVALUATION</u>	5. TYPE OF REPORT & PERIOD COVERED Technical Report 1979-80	
7. AUTHOR(s) R. M. Showers	6. PERFORMING ORG. REPORT NUMBER MS-EES-TR-80-1	
11. CONTROLLING OFFICE NAME AND ADDRESS Naval Regional Contracting Office Philadelphia, Newport Division Building No. 132T, Newport, RI 02840	8. CONTRACT OR GRANT NUMBER(s) N00140-79-C-6628	
9. PERFORMING ORGANIZATION NAME AND ADDRESS University of Pennsylvania Moore School of Electrical Engineering Philadelphia, Pa. 19104	10. PROGRAM ELEMENT, PROJECT, TASK AREA & WORK UNIT NUMBERS // 1 - 1 - 1	
14. MONITORING AGENCY NAME & ADDRESS (if different from Controlling Office) Code 344 Naval Underwater Systems Center New London Laboratory New London, CT. 06321	12. REPORT DATE December 31, 1980	
	13. NUMBER OF PAGES 101	
	15. SECURITY CLASS. (of this report) Unclassified	
	15a. DECLASSIFICATION/DOWNGRADING SCHEDULE	
16. DISTRIBUTION STATEMENT (of this Report) This report was prepared Rhode Island, under contract number all reports shall be with the Water Systems Center.	DISTRIBUTION STATEMENT A Approved for public release; Distribution Unlimited	
17. DISTRIBUTION STATEMENT (of the abstract entered in Block 20, if different from Report)		
18. SUPPLEMENTARY NOTES		
19. KEY WORDS (Continue on reverse side if necessary and identify by block number)		
Electromagnetic Compatibility Electromagnetic Interference Interference Prediction Interference Limits	System Evaluation	
20. ABSTRACT (Continue on reverse side if necessary and identify by block number) This report is concerned with the development of a quantitative model for predicting and evaluating the effectiveness of electrical-electronic systems from the point of view of their electromagnetic compatibility characteristics. The prediction is based upon techniques for computing protection margins in all cases where undesired electromagnetic interaction between components is possible. Methods of controlling the interaction to achieve compatibility are discussed in terms of quantitative analytic models which are usable for establishing limits and installation practices where appropriate.	Continued	

Unclassified

SECURITY CLASSIFICATION OF THIS PAGE(*When Data Entered*)

The report is divided into two parts. Part I discusses various models for generation of both conducted and radiated interference. Using these and associated susceptibility characteristics of receivers, appropriate coupling models are defined. From this work Part II develops a methodology for predicting electromagnetic compatibility "protection margins." As a part of this approach, reference is made to a set of "nominal" conducted and radiated levels. Using these levels, many of the detailed computations that would otherwise be necessary can be avoided.

SECURITY CLASSIFICATION OF THIS PAGE(*When Data Entered*)

## ABSTRACT

This report is concerned with the development of a quantitative model for predicting and evaluating the effectiveness of electrical-electronic systems from the point of view of their electromagnetic compatibility characteristics. The prediction is based upon techniques for computing protection margins in all cases where undesired electromagnetic interaction between components is possible. Methods of controlling the interaction to achieve compatibility are discussed in terms of quantitative analytic models which are useable for establishing limits and installation practices where appropriate.

The report is divided into two parts. Part I discusses various models for generation of both conducted and radiated interference. Using these and associated susceptibility characteristics of receivers, appropriate coupling models are defined. From this work Part II develops a methodology for predicting electromagnetic compatibility "protection margins." As a part of this approach, reference is made to a set of "nominal" conducted and radiated levels. Using these levels, many of the detailed computations that would otherwise be necessary can be avoided.

RE: Classified Reference, Distribution  
Unlimited-  
No change per Mr. Ned Shaw, NUSC/Library

Accredited For	
ATIS	STAR&I
DTIC	NSF
Unrestricted	
Classification	
<b>PER LETTER</b>	
Pv.	
Distribution/	
Availability Codes	
Avail and/or	
Dist	Special
A	

## CONTENTS

<b>Abstract.....</b>	<b>ii</b>
<b>List of Figures.....</b>	<b>v</b>
<b>PART I - MODEL DEVELOPMENT</b>	
<b>1.0 GENERAL.....</b>	<b>1</b>
<b>1.1 Introduction.....</b>	<b>1</b>
<b>1.2 Classification of Mechanisms.....</b>	<b>1</b>
<b>2.0 MODEL DEVELOPMENT.....</b>	<b>3</b>
<b>2.1 Technical Considerations.....</b>	<b>3</b>
<b>2.1.1 Bandwidth.....</b>	<b>3</b>
<b>2.1.2 Pulse Spectra.....</b>	<b>4</b>
<b>2.1.3 Coupling Models.....</b>	<b>4</b>
<b>2.2 Conducted Emissions.....</b>	<b>8</b>
<b>2.2.1 Source Measurements.....</b>	<b>10</b>
<b>2.2.2 Nonlinear Power Line Loads.....</b>	<b>10</b>
<b>2.2.3 Common-Mode Emission.....</b>	<b>11</b>
<b>2.3 Radiated Emissions.....</b>	<b>21</b>
<b>2.3.1 Loop Emission.....</b>	<b>22</b>
<b>2.3.2 Typical Source Characteristics.....</b>	<b>25</b>
<b>2.3.2.1 Power Conductor Loops.....</b>	<b>25</b>
<b>2.3.2.2 Magnetic Devices.....</b>	<b>27</b>
<b>2.3.2.3 Application of Inverse-Square-Distance Relationship.....</b>	<b>31</b>
<b>2.3.3 Radiation from Cables.....</b>	<b>31</b>
<b>2.3.3.1 Parallel-Wire Model.....</b>	<b>31</b>
<b>2.3.3.2 Application to Coaxial Cables and Common Mode.....</b>	<b>35</b>
<b>2.3.3.3 Twisted Pair Cable.....</b>	<b>37</b>
<b>2.3.4 Electric Sources.....</b>	<b>37</b>
<b>2.4 Immunity Models.....</b>	<b>42</b>
<b>2.4.1 Bandwidth Considerations in Susceptibility Estimation.....</b>	<b>42</b>
<b>2.4.2 Wire Loops.....</b>	<b>45</b>
<b>2.4.3 Cable Susceptibility.....</b>	<b>47</b>
<b>PART II - METHODOLOGY IMPLEMENTATION</b>	
<b>3.0 METHODOLOGY FOR EMC PREDICTION AND ANALYSIS.....</b>	<b>48</b>
<b>3.1 System Breakdown.....</b>	<b>48</b>
<b>3.2 The Protection Margin.....</b>	<b>49</b>

	<u>Page</u>
3.2.1 Mechanisms of Interference.....	49
3.3 Limit Setting Philosophy.....	52
4.0 NOMINAL LEVELS.....	52
4.1 Conducted Emissions, Differential Mode.....	54
4.2 Conducted Susceptibility Limit, Differential Mode.....	54
4.3 Application to Cabinet Emissions and Susceptibility.....	56
4.4 Common-Mode Emission.....	59
4.5 Common-Mode Susceptibility.....	59
4.6 Electric Field Limits.....	61
4.6.1 Internal and External Limits.....	63
4.7 Broadband Limits.....	65
5.0 PROTECTION MARGIN CALCULATIONS.....	65
5.1 Introduction.....	65
5.2 Magnetic Field Coupling.....	67
5.2.1 Cabinet-to-Cabinet Coupling.....	67
5.2.1.1 Magnetic Dipole Source.....	70
5.2.1.2 Cabinet-to-Cable Calculations.....	72
5.2.1.3 Cable-to-Cabinet Calculations.....	72
5.2.1.4 Cable-to-Cable Calculation.....	73
5.3 Conductive Coupling.....	73
5.3.1 Differential-Mode Conducted Coupling.....	73
5.3.2 Common-Mode Conducted Coupling.....	74
5.4 Isolation Factors.....	74
5.4.1 Case-to-Case and Case-to-Cable Coupling.....	74
5.4.2 Cable-to-Cable and Cable-to-Case Coupling.....	75
5.4.2.1 Differential Mode.....	75
5.4.2.2 Common-Mode Source Cable.....	77
5.4.3 Common-Mode Susceptor Cable.....	79
5.4.4 Summary.....	79
5.5 Broadband Interactions.....	79
5.5.1 Circuit Model.....	83
5.5.2 Loop Coupling Model.....	83
5.5.3 Common-Mode Cable Coupling.....	86
5.5.4 Calculation of Protection Margins.....	87
5.5.5 Application to Fields Produced by Power Supplies....	90
5.5.6 Conducted Broadband Susceptibility.....	91
5.5.7 Experimental Tests.....	93
5.5.8 Summary.....	94
REFERENCES.....	95
APPENDIX - COMPARISON OF ERRORS INCURRED IN EXTRAPOLATING MAGNETIC FIELD STRENGTH AT VARIOUS DISTANCES.....	96

## LIST OF FIGURES

<u>Figure Number</u>		<u>Page</u>
1	Basic Interference Mechanisms.....	2
2	Trapezoidal Pulse Model.....	5
3	Envelope of Spectrum of Pulse of Figure 2.....	6
4	Broadband Conducted Emission Sources.....	7
5	Equivalent Circuit, Conducted Interference Source...	9
6	Power Frequency Harmonics--Comparison of Data with $1/f$ and $1/f^2$ Models.....	12
7	Simplified Model of Current Generator Characteristics	13
8	Harmonic Voltages Predicted on a 115 V, 60 Hz Line when $L_L = 50 \mu\text{H}$ .....	14
9	Harmonic Voltages Predicted on a 115 V, 400 Hz Line when $L_L = 50 \mu\text{H}$ .....	15
10	Possible Source of Common-Mode Currents.....	16
13	Magnetic Flux Density from Circular Current Loop on Axis and in Plane of Loop.....	23
14	Normalized Magnetic Field Strength from Circular Loop on Axis and in Plane of Loop.....	24
15	Maximum Flux Density from a Circular Loop.....	26
16	Measured Magnetic Flux Density - Typical Sources....	28
17	Predicted Electronic Equipment Magnetic Flux Emissions as a Function of Apparent Power (at the Fundamental Frequency and $r = 0.07$ Meter).....	29
18	Parallel-Wire Model.....	32
19	Flux Density from Parallel Conductors.....	34
20	Spacing of Conductors in the Equivalent Two-Wire Line as a Function of Frequency for Different Cables.....	36

<u>Figure Number</u>		<u>Page</u>
21	Common-Mode Radiation Model.....	38
22	Correction Factor for Estimating Field from Twisted Pair Cables.....	39
23	Magnetic Field Emissions from "TNW" Cables.....	40
24	Fundamental Frequency Flux Density from Cables Carrying Recommended Limit Currents.....	41
25(a)	Electric Dipole Model--Source Case Isolated from Ground.....	43
25(b)	Magnetic Dipole Model--Source Case Grounded, Power Line Close to Ground Plane.....	43
25(c)	Parallel-Wire Model--Source Case Grounded, Power Line away from Ground Plane.....	44
26	Cable and Loop Susceptibility.....	46
27	Protection Margin Computation.....	50
28	Protection Margin Computation.....	51
29	SES Interaction Chart.....	53
30	Conducted Emission Limits.....	55
31	Conducted Susceptibility Limits.....	57
32	Magnetic Field Limits.....	58
33	Protection Distances from Power Lines Meeting Conducted Limit of Fig. 30.....	60
34	Common-Mode Voltage Induced by Limit Field below 20 kHz.	62
35	Electric-Field Limits, 1 meter from Source Case.....	64
36	Narrow-band-Broadband Correction Factor (to be added to Narrow-band Limits to Obtain Broadband Limits in dB/unit/ MHz).....	66
37	Proposed Environmental Limits (Narrow-band).....	68
38	Entries in Protection Margin Calculation.....	69

<u>Figure Number</u>		<u>Page</u>
39	Minimum Spacing of Magnetic Source and Susceptor as a Function of Susceptor Sensitivity and Source Strength. Frequency = 60 Hz; Source Strength = 1.0, 0.1, 0.01 A-m <sup>2</sup> , Susceptor Area = 1 cm <sup>2</sup> .....	71
40	Twisted Pair Source Cable, Field Reference Line.....	76
41	Magnetic Field Reference Line, Parallel Wire or Common- Mode Source.....	78
42	Spectrum of Current Step of 1 Ampere.....	88
43	Broadband Magnetic Field Emission Spectrum.....	89
A.1	Geometrical Arrangement.....	98
A.2	<u>Predicted Field</u> vs Distance ( $\frac{1}{r^2}$ assumed, $r_m = 7$ cms) ... <u>True Field</u>	99
A.3	<u>Predicted Field</u> vs Distance ( $\frac{1}{r^3}$ assumed, $r_m = 7$ cms) ... <u>True Field</u>	101
TABLES		
I	Predicted Common-Mode Current (mA).....	19
II	Low-Frequency Magnetic Coupling Models.....	80

PART I

MODEL DEVELOPMENT

## 1.0 GENERAL

### 1.1 Introduction \*

A particular configuration or system of electrical and electronic components or subsystems is said to be electromagnetically compatible when the performance of any component is not degraded by the simultaneous operation of any other component or groups of components in that or nearby systems. It is desirable to predict, in the design stages of a system, whether any incompatibility is likely to occur, or the conditions under which it is likely to occur. The results can then be used in designing the system.

To predict compatibility, one must know for each system component the electromagnetic interference level at that component at which its performance begins to be degraded as a function of the desired signal level. The ratio of the actual value of the latter to the former is called the compatibility or "protection" margin. If it is greater than unity for all system components, the system is said to be compatible. If it is less than unity for a particular pair of components, then performance degradation will occur.

The level of interference at a particular component, which we designate the "susceptor", depends upon the level produced by the source of interference and the coupling between the source and that component. The level at which the susceptor's performance is degraded depends on the characteristics of the susceptor itself. Thus, to predict compatibility margins one must have models for interference sources, susceptors, and the couplings between them.

This report appears in two parts. It is the purpose of Part I to develop appropriate models applicable to non-antenna coupled interference, and to determine the conditions under which they should be applied. The emphasis is on EMC phenomena at frequencies below about 1 MHz, but the discussion is applicable, in principle, at higher frequencies as well. Part II discusses the prediction methodology, in which extensive use is made of the models discussed in Part I.

### 1.2 Classification of Mechanisms

The mechanisms by which interference is coupled from the source to the susceptor can be classified as follows (see Fig. 1). Although non-antenna-coupling mechanisms are of primary consideration, the techniques discussed can also be applied to antenna-coupling mechanisms.

- (a) Radiation from source case to susceptor case and cables [(1) and (2) in Fig. 1].
- (b) Radiation from source cables (especially the power cable) to susceptor case and cables [(3) and (4)].

\*Note: This report is basically a revision of a report, Systems Electromagnetic Compatibility Evaluation, originally published in 1973. It contains much reorganization of material and changes in a number of the original models. See Ref. 11.

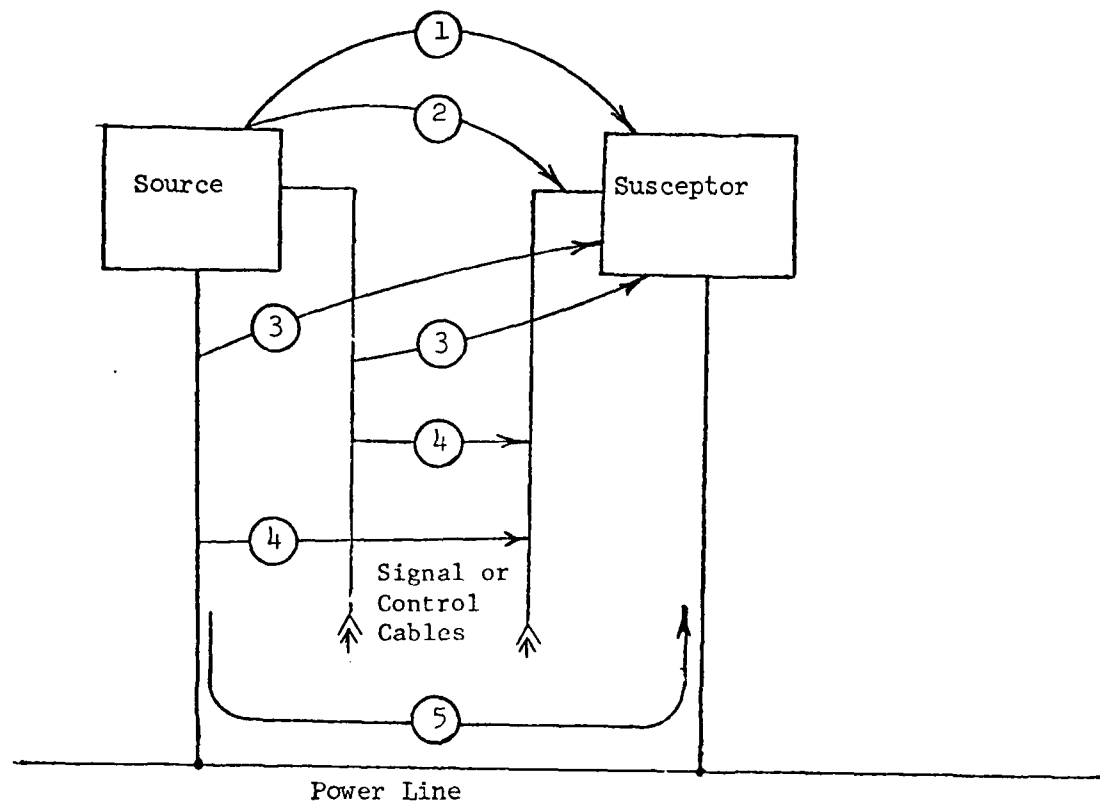


Figure 1. Basic Interference Mechanisms

- (c) Direct conduction from source to susceptor via a common conductor, for example, the power line (5).

In all cases, the undesired signal is presumed to originate within the source. In (a) it is radiated directly from the source enclosure, while in (b) and (c) the source is presumed to generate the undesired signal in the form of currents on the conductors connected to it. The undesired signal presents itself at the susceptor either in the form of an electric or magnetic field at the susceptor case, or as a voltage on the cables connected to the susceptor.

## 2.0 MODEL DEVELOPMENT

In order to compute protection margins, either actual data or models for levels and coupling mechanisms are required. The use of models (to the extent that they are valid) avoids the necessity for gathering large amounts of statistical data. Such models must be validated, at least sufficiently to provide predictions in which one can have a high level of confidence. Of course, in any given case, where the predicted margin is marginal or negative, there is no substitute for properly measured data.

### 2.1 Technical Considerations

#### 2.1.1 Bandwidth

In interference prediction work, it is convenient to analyze phenomena that occur as a function of frequency. Thus, in characterizing sources, one uses a frequency spectrum presentation of the emission level. The type of presentation depends upon the character of the source. If the source has a dominant output at a particular frequency, or frequencies, this output must be presented as a current or voltage level at those particular frequencies. In that case, the dimensions are amperes or volts. On the other hand, the spectrum may be continuous such as obtained with a pulse or a series of pulses and these pulses are repeated at random times and have random amplitudes. Then the spectrum must be specified in terms of a level (such as volts or amperes) per unit frequency range.

Electrical waveforms can also be characterized in the time domain. The two characterizations are related, of course, by the Fourier transform [1]. Thus, in theory, by knowing the form of the pulse in either domain the form in the other may be found. In practice, however, the computation of Fourier transforms can be laborious, especially since in the frequency domain both amplitude and phase information are necessary. If measurements are to be made on broadband sources it would appear to be most convenient to have information from both domains, in particular:

1. Time domain: peak value and rise time (or maximum slope), duration.

## 2. Frequency domain:

- a) spectrum amplitude as a function of frequency (peak value in a reference bandwidth:  $\mu\text{T}/\text{MHz}$ ,  $\mu\text{A}/\text{kHz}$ , etc.)
- b) levels at discrete frequencies.

Frequency domain measurements may be difficult in the case of single-occurrence transients or transients occurring at a low average repetition rate. In such cases a complete time domain description might be obtained with transient recording devices such as an image retention oscilloscope, and then the Fourier transform applied to it to obtain frequency domain information.

### 2.1.2 Pulse Spectra

A useful model for a pulse is the simple trapezoid shown in Fig. 2. Its spectrum is [1]:

$$S(f) = 2AT \frac{\sin \pi f\tau}{\pi f\tau} \frac{\sin \pi fT}{\pi fT} \quad (1)$$

where  $f$  is the frequency in Hz,  $T$  and  $\tau$  are in seconds, and  $S(f)$  is in the units of A per Hz.

The sinusoidally varying terms in (1) make the spectrum difficult to plot precisely. It is perhaps more useful to plot the loci of the maximum values versus  $f$ , and this is done in Fig. 3. If  $A$  is in volts the ordinate values are in units of volt-seconds or volts per Hertz.

As examples of broadband conducted interference sources, the spectra of a data-processing system clock pulse and the MIL-STD-1399 2500 V line transient are presented in Fig. 4. These spectra are taken from Ref. [2]. The duration,  $T$ , used in computing these spectra was that above 10% of the peak value of the pulse. In the trapezoidal pulse, the duration is that above the 50% level. To convert non-trapezoidal pulses to a trapezoidal equivalent, the duration  $T$  would be chosen such that

$$\text{area of pulse} = \text{peak value} \times T \text{ (trapezoidal equivalent)}$$

### 2.1.3 Coupling Models

There are three major types of coupling models--one for conduction, another for magnetic coupling, and the third for electric coupling. For conduction a four-terminal network model is used in which current is injected in the input terminal pair, causing a voltage to appear at the output terminal pair. The ratio of the output voltage to the input current is defined as the transfer impedance of the network. Such coupling networks can be used for both differential-mode and common-mode propagation mechanisms for two-conductor lines, such as single-phase power lines.

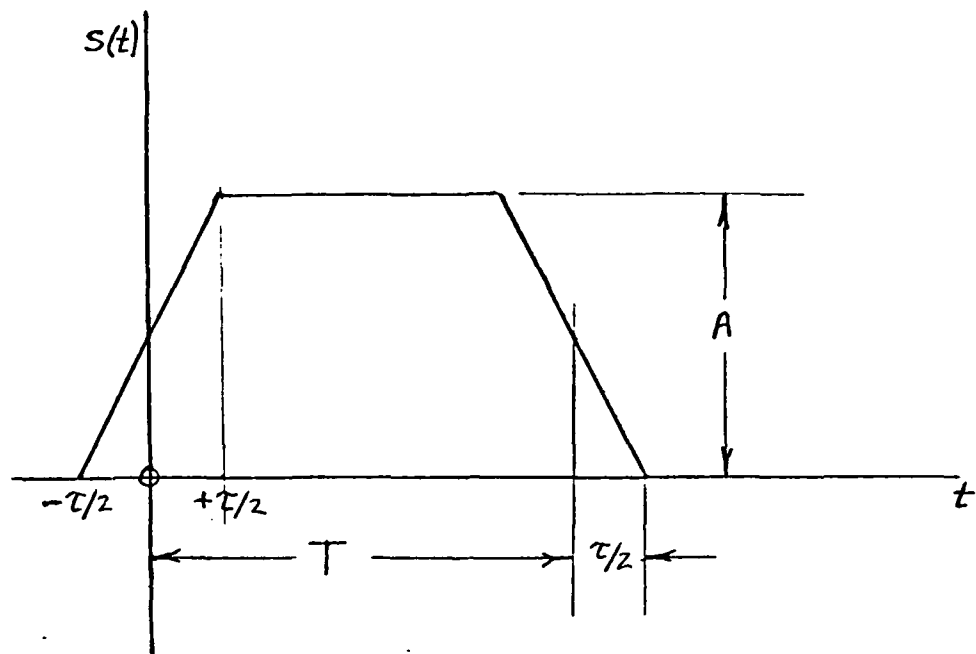
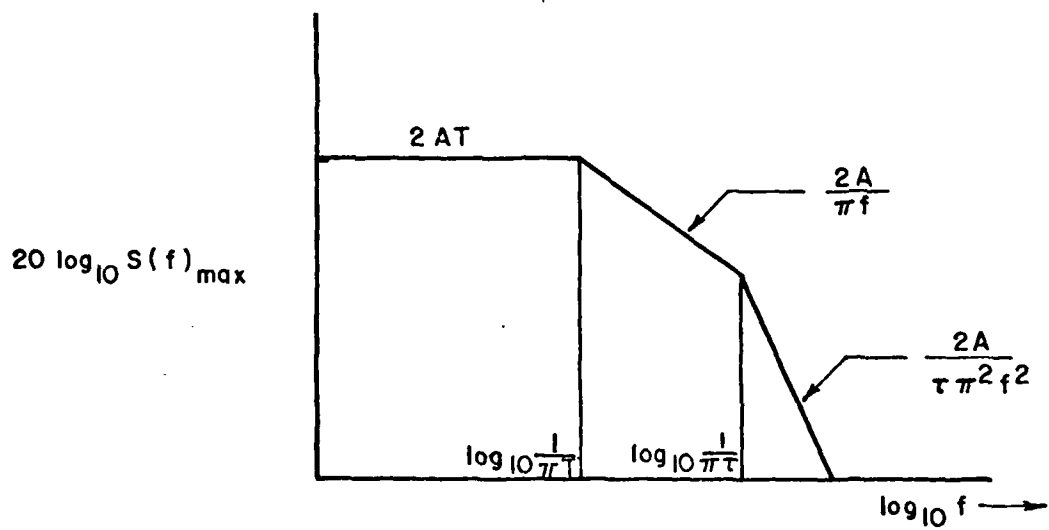


Figure 2. Trapezoidal Pulse Model



**Figure 3 Envelope of Spectrum of Pulse of Figure 2**  
 **$S(f)$  Has Dimensions A·s or A/Hz**

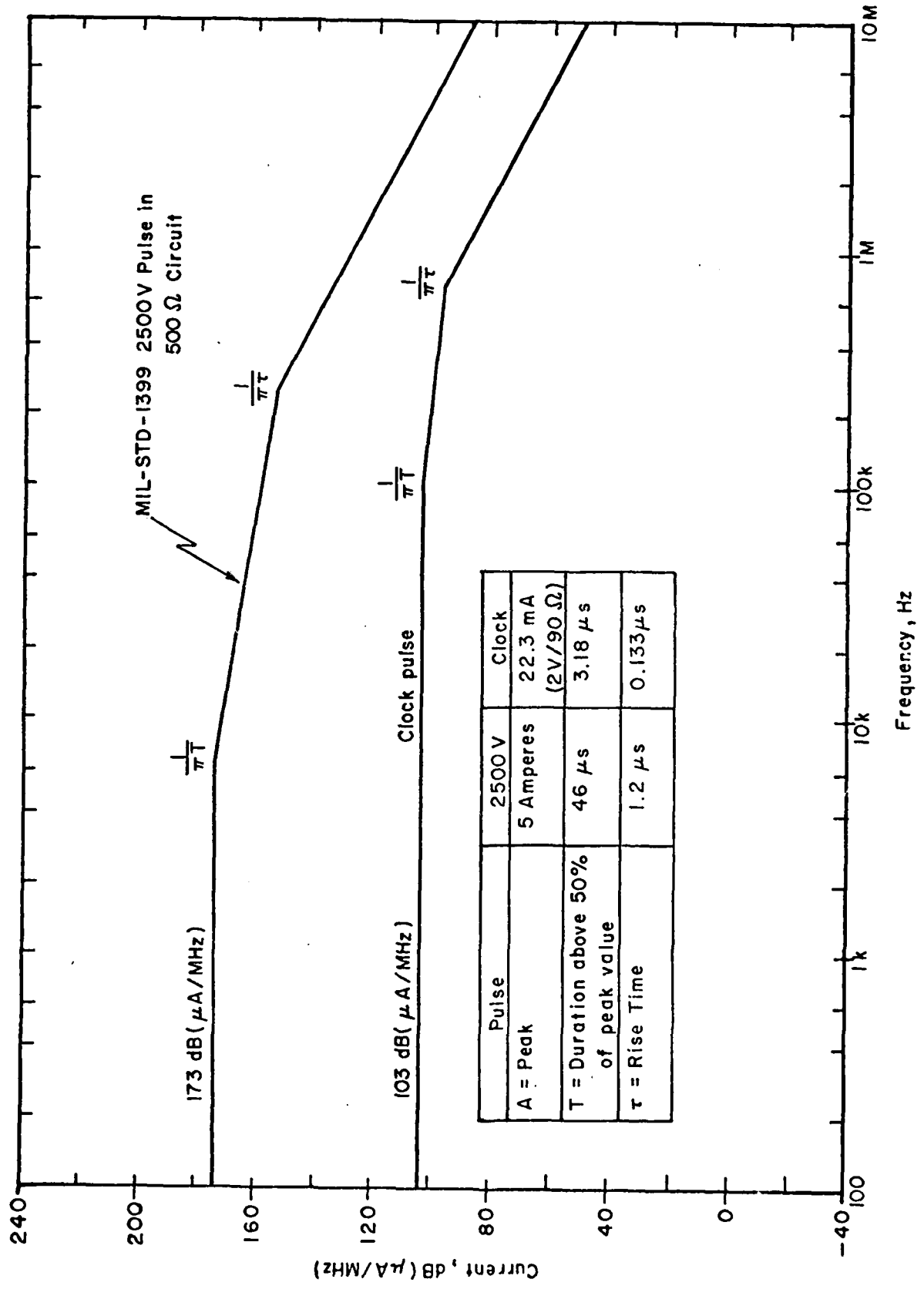


Figure 4 Broadband Conducted Emission Sources [ 2 ]

In the magnetic coupling model, the voltage is induced in the susceptor as a consequence of Faraday's law, which relates the induced voltage to the rate of change of the magnetic flux density in a closed loop. The coupling between a source and a susceptor is dependent upon the nature of the source and the dimensions of both the source and the susceptor, as well as the distance between them. If the distance is large compared with the dimensions of either, a dipole model generally can be applied; that is, the source is represented as a dipole of a specified strength in ampere-meters<sup>2</sup> and susceptor is represented as a loop intercepting a total flux  $\phi$ . The coupling varies as the reciprocal third power of the distance between the equivalent source dipole and the susceptor loop. In cases where the separation between the magnetic source and the susceptor is not large compared with their dimensions, it is not possible, in general, to conveniently separate the coupling model into three parts, namely, the source, the susceptor and the coupling between them. However, in subsequent discussion, typical sources and susceptors will be described, but the coupling factors may appear in the same discussions.

In the case of electric coupling, one can theoretically define models which are the analog of those for magnetic coupling. However, electric coupling is usually not very significant and dipole models are not very realistic for the following reasons:

- a) Since cabinets on most devices are good conductors, currents flow on them and the effective dipole sources or susceptors have dimensions which are not small compared with cabinet separations.
- b) Since the cabinets have good conductivity, as do shields on cables, there is substantial attenuation of electric fields before they reach sensitive circuits.

For these reasons, very little attention is given to electric coupling in this report.

## 2.2 Conducted Emissions

Many conducted interference sources may be modeled by a simplified two-terminal Norton equivalent circuit as shown in Fig. 5. The two terminals in this representation correspond to either the two active conductors of a two-conductor power or signal line operating in the "differential" mode, or, if operating in the "common mode" a single wire "equivalent" for these two conductors and a ground connection or ground plane. The impedances  $Z_S$  and  $Z_L$  are the equivalent source and load impedances, respectively, in the differential or common mode configuration.  $I_S$  and  $I_L$  are the source short-circuit current and the current flowing in the load  $Z_L$ , respectively, and constitute a complete characterization of a "linear" source. However,  $I_S$  and  $Z_S$  may be a function of the source operating conditions and may be a function of the load if the source itself is "nonlinear." The source can also be characterized by the Thevenin equivalent in which the open-circuit voltage

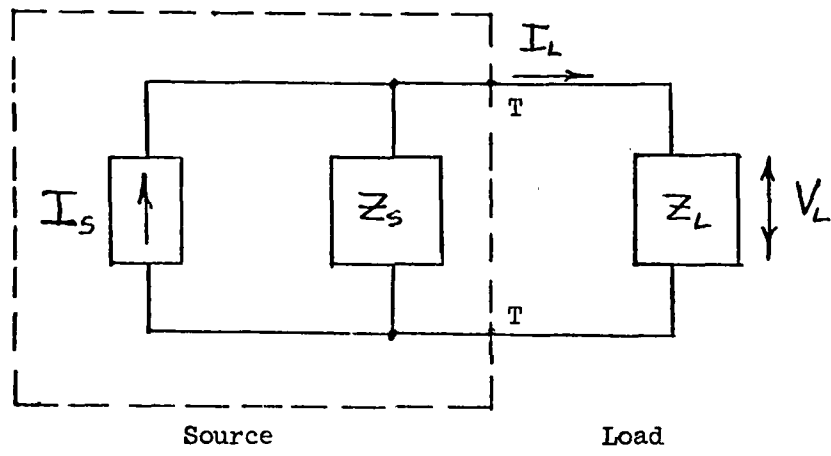


Figure 5. Equivalent Circuit, Conducted Interference Source

$$V_S = I_S Z_S \quad (2)$$

appears in series with  $Z_S$  and the terminals (T).

### 2.2.1 Source Measurements

Although a knowledge of both  $I_S$  and  $Z_S$  is necessary to characterize a source, explicit measurement is usually made only of  $I_S$ .  $Z_S$  is not usually known. Values of  $Z_S$  are frequently "inferred" in using source data or a value of  $Z_S$  is assumed, e.g.  $Z_S = \infty$  (in other words, the measured source current is assumed to flow under all loading conditions).

In the following we describe some typical sources. We consider those that may be important in the frequency range below about 100 kHz. In this range the major emissions are, directly or indirectly, due to the power frequency current and its harmonics, active sources such as sonar and VHF transmitters, and switching transients.

### 2.2.2 Nonlinear Power Line Loads

Nonlinear loads in 60 and 400 Hz power circuits can generate large harmonic components up to several hundred amperes that fall in the same frequency range as some sensitive low-frequency electronic equipment. The harmonic levels depend on the loads connected to the power line, and on the degree of nonlinearity in the load. Rectifier power supplies are typical sources [3].

For a supply having a large inductive filter on the secondary side, the current  $I_S$  in the line at any harmonic present is determined by the relation:

$$I_n = \frac{1}{n} I_1 \text{ (rms values)} \quad (3)$$

where  $I_1$  is the rms value of the fundamental, and

$I_n$  is the rms value of the  $n^{\text{th}}$  harmonic

Values of  $n$ , specifying which harmonics are present, are given by:

$$n = s.q + 1, s. = 1, 2, 3, \dots \quad (4)$$

where  $q$  is the pulse number associated with the particular rectifier configuration being considered.

For example, a simple wye-wye transformer connection with a midpoint diode configuration has a  $q$  value of three; and a delta-wye transformer with a bridge diode configuration has a  $q$  value of six.

In practice, relation (4) applies at best only for low-order harmonics, e.g. 5 or 7, and above that for various reasons the current falls off with harmonic order at a faster rate.

A comparison of the levels predicted by  $1/n$  and  $1/n^2$  models with harmonic levels actually measured is shown on Fig. 6. A detailed discussion of the model for conducted line harmonic level calculation is given in Ref. [4].

In the absence of further information, it is recommended that harmonics be assumed to vary as the (-1) power of the frequency out to the 5th harmonic and the (-1.5) power above that.

The  $1/n^P$  decrement is maintained up to the frequency range at which measured emissions cease to be characterizable as power line harmonics. Available data appear to indicate that this occurs at frequencies above about 100 kHz. In this range, therefore, it seems reasonable that a transition should occur to a limit that is constant for all devices. The level of this limit could be the level of the present MIL-STD-461 limit at the high frequency end.

#### 2.2.2.1 Simplified Model

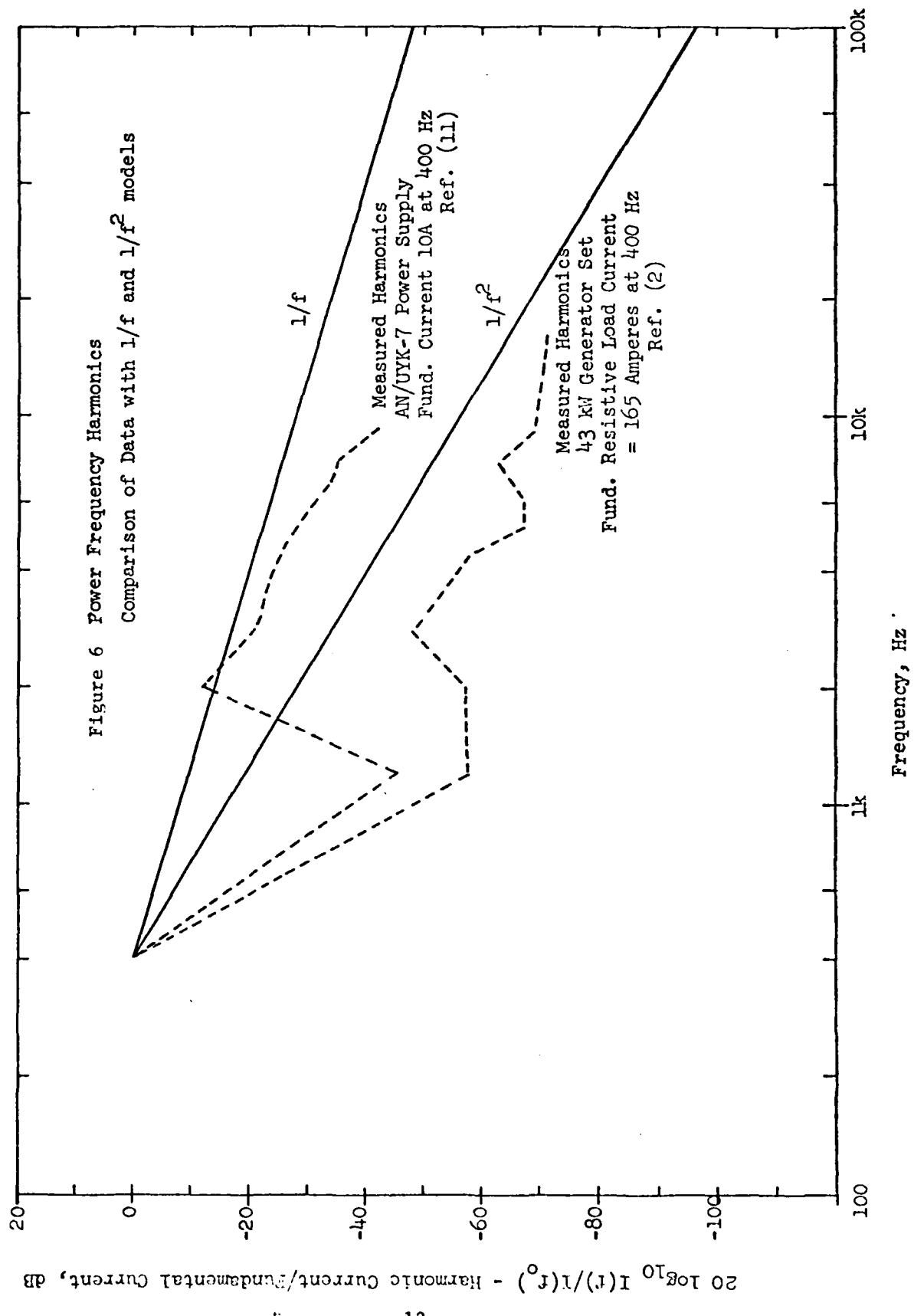
In order to get order of magnitude estimates of voltage levels, one can use the simplified model shown in Fig. 7. Here the total nonlinear load is represented by the resistance  $R$  and the total inductance of the generator and line connecting it to the point at which harmonic levels are desired is represented by  $L$ . In such a circuit, assuming harmonic current levels fall off as  $1/n^L$ , where  $n$  is the harmonic number, the voltage levels for the harmonics that appear are constant out to a certain harmonic number and fall off as  $1/n$  at higher harmonic numbers. The result is given in graphical form in Figs. 8 and 9 for 60 Hz and 400 Hz circuits, respectively, and for  $L_L = 50 \mu\text{H}$ . In using these curves for low orders of  $n$ , one follows the horizontal dotted line corresponding to the total line current, out to the intersection with the sloping ( $1/n$ ) curve, and then follows the sloping curve. For other values of inductance, the horizontal dotted line is raised or lowered in proportion to the change from  $50 \mu\text{H}$ .

#### 2.2.3 Common-Mode Emission

To estimate common-mode current emission levels requires knowledge of the power cable circuit configuration and the location and size of line-to-ground capacitors. A three-phase ungrounded system is shown in Fig. 10. Boxes 1 and 2 represent single-phase loads placed on two different phases of the line. The capacitors represent intentional filter or stray capacitances between the power line and the load cabinets connected to the ground plane or common safety "ground" wire.

The common-mode current  $I_C$  would then be equal to the line-to-line voltage  $V_{ac}$  divided by the capacitive reactance of  $C_{L1}$  and  $C_{L2}$  in series:

$$I_C = 2\pi f \frac{C_{L1} C_{L2}}{C_{L1} + C_{L2}} \cdot V_{ac} \quad (5)$$



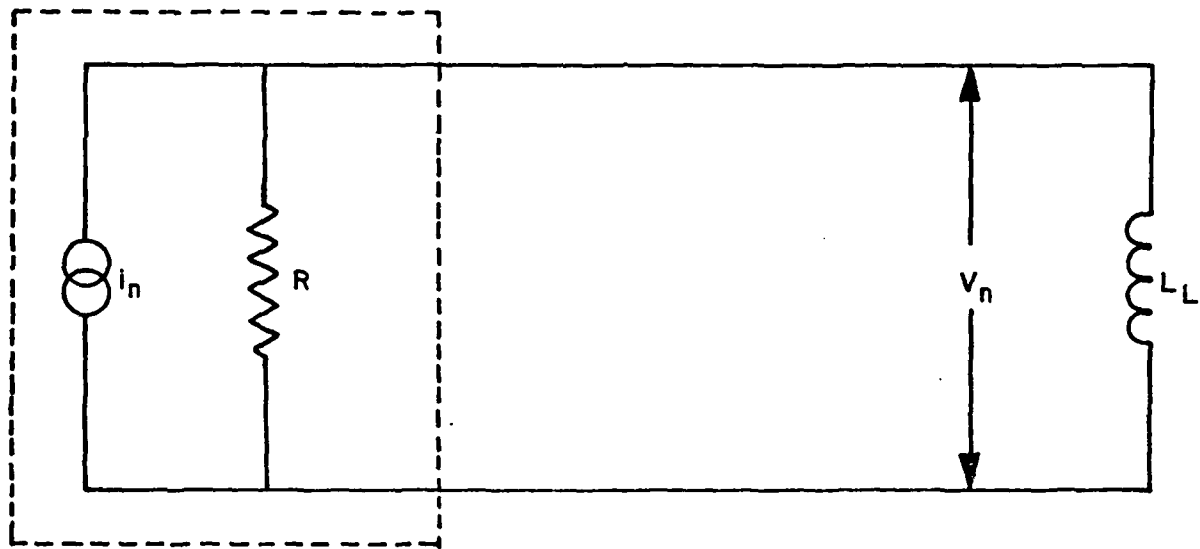


Figure 7 Simplified Model of Current Generator Characteristics

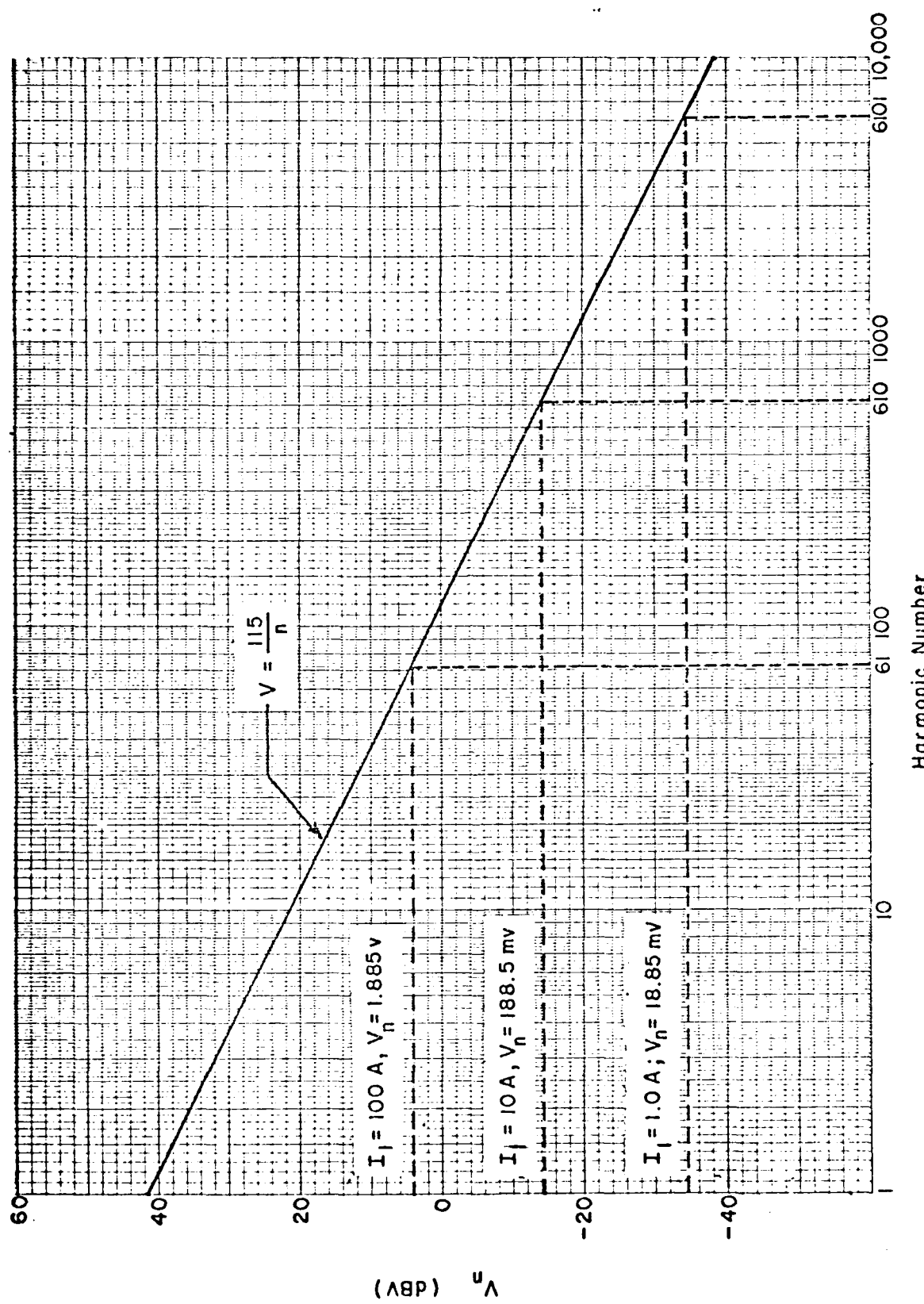


Figure 8 Harmonic Voltages Predicted on a 115 V, 60 Hz Line When  $L_L = 50 \mu\text{H}$

NO. 340-1510 DIETZGEN GRAPH PAPER  
SEMI-LOGARITHMIC  
5 CYCLES X 10 DIVISIONS PER INCH

EUGENE DIETZGEN CO.  
MADE IN U. S. A.

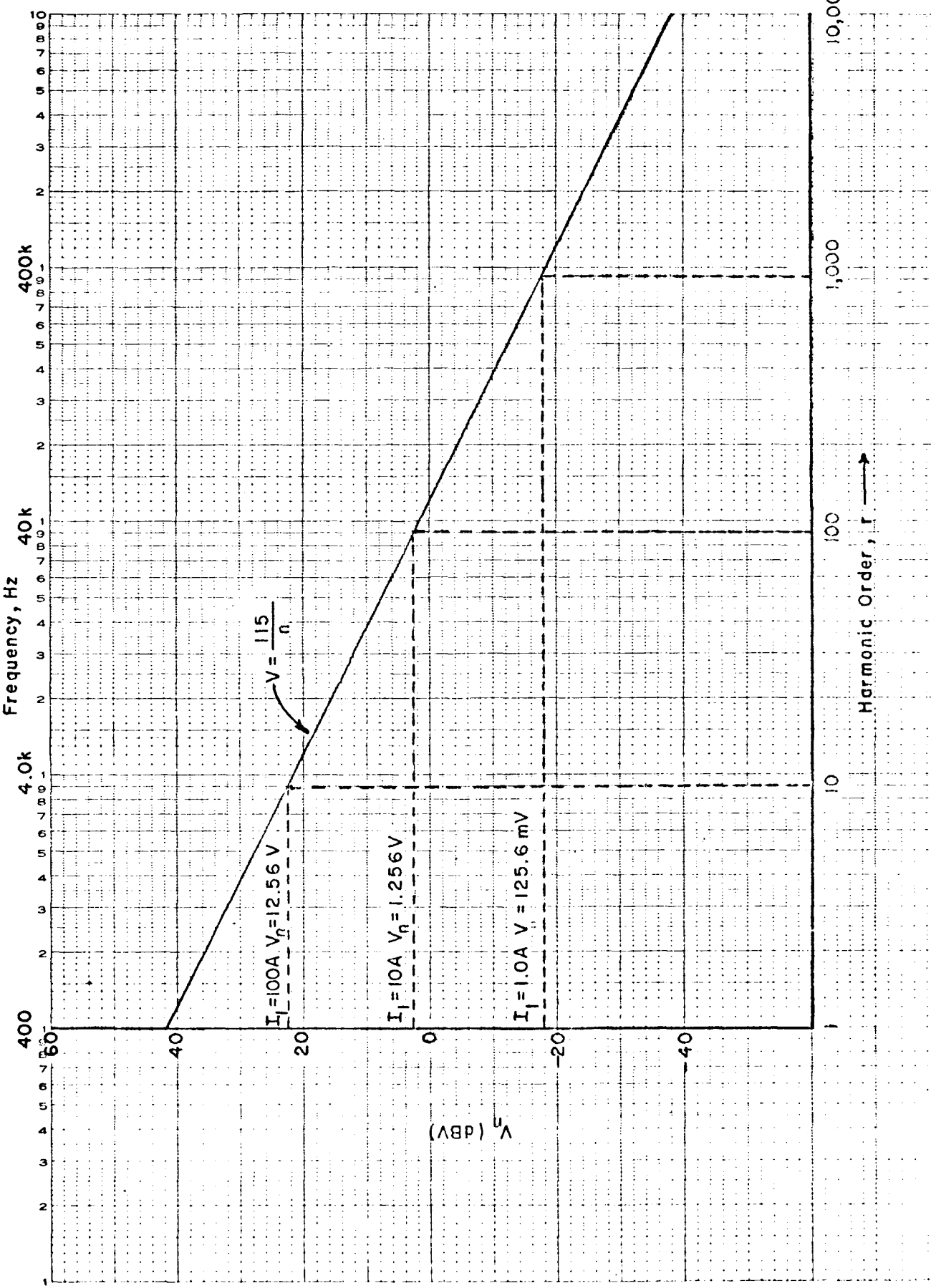


Figure 9 Harmonic Voltages Predicted on a 115V, 400 Hz Line When  $L_L = 50 \mu H$

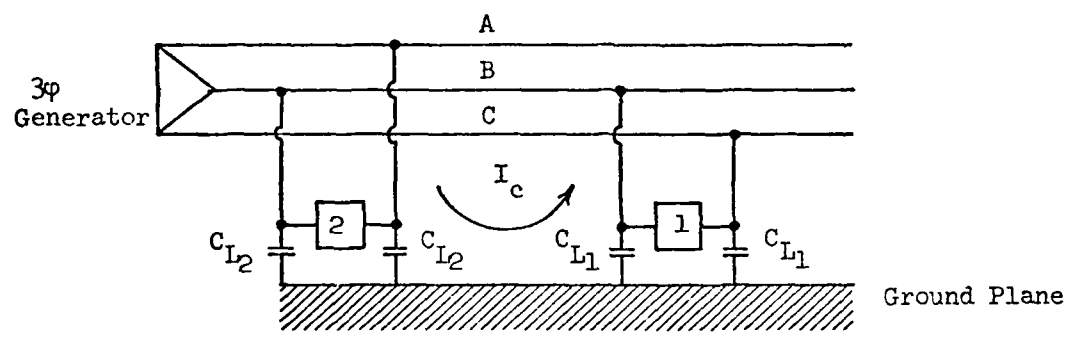


Figure 10 Possible Source of Common-Mode Currents

At the frequencies of the power line harmonics,  $V_{ac}$  may be obtained from the model described in the previous paragraph or estimated more accurately using Ref. [4].

Thus, common-mode current at low order harmonics will rise with frequency initially at 20 dB/decade, and then level off and remain constant or fall off with harmonic order according to whether the current generated falls off with frequency at  $1/f$  or  $1/f^2$ .

To estimate the order of magnitude of the common-mode current, consider  $C_{L1} = C_{L2} = 0.05 \mu F$ , corresponding to the common case of RF bypass capacitors on the power line input to a receiver. Then the series capacitance  $C_{L1}C_{L2} = (1/2) \times 0.05 = 0.025 \mu F$ , and

$$I_c = 2\pi \times 25 \times 10^{-9} \times f \times V_{ac}$$

$$\approx 0.15 f \text{ milliamperes} \quad (6)$$

for  $V_{ac} = 1 \text{ V}$

and  $f$  in kHz

As a practical matter, the linear rise in  $I_c$  with frequency is limited to those frequencies below the break point in Figs. 8 or 9. Above this frequency the current would tend to remain constant or decrease with frequency.

#### 2.2.3.1 Model for Estimating Common-Mode Current Associated with Power Systems Having Multiple Line-to-Ground Filters

##### a) Assumptions

A 3-phase circuit is assumed and, initially, 3-phase loads. Also, it is assumed that there are a sufficient number of filtered loads connected into the system so that they are, overall, effectively balanced so that the ground plane or structure assumes a potential near the neutral point of the 3-phase supply. If this is not actually true, it is not considered that it would significantly alter the conclusions derived here.

In accordance with this model, the line-to-neutral voltage is assumed to be equal to the line-to-line voltage divided by the square root of 3. Then, for a capacitance  $C$ , one would expect to obtain a current

$$I_c = \frac{V_L}{\sqrt{3}} \omega C$$

in each capacitor. In a perfectly balanced filter with all the  $C$ 's identical on all of the phases, the total structure current would add up to zero. However, it has been stated that typical capacitors have considerable tolerance (as much as 35%) so that, in general, one can expect a net unbalanced filter current  $I_f$  of approximately  $1/3$  of the current flowing in a single capacitor.

$$I_f = \frac{V_L}{3\sqrt{3}} \omega C \quad (7)$$

b) Effects of Multiple Filters

When several filters appear on the same line, they will each produce currents which should be summed to obtain the total current that will flow on that line. Just how these currents will distribute themselves on the cables leading to the equipments connected to such a line depends upon the exact configuration. However, the current in one load will not necessarily be in the same phase as that in another, since, with a 3-phase load, the phase of the current will depend on which capacitor is connected to which phase.

Figure 11 shows 10 loads connected to a common line. The total current to the structure must add to zero if no other loads with filters are involved.

To simplify the argument, we assume that the currents in individual loads will have phases distributed at random. With random phasing, the currents add as the square root of the number of filters; that is, 9 filters (having the same values of capacitance) will produce a total current approximately equal to 3 times the current produced by a single load. It is quite conceivable that this total current could be impressed upon a susceptible device, say the 10th load shown on Fig. 11. At first glance, one might conclude that this result contradicts Eq. 7. On reflection it can be concluded that what really happens is that in a closed circuit of this kind an adjustment in the structure potential occurs which enables the total structure current to add to zero, but which causes currents in individual loads to well exceed the level calculated by Eq. 7.

Thus, with multiple loads we can expect the maximum structure current impressed on a susceptible load to be given by:

$$I_s = \frac{V_L \omega C \sqrt{n}}{3\sqrt{3}} \quad (8)$$

where  $n$  is the number of loads (having about equal capacitance values). Thus, for the sake of calculations, we assume that 9 loads are representative and that, therefore, Eq. 8 becomes:

$$I_s = \frac{V_L \omega C}{\sqrt{3}} \quad (9)$$

c) Estimated Currents

Table I gives the estimated structure currents for line-to-ground capacitors of  $0.02 \mu F$  (as called for in present "TRIDENT specifications) and  $1.25 \mu F$  (this value has been found installed in a number of TRIDENT equipments).

TABLE I PREDICTED COMMON-MODE CURRENT (mA)

	Harmonic	1	5	7	11	13	38
L-G Cap ( $\mu\text{F}$ )	Frequency (kHz)	0.4	2.0	2.8	4.4	5.2	15.2
	Voltage	120	5.0	4.2	3.4	3.1	0.2
0.02	Current, mA	3.5	0.72	0.88	1.072	1.17	0.22
2.5	Current, mA	220	45	55	67	73	15

For the voltage levels, we assume the following. At 400 MHz, the line-to-line voltage is 120 volts. At the 5th harmonic, the line-to-line voltage is assumed to be 5 volts and varies by the inverse square root of frequency for components to the 13th. At VLF (15 kHz) the line-to-line voltage is assumed to be 0.2 volts. These values are roughly in accordance with values predicted theoretically and measured experimentally.

The values of structure current for a maximum line-to-ground capacitance of 0.02  $\mu\text{F}$  are seen to be of the order of 1 mA. At 400 Hz, 5 mA is a reasonable expectation. However, if the line-to-ground capacitance is 1.25  $\mu\text{F}$ , several hundred mA may be expected.

#### d) Single-Phase Loads

For a single-phase load, we adopt an analysis slightly different from the one given in Ref. [5]. In particular, here we have two capacitors connected in series across one phase of the 3-phase system with their center point connected to neutral. In this case, the current flowing in each capacitor is given by:

$$I = \frac{V_L \omega C}{\sqrt{3}} \quad (10)$$

When the current through the second capacitor is added vectorially to that in the first capacitor, one obtains a resultant current which, in fact, has a magnitude equal to that given by Eq. 10, as shown in Fig. 12. Assume the two capacitors are equal with a value of  $C \mu\text{F}$  and placed from phases A and B to neutral.

The current  $I_{C(A)}$  in the capacitor on phase A has a vector value  $j V_A \omega C$ . Similarly, that for phase B has the current  $I_{C(B)}$  shown. The

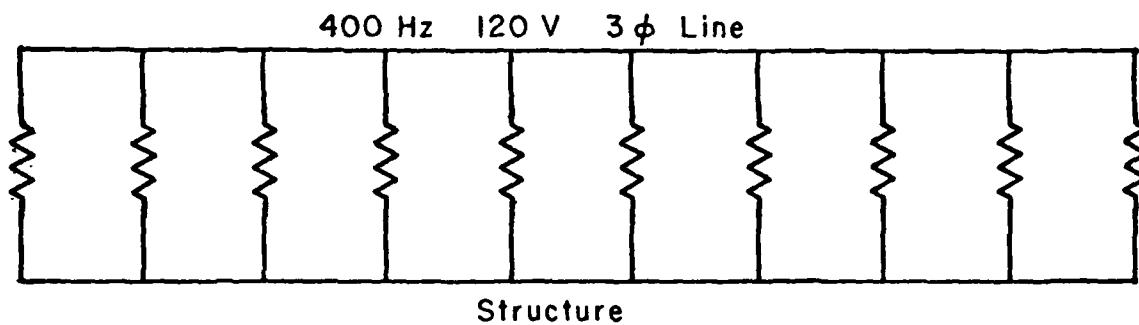


**Figure II** Multiple Loads on a Common Line

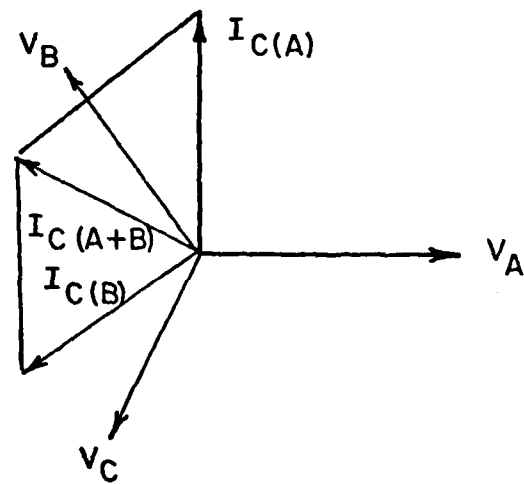


**Figure I2** Capacitor Current Addition for Filter in Single Phase Load

net current  $I_{C(A+B)}$  has the same magnitude as that due to either capacitor alone. Thus, it may be noted that a single-phase filter will produce three times as much current as a 3-phase filter having the same line-to-ground capacitance. Conceivably, this current could be more important than that from 3-phase filters. For the time being, we assume that single-phase filters are less than 1/3 as numerous as 3-phase filters, and, therefore, will contribute less structure current than 3-phase filters.

### 2.3 Radiated Emissions

Radiated fields from power lines and cables arise directly or indirectly from the above conducted emissions.

The basic model for direct magnetic field radiation from equipment cases is a magnetic dipole of moment  $M_m$ . For an infinitesimal source the magnetic field strength at a distance  $r$  is given by (in spherical coordinates)

$$H_\theta = \frac{M_m \beta^3}{4\pi} \left( -\frac{1}{\beta r} + j \frac{1}{(\beta r)^2} + \frac{1}{(\beta r)^3} \right) \sin \theta \quad (11)$$

$$H_\phi = \frac{2M_m \beta^3}{4\pi} \left( \frac{1}{(\beta r)^3} + j \frac{1}{(\beta r)^2} \right) \cos \theta$$

where

$$\beta = \frac{2\pi}{\lambda} = \frac{2\pi f}{c}, \text{ (m}^{-1}\text{)}$$

$$f = \text{frequency, Hz (s}^{-1}\text{)}$$

$$c = \text{velocity of light} = 3 \times 10^8 \text{ meters/s, and}$$

$$M_m = \text{dipole strength, (A-m}^2\text{)}$$

For  $\beta r \ll 1$ , the magnetic field strength is

$$H_\theta = \frac{M_m \sin \theta}{4\pi r^3} \quad (12)$$

$$H_\phi = \frac{2M_m \cos \theta}{4\pi r^3}$$

For example, if  $r < 20$  meters and  $f < 1$  MHz, it is sufficiently accurate to model the magnetic field strength as falling off as  $(1/r)^3$ .

The magnitude of the maximum magnetic flux density is given in terms of the maximum magnetic field strength and the dipole strength by

$$|B| = \mu_0 |H| \approx \frac{\mu_0 |M_m|}{3} \frac{1}{2\pi r} \quad (13)$$

[In making predictions, we ignore the significance of the angle  $\theta$  in Eq. 11 in order to simplify calculations. As a matter of fact, the probability that the susceptor will be oriented to respond to a null direction of the field is quite small. Furthermore, retaining such directional information and including it in the calculations requires complications that cannot be justified practically.] If the flux density  $B'$  is measured at a distance  $r'$ , then the magnitude of the flux density at any other distance from a small dipole is found by

$$\frac{B}{B'} = \left( \frac{r'}{r} \right)^3 \quad (14)$$

The magnetic dipole model is generally valid at distances from the center of the source large compared with the maximum dimensions of the source.

### 2.3.1 Loop Emission

If the distance to the magnetic source is not large compared with its maximum dimensions, a still simple, but frequently adequate, source model is a current loop. The equations for the field from a loop are fairly complex off the axis of the loop; however, an asymptotic approximation may be used to estimate the worst case field. In the following we continue to assume the distances involved are small, i.e. the distance from the point of interest to the magnetic source current or dipole, and the frequency are such that  $Br \ll 1$ . Accordingly, only the "static" magnetic field components have to be considered.

To demonstrate the nature of variations, we make use of exact calculations of a model of a magnetic source consisting of a circular loop of wire of radius  $a_0$ . Figure 13 shows the variation of the flux density as a function of distance measured from the center of the loop in the two directions which represent the extremes that one would find, namely, in a direction in the plane of the loop and in a direction along the axis of the loop. At large distances the flux density varies inversely as the cube of the distance in both directions with that along the axis being 6 dB higher than that in the loop plane. At close distances the flux density is lowest along the axis of the loop and approaches an asymptotic value that depends upon the loop radius, being (for loops of equal dipole strength) lower for loops having the larger radii. For a direction in the plane of the loop the flux density increases rapidly without limit as the position approaches the location of the actual loop conductor. Figure 14 shows the same information as shown on Fig. 13 except normalized with respect to the loop radius  $a$ .

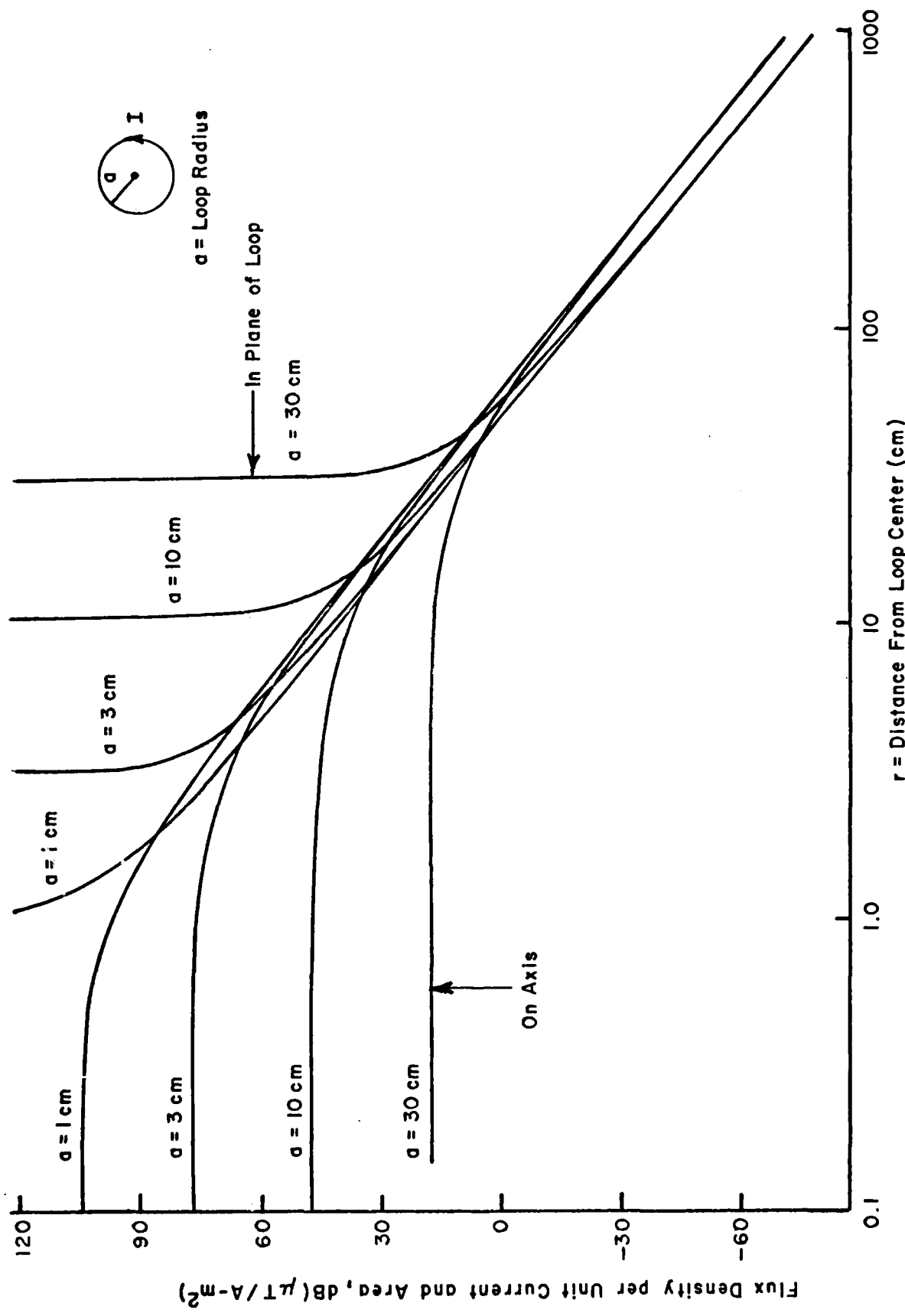


Figure 13 Magnetic Flux Density From Circular Current Loop on Axis and in Plane of Loop

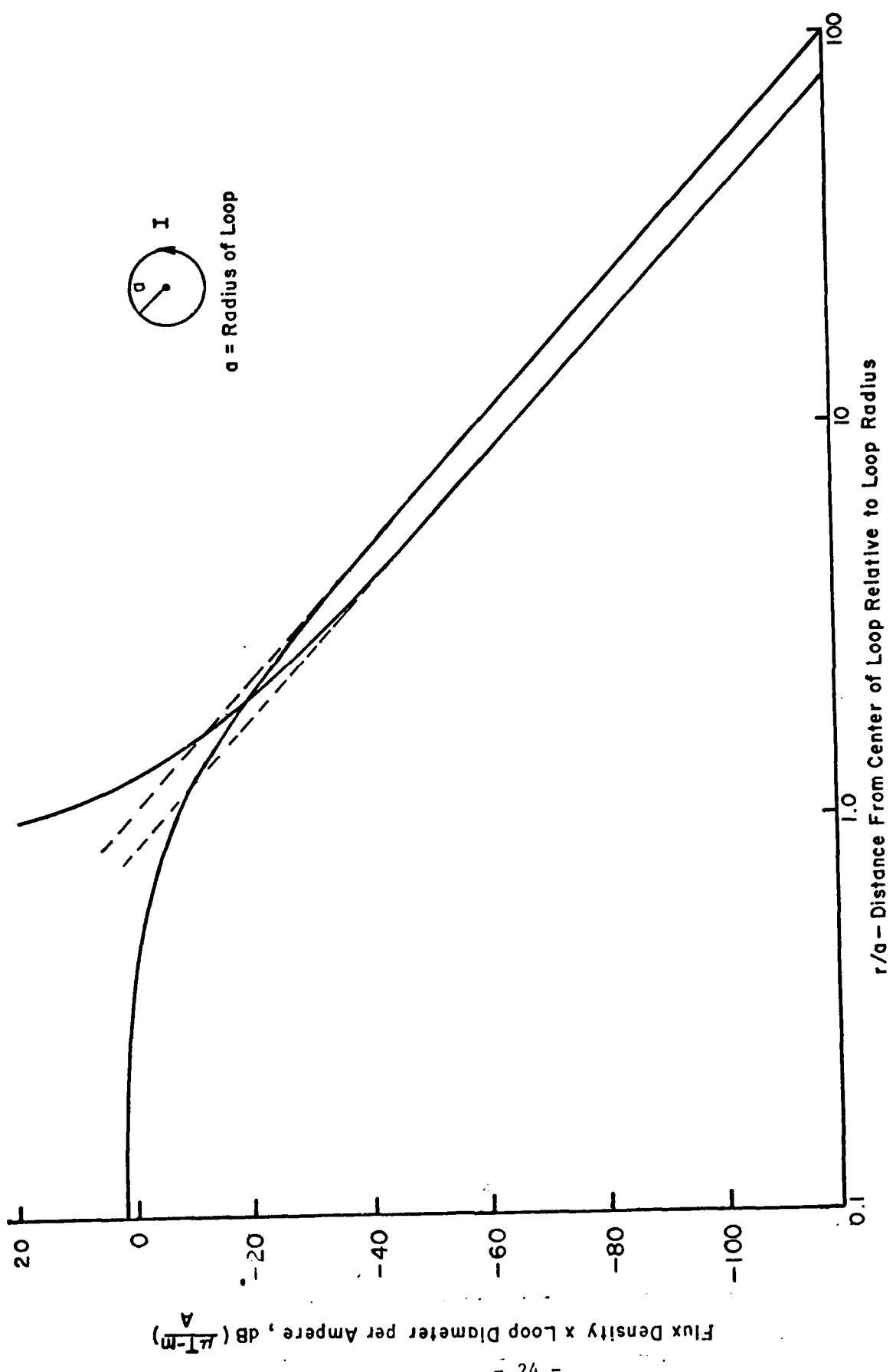


Figure 14 Normalized Magnetic Field Strength From Circular Current Loop on Axis and in Plane of Loop

As a practical matter, it should be recognized that (1) in the usual device it is generally not possible to get closer to the effective loop than the loop radius itself, and (2) that the measurement is made with a loop of finite diameter and therefore, will, in fact, average the flux density over the loop area. Because of these factors it is considered reasonable to expect that the actual value of the flux density at any distance  $R$  from the effective center of the dipole will lie between the two straight lines shown on Fig. 14 which are drawn coincident with the actual lines at large distances. In any event, one would not expect it to exceed the upper curve. Thus, a prediction of coupling based upon the upper curve should provide us with a conservative estimate of any possible interaction effects due to a source of this type.

Very close to a loop, in the plane of the loop, the field is similar to that of a long straight conductor, or

$$B = \frac{\mu_0 I_L}{2\pi r}, \quad r \ll d \quad (15)$$

where  $r$  = distance from nearest point on circumference of loop, and  $d$  = diameter of loop. Farther from the loop, it acts like a magnetic dipole of moment  $\frac{\pi d^2}{4} I_L$ , so that the maximum flux density is, by Eq. 13 above

$$B = \frac{\mu_0 I_L d^2}{8r^3}, \quad r \gg d \quad (16)$$

The asymptotes (15) and (16) are plotted in Fig. 15 for various values of  $d$ .

On the axis of the loop, close to the loop,  $B$  is constant with  $r$  and is given by

$$B = \frac{\mu_0 I_L}{d}, \quad r \ll d, \text{ on axis} \quad (17)$$

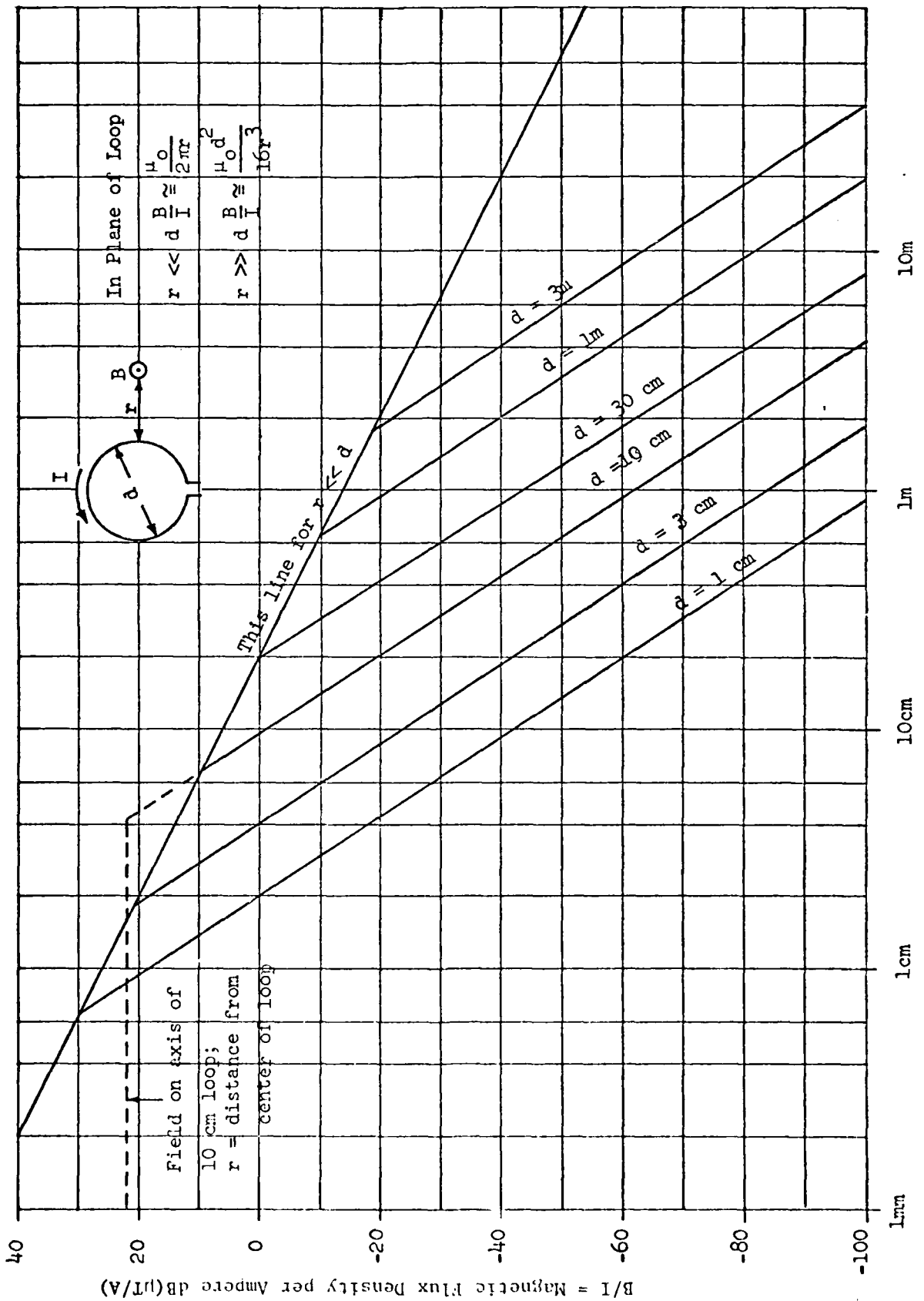
This value of  $B$  for one value of  $d$  is plotted also in Fig. 15 for comparison.

### 2.3.2 Typical Source Characteristics

#### 2.3.2.1 Power Conductor Loops

One magnetic field source at low frequencies is constituted of the power conductors inside an equipment cabinet. As an example, we could consider that the two conductors of a single-phase power circuit, after entering the cabinet, separate and run in opposite directions within the cabinet before closing at a transformer, switch, or other device. If we assume the cabinet is 3 ft square, we could approximate the field generated as that from a circular loop 2.5 ft in diameter. Thus, the flux density

Figure 15 Maximum Flux Density from a Circular Loop



generated would correspond to a curve on Fig. 15 for  $d = 0.76$  meter. At distances beyond about 0.76 m the flux density falls off as  $1/r^3$ . Closer it falls off as  $1/r^2$  or less, depending on how closely one approaches an actual conductor. Along the axis of the actual loop, the maximum flux density would be 12 dB above a microtesla for each ampere of current. One should note, however, that since the field of concern is that external to the cabinet, one is prevented by the cabinet from approaching the actual loop at a distance such that the inverse cube law ceases to apply. Also, one should be cautious in assuming a loop area equal to the maximum possible. Such a design is not, of course, good practice from an EMC point of view.

Switchboards can be significant radiators because of the practice of separating conductors and their associated switch contacts. Typically, in a circuit breaker panel, one can assume the effective loop area is about 25% of the total cabinet face area.

#### 2.3.2.2 Magnetic Devices

Frequently, the source contains magnetic material such as a power transformer, fluorescent lamp ballast, filter choke, motor, generator, or relay. An analysis similar to the above applies except for two things: (1) the size of the effective source is likely to have a small effective loop diameter, therefore the  $1/r^3$  variation extends into closer distances, and (2) the source strength is likely to be higher because of the larger number of turns of wire used to excite the magnetic material.

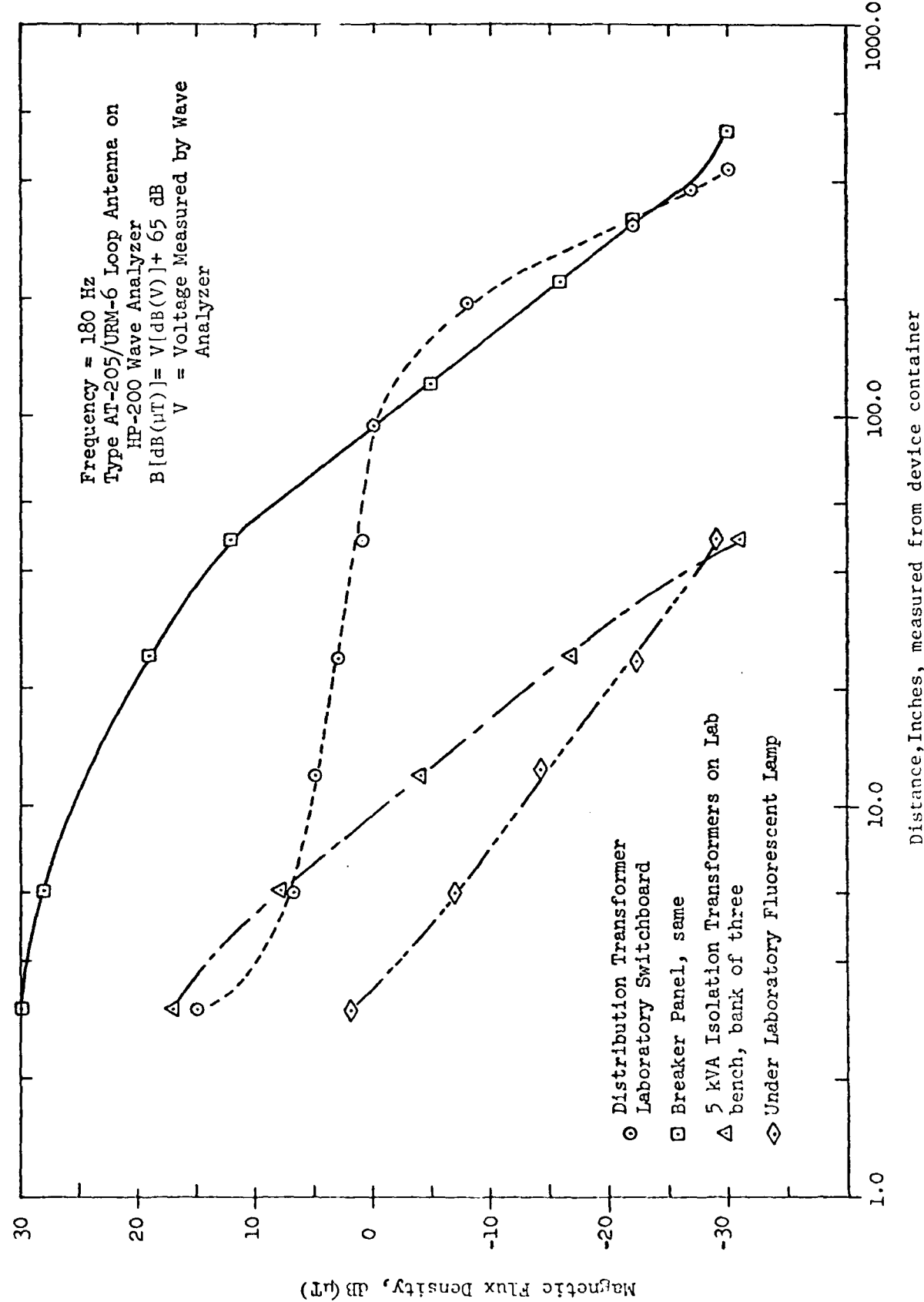
The field as a function of distance is shown for several devices on Fig. 16. The distance is measured from the container of the device.

For many devices there is little or no information available on the nature of, or strength of, sources of magnetic field. Tests at the Naval Underwater Systems Center have shown that many magnetic devices such as motors, generators and power transformers have fields which depend, to a major extent, on the power consumed. The data taken have been used to prepare Fig. 17\*, which shows the flux density to be expected at a distance of 7 cms from a cabinet containing a device with the indicated value of volt amperes.

In deriving this curve, the edge of the device was assumed to be a distance of 2 inches from the cabinet, and no attenuation of the field due to the cabinet was considered. In using this figure, it should be recognized that errors of as much as 10 dB can be expected on an average and higher values in individual cases. The flux density given in Fig. 17 is that at fundamental frequency. It can be expected to fall off at harmonic frequencies in accordance with the following relations, which have been derived empirically:

\* This figure was originally drawn by Mr. R. Russell during a technical conference held at General Dynamics, Electric Boat Div., and is based upon data taken at the Naval Underwater Systems Center, NUSC C51000 Program, Data Packages 1, 2 and 3, 29 May 1975.

Figure 16 Measured Magnetic Flux Density - Typical Sources



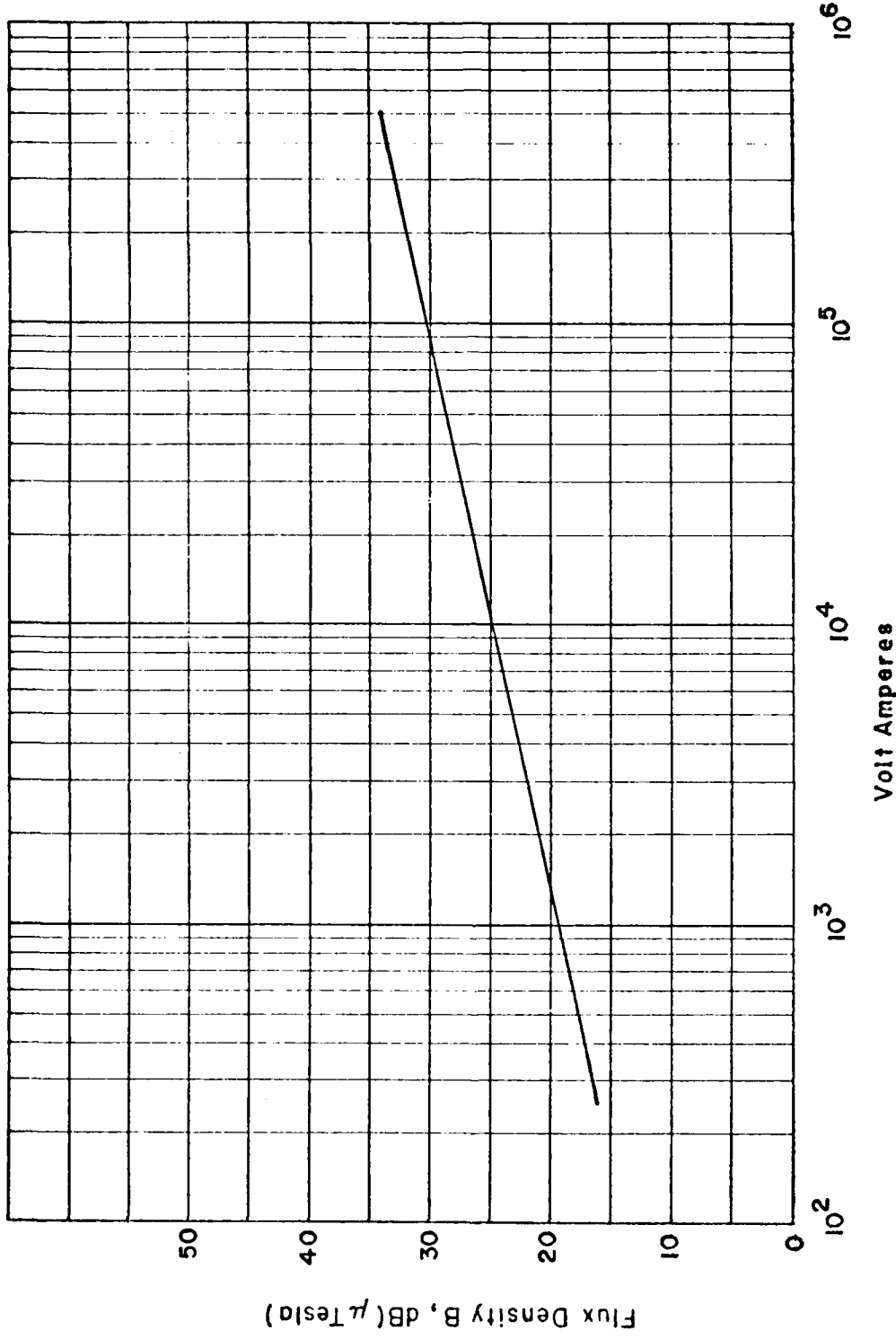


Figure I7 Predicted Electronic Equipment Magnetic Flux Emissions as a Function of Apparent Power (at the Fundamental Frequency and  $r = 0.07$  Meter)

For 60 Hz lines

$$\begin{aligned} B(f) &= B_{60} \times \frac{60}{f} & f < 1 \text{ kHz} \\ &= B_{60} \times \frac{60}{1000} \left( \frac{1000}{f} \right)^{1.5} & f > 1 \text{ kHz} \end{aligned} \quad (18)$$

For 400 Hz lines

$$\begin{aligned} B(f) &= B_{400} \times \frac{400}{f} & f < 5 \text{ kHz} \\ &= B_{400} \times \frac{400}{5000} \times \left( \frac{5000}{f} \right)^{1.5} & f > 5 \text{ kHz} \end{aligned} \quad (19)$$

Caution in using these relations should be observed as follows:

a) Recent devices frequently use switching type power supplies which contain transformers operating at the switching frequency, rather than the power frequency. The flux density algorithm may be applied in such cases at the switching frequency and its harmonics. However, in such cases it is important to account for shielding effectiveness of cabinets and special shields.

b) Audio transformers operating at high levels will not be attenuated with frequency in accordance with Eqs. 18 and 19 because the cores are being intentionally driven. However, again, any effects of metal shields either around the transformers or because of cabinets must be accounted for.

The magnetic devices for which Fig. 17 applies can be represented as magnetic dipoles in so far as the field produced is concerned. Rewriting Eq. 13, one gets

$$M_m = \frac{2\pi r^3 B}{\mu_0} \quad (20)$$

where  $r$  is the distance to the location of the center of the magnetic source. This can be written in dB as

$$M_m (\text{dB AT-m}^2) = B(\text{dB}\mu\text{T}) + 60 \log_{10} r + 14 \quad (21)$$

Hence, assuming the source is within the cabinet and 12" (30 cms) from it, the levels shown on Fig. 17 are considered to be 37 cms from the actual center of the magnetic source. Then the effective dipole strength is given by

$$M_n (\text{dB AT-m}^2) = B(\text{dBT}) \approx 12 \quad (22)$$

Typical values of  $M_n$  at 60 Hz have been found to be [5]

Large power transformers (500 kVA)	24 dB (AT-m <sup>2</sup> )
Fluorescent lamp ballasts	0 dB
Large MG sets and power distribution panels	10 dB
Small motors and distributions panels	0 dB
1 turn loop, 1 ft in diameter carrying 1 ampere	-25 dB

### 2.3.2.3 Application of Inverse-Square-Distance Relationship

In Fig. 17 the flux density is given at a point 7 cms from the cabinet of the device. Experience has shown that the variation of the flux density with distance when measured to the cabinet (rather than measured to the center of the magnetic source itself) follows an inverse-distance-squared relationship rather well. However, errors in both directions (predicted field either too high or too low) can occur, depending upon the actual position of the source. Mathematical analysis has shown that in configurations considered most typical, the error will be on the low side by about 6 dB. A complete treatment of this subject appears in Appendix A.

### 2.3.3 Radiation from Cables

Models have been developed [6] for differential and common-mode radiation from parallel-wire, coaxial, and twisted-pair lines. Two basic models are all that are required to cover all these cases. The parallel-wire model suffices for all common-mode emissions above a ground plane and for differential-mode emissions on parallel wire and coaxial lines. A separate model, which may be evaluated numerically by means of a correction factor applied to the parallel wire model, is required for the differential mode, twisted pair case. These two models are now presented.

#### 2.3.3.1 Parallel-Wire Model

The parallel-wire model is shown in Fig. 18. It consists of two infinitely long parallel conductors carrying equal and opposite currents  $I$ . They are separated by a distance  $d$ .

Taking the origin between the conductors as shown, the magnetic field strength at any point  $(x,y)$  is given by:

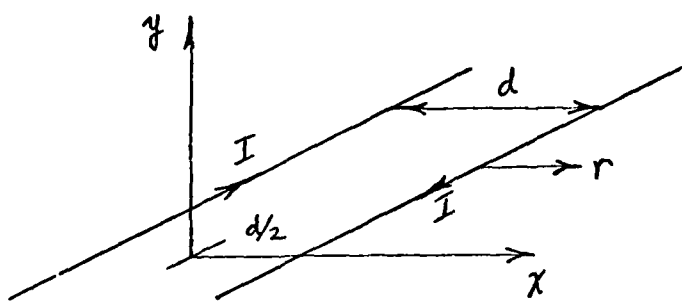


Figure 18 Parallel-Wire Model

$$H_x = \frac{Iy}{2\pi} \left[ \frac{1}{\left(x + \frac{d}{2}\right)^2 + y^2} - \frac{1}{\left(x - \frac{d}{2}\right)^2 + y^2} \right] \quad (23)$$

$$H_y = \frac{I}{2\pi} \left[ \frac{\left(x - \frac{d}{2}\right)}{\left(x - \frac{d}{2}\right)^2 + y^2} - \frac{\left(x + \frac{d}{2}\right)}{\left(x + \frac{d}{2}\right)^2 + y^2} \right]$$

That is, the net field strength at any point is the difference between the field strengths from the two wires taken individually.

Close to the line, the maximum field occurs just beyond one of the two conductors, where the subtractive effect of the far conductor is minimal. Far from the line, the field at a given distance from the line is the same all around the line. Thus, the worst case field is estimated by plotting field as a function of  $r = x - d/2$ ,  $y = 0$ , where  $r$  = distance from the near conductor in the plane of the line. The plotting and modeling is made easier by recognizing that the general expression

$$H(y = 0) = \frac{I}{2\pi} \left[ \frac{1}{r} - \frac{1}{r + d} \right] = \frac{Id}{2\pi r(r + d)} \quad (24)$$

reduces to

$$H \approx \frac{I}{2\pi r} \text{ for } r \ll d \quad (25)$$

and

$$H \approx \frac{Id}{2\pi r^2} \text{ for } r \gg d \quad (26)$$

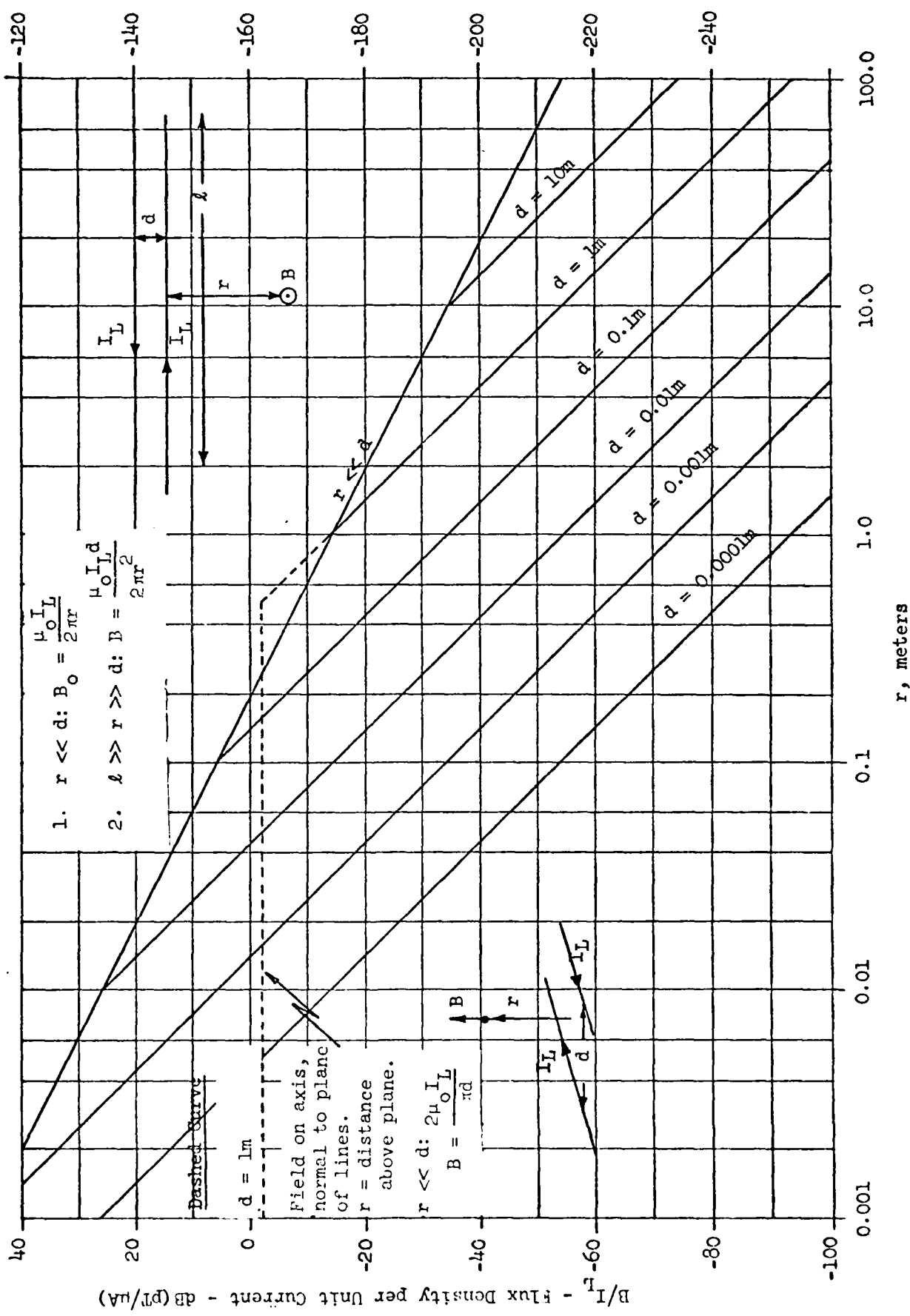
i.e., close to the line the field is the same as that for a single conductor, falling off as  $1/r$ , while far from the line it falls off as  $\frac{1}{r^2}$ . The asymptotes (25) and (26) are plotted in Fig. 19 for various values of  $d$ . Magnetic flux density

$$B = \mu_0 H$$

is plotted instead of field strength.

For comparison, one plot is shown of the flux density variation along a line perpendicular to the plane of the conductors midway between them. This is the field for  $x = 0$ :

Figure 19 Flux Density from Parallel Conductors



$$H_x(x = 0) = \frac{Iy}{2\pi} \left[ \frac{1}{y^2 + \frac{d^2}{r}} \right] = 0$$

$$H_y(x = 0) = \frac{Id}{2\pi \left( y^2 + \frac{d^2}{4} \right)}$$

which becomes

$$H \approx \frac{2I}{\pi d} \quad \text{for } y \ll d \quad (27)$$

and

$$H \approx \frac{Id}{2} \quad \text{for } y \gg d \quad (28)$$

i.e. the field is constant with distance from the line, close to the line, but assumes a  $1/y^2$  variation far from the line, the same upper asymptote as Eq. 2.

Thus, Eqs. 25 and 26, as plotted on Fig. 19, represent estimates of the worst case field from the line.

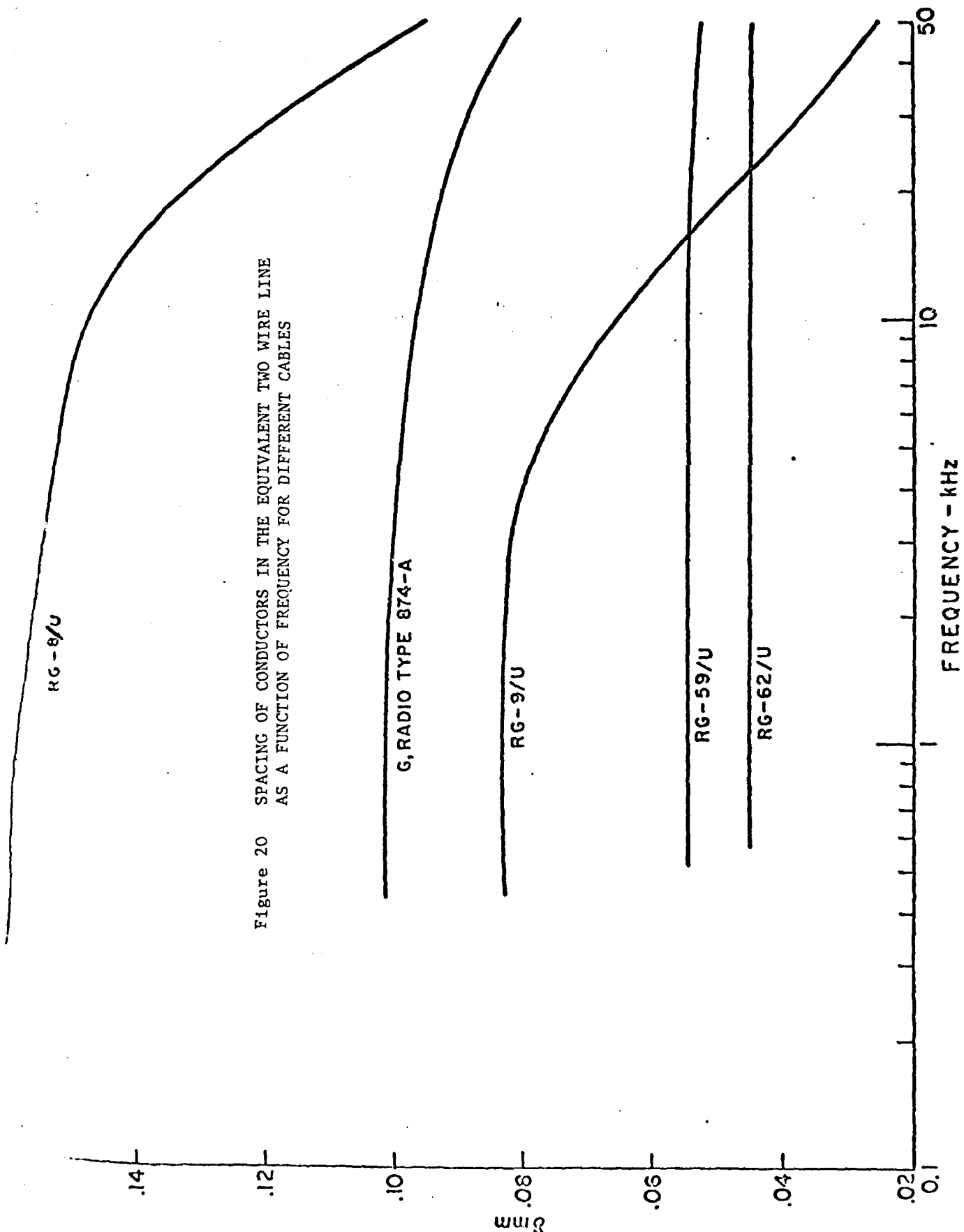
### 2.3.3.2 Application to Coaxial Cables and Common Mode

#### Coaxial Cables

The magnetic field from a differential mode current flowing in a coaxial cable results from the fact that the center conductor is not exactly in the center of the cable. Thus, it and the image of the shield are displaced by a distance  $\delta$ . Values of  $\delta$  for several common types of coaxial cable are shown in Fig. 20 [6]. The coaxial cable is thus effectively a parallel-wire line of separation  $\delta$  and the field from it may be computed by setting  $d = \delta$  in the above equations or in Fig. 19. This has been verified experimentally [7].

#### Common Mode

The "total" or "net" current flowing in all conductors in a cable (taking due account of direction and phase) is the "common-mode" current. If its value is other than zero the return current usually flows in the ground plane. Then the cable and its image in the ground plane form a parallel-wire line with separation  $d = 2 \times$  height above ground plane (Fig. 21). The field in such cases may, therefore, be calculated by using this value of  $d$  in the above equations.



### 2.3.3.3 Twisted Pair Cable

The maximum flux density radiated from a twisted pair cable of pitch  $p$  and conductor separation  $d$  a distance  $r$  away is given by [8] and [6].

For  $r \ll \frac{p}{3}$ , use parallel wire line model

$$B = \frac{\mu_0 I d}{2\pi r(r+d)} \quad (29)$$

For  $r \gg \frac{p}{3}$ ,

$$B = \frac{\mu_0 I}{\sqrt{pr}} \left( \frac{2\pi d}{p} \right) I_0 \left( \frac{2\pi d}{p} \right) e^{-2\pi r/p} \quad (30)$$

where

$I_0(x)$  = zeroth order modified Bessel function of the first kind.

The ratio of flux density for a twisted pair line to that of a parallel wire line is plotted as a function of  $r/p$  in Fig. 22. This ratio may be used to estimate the maximum flux density from a twisted pair line by correcting the values of the parallel-wire line by correcting the values of the parallel-wire flux density in Fig. 19 by this factor. The value used for  $d$  in Fig. 21 is the separation of the two conductors.

The twisted pair model can be easily extended to a twisted triad [9]. The work has been carried out for various cables. Examples for TNW type cables are shown in Fig. 23, which show for each cable the magnetic flux density as a function of distance from the cable when it is carrying its maximum rated current (shown on each curve).

Similar data are shown for type DSGA cables on Fig. 24.

### 2.3.4 Electric Sources

At the higher frequencies, say above 100 kHz, the electric field strength radiated from a cabinet or cable may become the dominant component of an interference signal affecting a particular susceptible device. Models have been derived to relate these fields to source parameters [2], [10].

#### 2.3.4.1 Models

The models used in predicting electric field strength from a given source depends upon the configuration of the source case and the power cable connected to it, and the ground plane. In general, the electric field is due to the common-mode current flowing in the power conductor. If the case is isolated from ground then the field is due to the electric

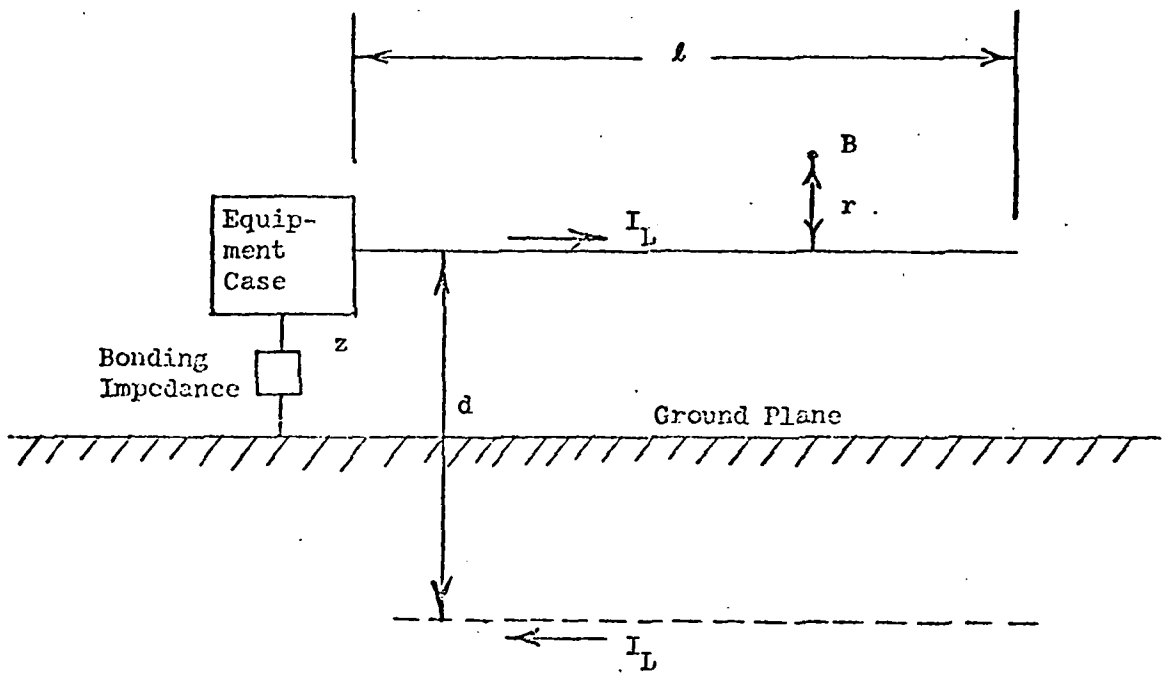


Figure 21 Common-Mode Radiation Model

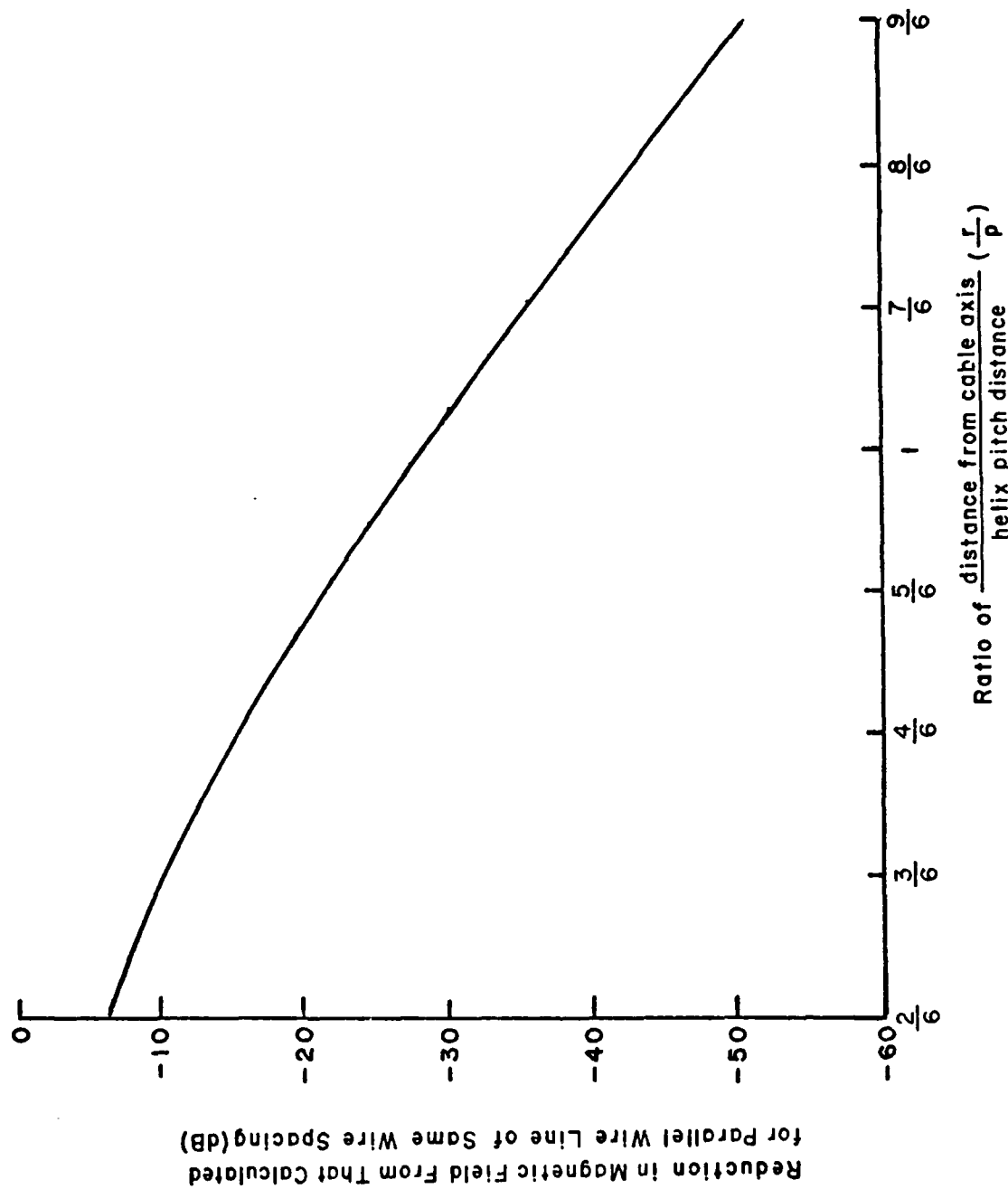


Figure 22 Correction Factor for Estimating Field From Twisted Pair Cables

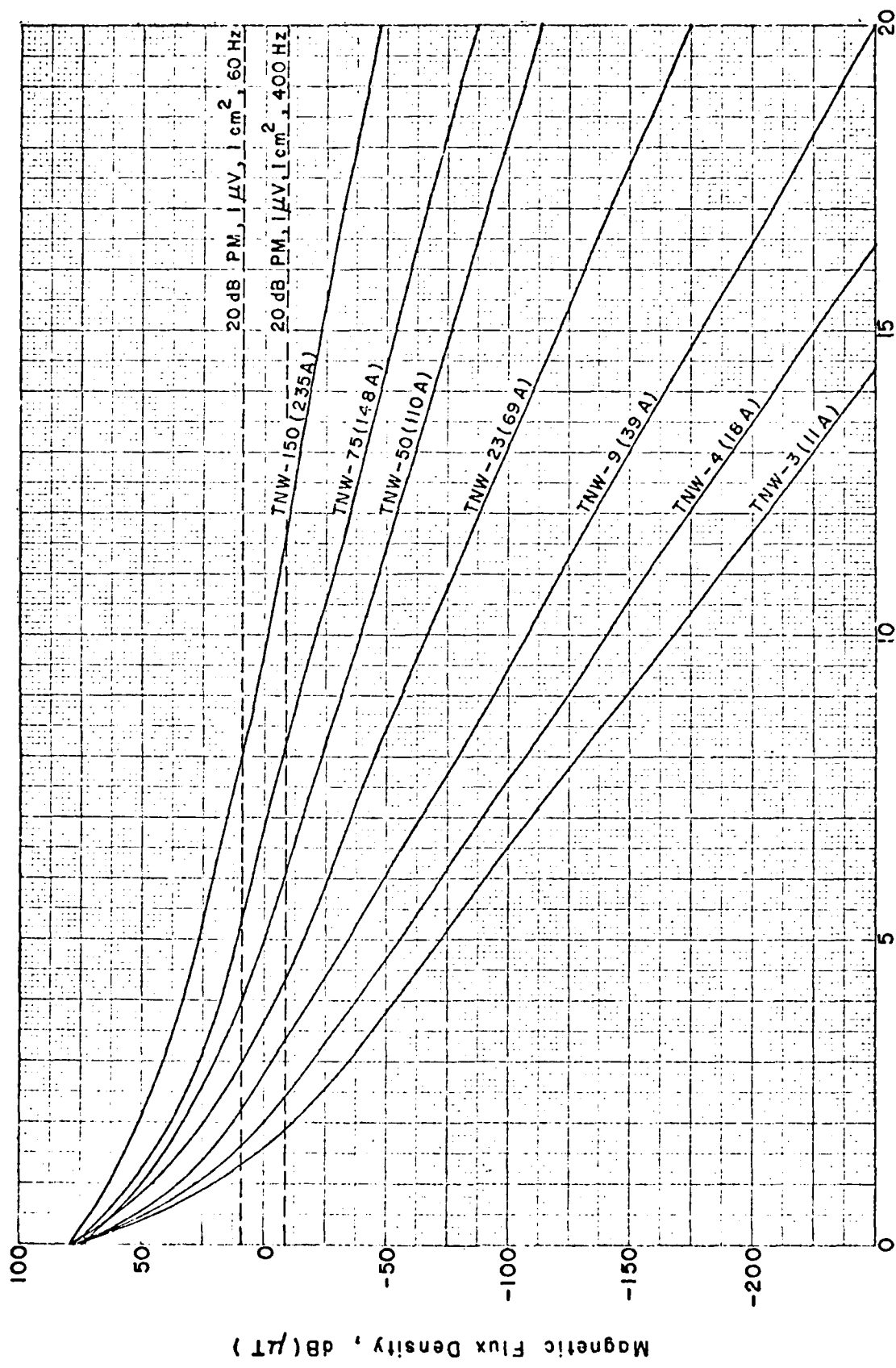


Figure 23 Magnetic Field Emissions From "TNW" Cables

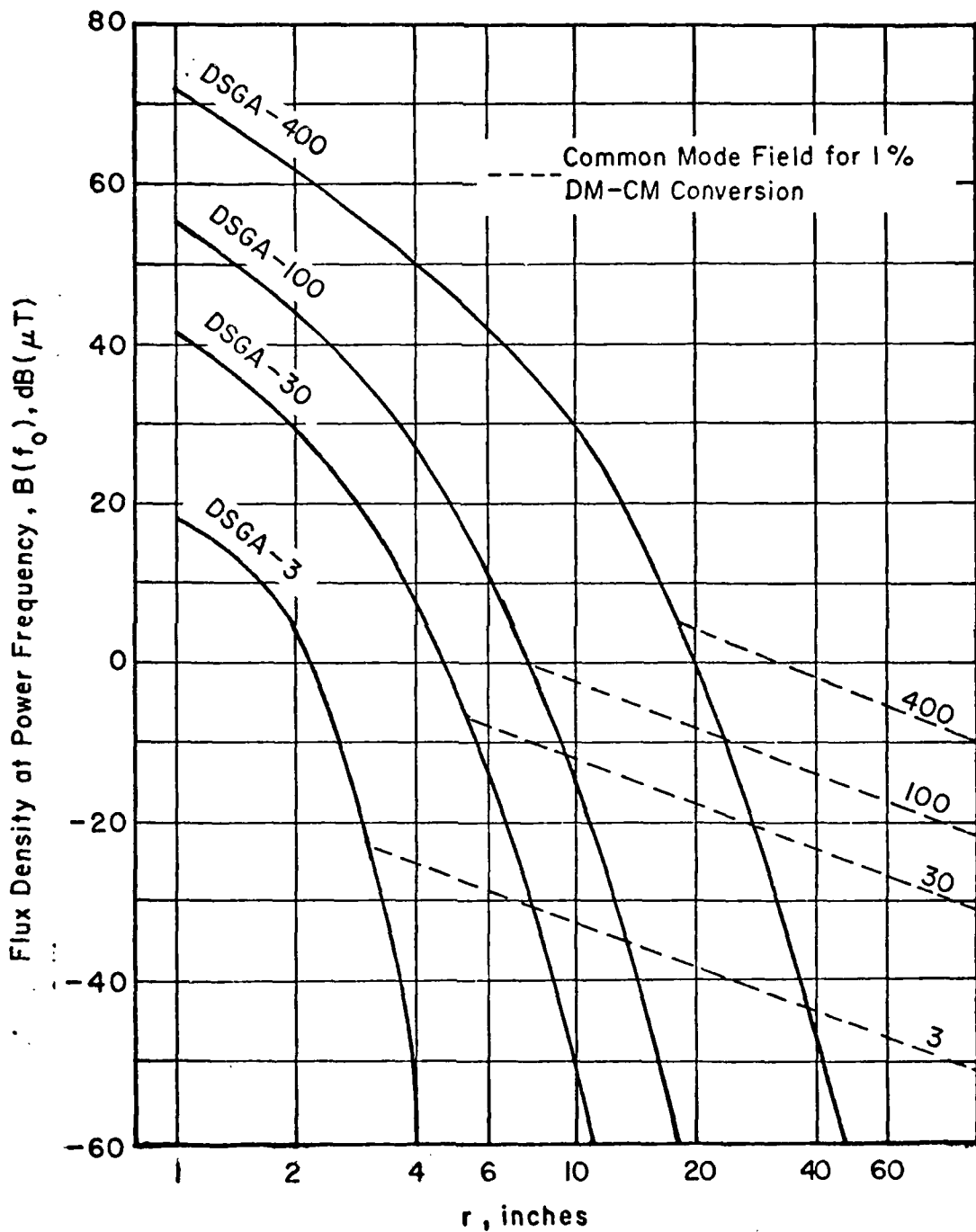


Figure 24 Fundamental Frequency Flux Density From Cables Carrying Recommended Limit Currents

dipole it forms with its image in the ground plane. If the case is well grounded, then the source is modeled as a magnetic dipole or parallel-wire line, depending on the separation of the power cable from the ground plane (see Fig. 25). These statements and the specific details that follow have been supported by experimental work as reported in [10].

#### Electric Dipole Model (Fig. 25(a))

The electric field strength from an electric dipole is given by

$$E_\theta = \frac{M_e \beta^3}{4\pi\epsilon_0} \left[ -\frac{1}{j\beta r} + \frac{1}{(\beta r)^2} + \frac{1}{j(\beta r)^3} \right] \sin \theta \quad (31)$$

$$E_r = \frac{2M_e \beta^2}{4\pi\epsilon_0 r} \left[ -\frac{1}{j\beta r} + \frac{1}{(\beta r)^2} \right] \cos \theta \quad (32)$$

where

$$\beta = 2\pi/\lambda$$

$\lambda$  = wavelength

$$M_e = \text{dipole moment} = \frac{Ih}{2\pi f}$$

$I$  = common-mode current

$h$  = dipole height = 2 × height above ground plane

$\theta$  = vertical angle of point at which the field is calculated, from dipole axis

$r$  = distance from center of dipole to point at which field is calculated.

This model applies when the device contains no external ground other than the power cord.

#### 2.4 Immunity Models

##### 2.4.1 Bandwidth Considerations in Susceptibility Estimation

In making a prediction of the effect of a given source on a particular susceptor, one must determine the susceptor's susceptance bandwidth. There is no difficulty if the source has only a single dominant frequency component which falls within the acceptance bandwidth of the susceptor. In that case a susceptibility threshold can be calculated directly from measurement of single frequency sensitivity characteristics of the device. For a broadband source having a spectrum that is relatively

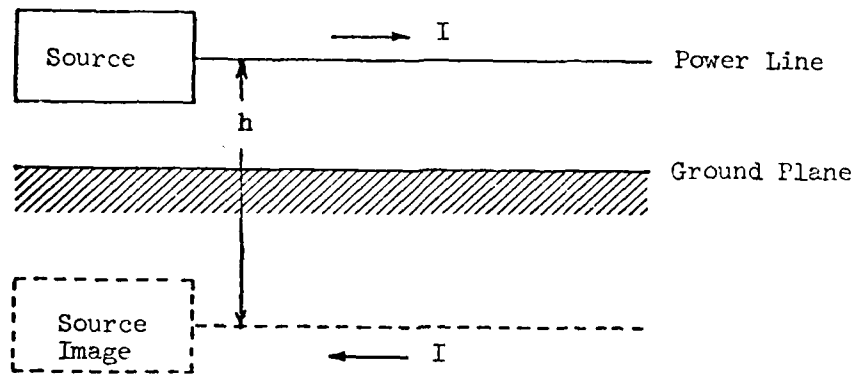


Figure 25(a) Electric Dipole Model - Source Case Isolated from Ground

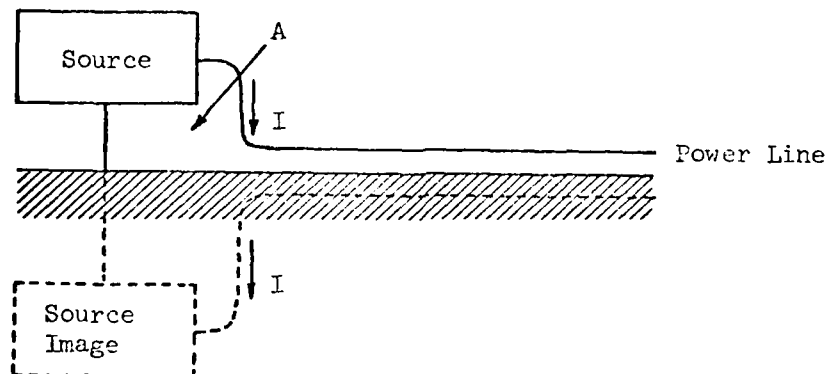


Figure 25(b) Magnetic Dipole Model - Source Case Grounded, Power Line Close to Ground Plane

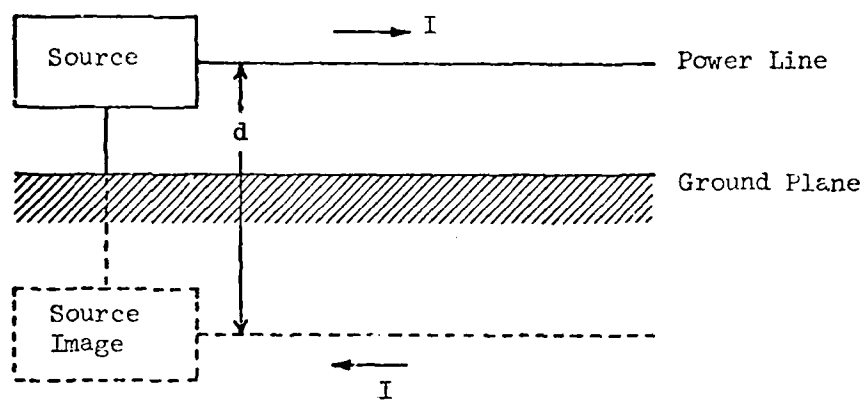


Figure 25(c) Parallel-Wire Model - Source Case Grounded,  
Power Line away from Ground Plane

flat over the acceptance bandwidth of the susceptible device, the procedure is also fairly straightforward; the spectrum amplitude is multiplied by the acceptance bandwidth of the device in order to get equivalent peak input voltage to the device.

The situation is more complicated when one has a source with a number of discrete components which lie within the acceptance bandwidth of the device. In this case, one must find out how the several components add together to produce susceptibility. This may or may not be a simple procedure. Thus, whether or not the phenomena which are being considered are to be considered as narrowband or broadband phenomena depends not only upon the characteristics of the source, but also upon the characteristics of the receiver as a susceptible device.

It is customary in interference prediction work to try to distinguish between strictly narrowband phenomena, i.e. we assume that a source with a discrete spectrum interferes with a possible susceptor through the mechanism of its sensitivity to single-frequency components, and that a source with a wide band or continuous spectrum interferes with a possibly susceptible device as a result of its sensitivity to broadband or continuous signals. This procedure simplifies the calculations, but does not necessarily take into account all of the possible interaction mechanisms. Its validity is dependent upon particular source and receiver or susceptor characteristics. There is no specified procedure for evaluating the more complicated cases; investigators are simply warned to be on the alert for the necessity to be concerned about this matter.

#### 2.4.2 Wire Loops

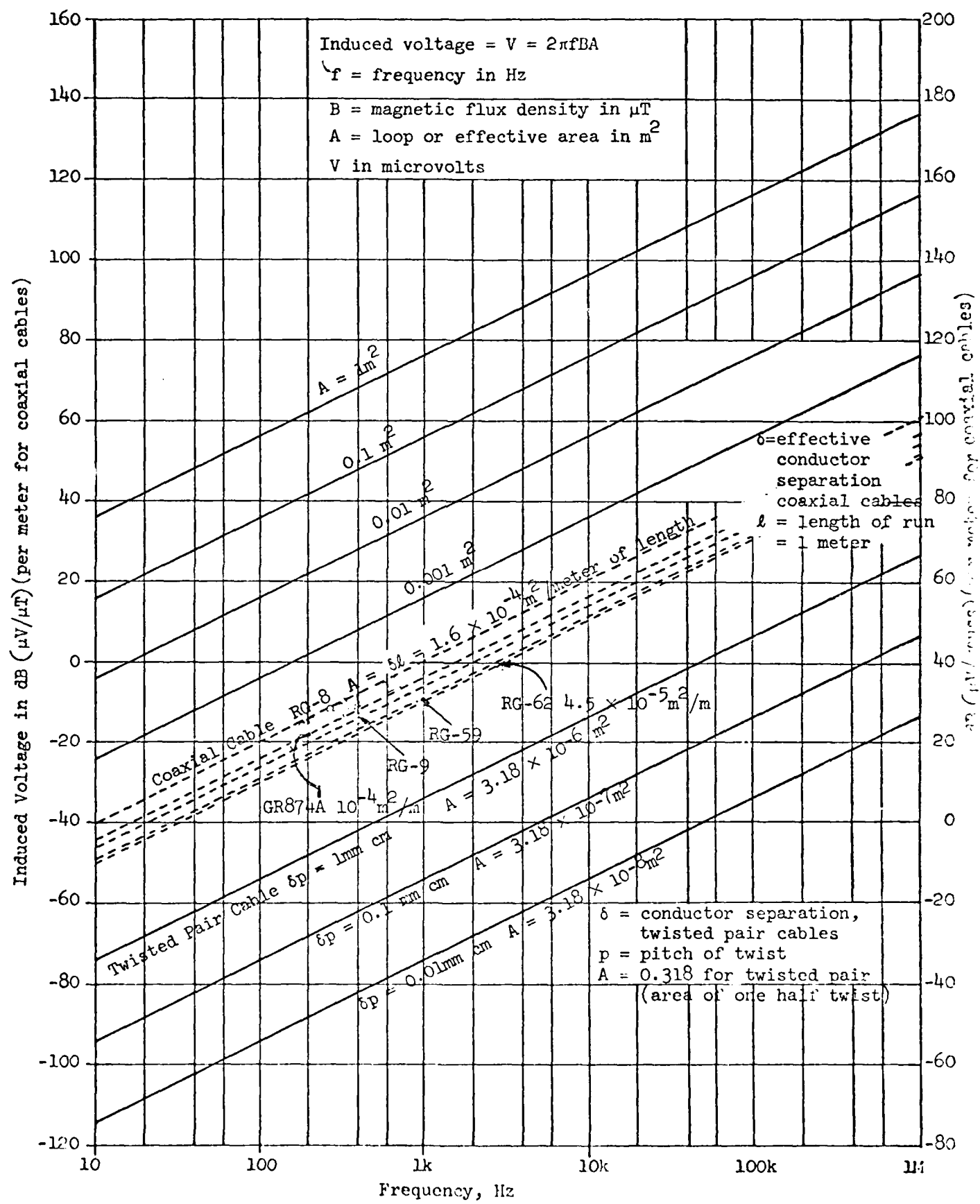
The voltage induced in a closed loop of wire by a magnetic field  $B$  is computed by Faraday's law:

$$V = \frac{d\phi}{dt} = \omega AB \quad (33)$$

where  $\phi = AB$  is the total magnetic flux linking the effective area  $A$  of the loop,  $B$  is the magnetic flux density, assumed uniform over  $A$ , and  $\omega$  is the radian frequency at which  $V$  is to be calculated. For narrowband interference,  $V$  and  $B$  are the amplitudes of the sinusoidal variations. For broadband interference, they are the spectral densities at frequency  $\omega$ .

The effective value of  $A$  can vary widely from one situation to another. To provide high immunity,  $A$  should be as small as possible, which in the case of sensitive input circuits requires maintaining a close spacing between the "hot" conductor and its return conductor. In some cases these leads have been known to have been routed on opposite sides of equipment cabinets. Where integrated circuit cards are used, a worst-case assumption would be that the area is equal to the card area. Figure 26 is a nomograph giving, for particular values of area  $A$  in square meters, voltage induced in dB with respect to a microvolt per microtesla of flux density as a function of frequency.

Figure 26 Cable and Loop Susceptibility



### 2.4.3 Cable Susceptibility

The effective area  $A$  depends on the cable. For a parallel wire line of length  $l$  and separation  $d$ ,

$$A = ld \quad (34)$$

For a coaxial cable of length  $l$  and eccentricity  $\delta$

$$A = l\delta \quad (35)$$

For a twisted pair cable it has been found that a good approximation to the voltage induced is that induced in one-half twist, so that the effective area for a cable of pitch  $p$  and separation  $d$  would be

$$A = 2 \times \frac{2}{\pi} \times \frac{d}{2} \times \frac{p}{2} = 0.318 pd \quad (36)$$

assuming a sinusoidal projection of the helical conductors [6].

The above formulas apply for the differential mode. For the common-mode voltage generated in a cable of length  $l$ , a distance  $h$  above the ground plane,  $A$  is the area of the ground loop, or

$$A = hl \quad (37)$$

It must be remembered in applying Eqs. 33 to 37 that this simple model assumes that the field is uniform over the effective area  $A$ , and that the cable is oriented for maximum pickup. If the maximum flux density in  $A$  is taken as the value of  $B$ , then  $V$  will be a conservative estimate.

For the twisted-pair cable model to be accurate,  $B$  must be uniform over the length of the cable. If this is not the case, then the voltages generated in successive half-loops will not necessarily cancel, thereby possibly increasing the effective area and the net voltage induced. In such cases, the effective area may be considered bounded by Eqs. 36 and 34, and the induced voltage may be assumed to be in a range consistent with those areas.

Figure 26 shows, for various cables, the voltages induced. In the case of coaxial cables the voltages are given per unit length since the voltage is proportional to the length subjected to the flux density. In the case of twisted pair cables the voltage is that induced in a single half loop in accordance with earlier discussion.

PART II

METHODOLOGY IMPLEMENTATION

### 3.0 METHODOLOGY FOR EMC PREDICTION AND ANALYSIS

The following procedure is recommended for organizing and carrying out EMC prediction and analysis work in a large system. It is based upon the concept that if the components of that system are built according to a specific set of emission and susceptibility standards, and are installed in accordance with a complementary set of installation procedures, such a system will be inherently compatible in so far as unintended radiation and susceptibility are concerned. However, since intended emissions may be quite large, and cannot be restricted in the same way as unintended emissions, and since frequently design sensitivities also must be higher than unintended susceptibilities, these must be taken into account.

The majority of possible interactions between electromagnetic emitters and electromagnetic "susceptors" will not necessarily be required to be subjected to detailed analysis. Detailed analyses may be necessary in the cases of those components which do not meet the emission and susceptibility standards and in those cases where the installation practices cannot be adhered to. Thus, one objective of this technology is to eliminate the detailed analyses in those cases for which it can be anticipated that the probability of degrading interaction is extremely low or zero.

The method to be described can be carried out either manually using graphical overlays, or analytically, using computer programs to perform the necessary comparisons. The major advantages of using a computer program over the manual technique is that it provides (1) an organized procedure for carrying out the analysis, (2) a readily accessible data bank, and (3) rapid analysis, using the most suitable models, or a comparison of two or more models.

#### 3.1 System Breakdown

For the purpose of evaluating the overall system performance, one might be tempted to divide the system into subsystems. The basis for this breakdown may be technical or administrative. Since most overall systems are procured on the basis of separate subsystems, from the point of view of fixing responsibilities for equipment characteristics, the subsystem division may be most convenient. Presumably, subsystems should be compatible within themselves before they are assembled into the overall system. Hence, one would be primarily concerned with incompatibilities between subsystems in evaluating the overall system performance.

A subsystem can be made up of many parts, for example, the external communications subsystem has among its components a VLF receiver, a VLF antenna, a multicoupler, other radio receivers with similar associated components, and auxiliary equipments for data recording and analysis. As a practical matter, the modeling techniques which have been developed really apply to "black boxes" and interconnecting cables, and accordingly each of the elements of the external communication subsystem have to be considered for emission and susceptibility characteristics. Furthermore, in most cases parts of various subsystems may be intermixed in a given location because of

designed operational interactions, hence detailed emission data on components within subsystems are required. In particular, for below-decks configurations, a more reasonable breakdown is by compartment. Generally, compartments are isolated from each other by barriers that are impervious to electromagnetic waves, although they can be coupled electromagnetically by common cables running through them. Such coupling should be accounted for in cable analysis.

### 3.2 The Protection Margin

The method of calculating the protection margin is illustrated in Fig. 27, where  $S$  represents the interference signal level,  $S'_{\text{source}}$  is that at the source,  $S_{\text{source}}$  is that presented to the susceptor, computed by use of an appropriate coupling model, and  $S_{\text{susc}}$  is the susceptibility level.

If the susceptibility level is very much higher than the corresponding emission level,  $S_{\text{source}}$  (after correction for the coupling factor between any two subsystems of concern), it is unlikely that degraded performance will result. On the other hand, if the relative magnitudes are reversed, then unless there is a substantial isolation between the two subsystems that is not otherwise taken into account, there can be substantial degradation in the performance of the overall system. The difference between the susceptibility level and the source level is defined as the protection margin. Obviously, one is interested in having the protection margin as large as is necessary to assure no degrading interaction.

#### 3.2.1 Mechanisms of Interference

Five classes of potentially interfering interactions are defined:

1. case-to-case (radiation, both electric and magnetic)
2. case-to-cable
3. cable-to-cable
4. cable-to-case
5. direct conduction

For each conductive mechanism, or for mechanisms involving coupling from or to cables, it must be recognized that both differential and common modes must be considered.

Appropriate coupling models, to arrive at the protection margins for each of the above interference mechanisms, are indicated in the flow chart of Fig. 28.

The protection margins computed will, in general, be a function of frequency; however, if only a single value is stated it is the minimum value over the frequency range.

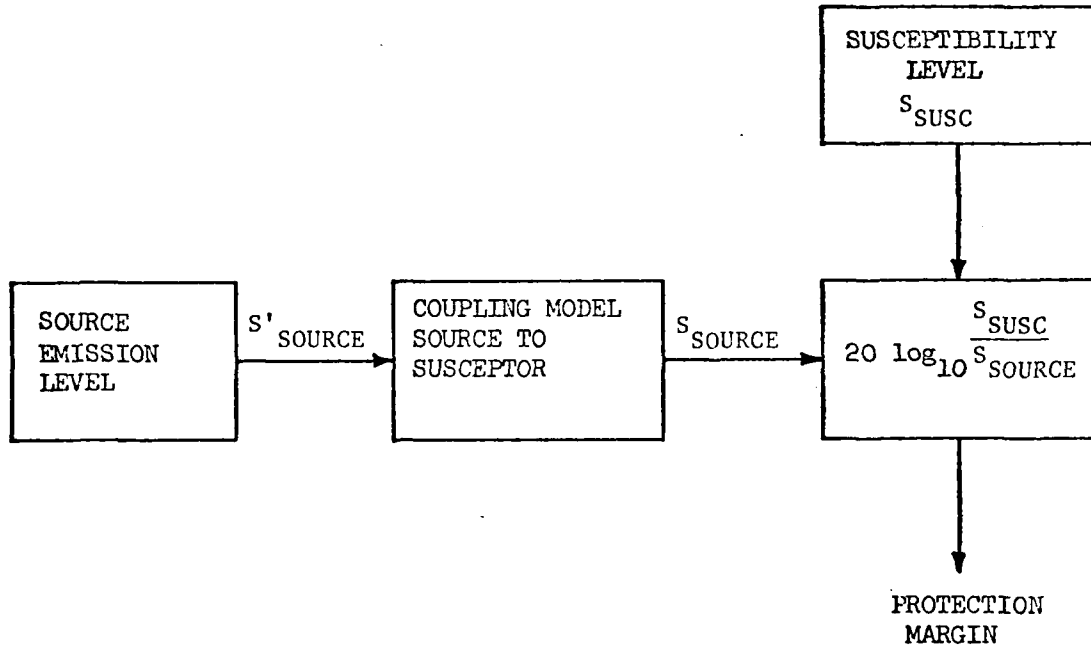


Figure 27 PROTECTION MARGIN COMPUTATION

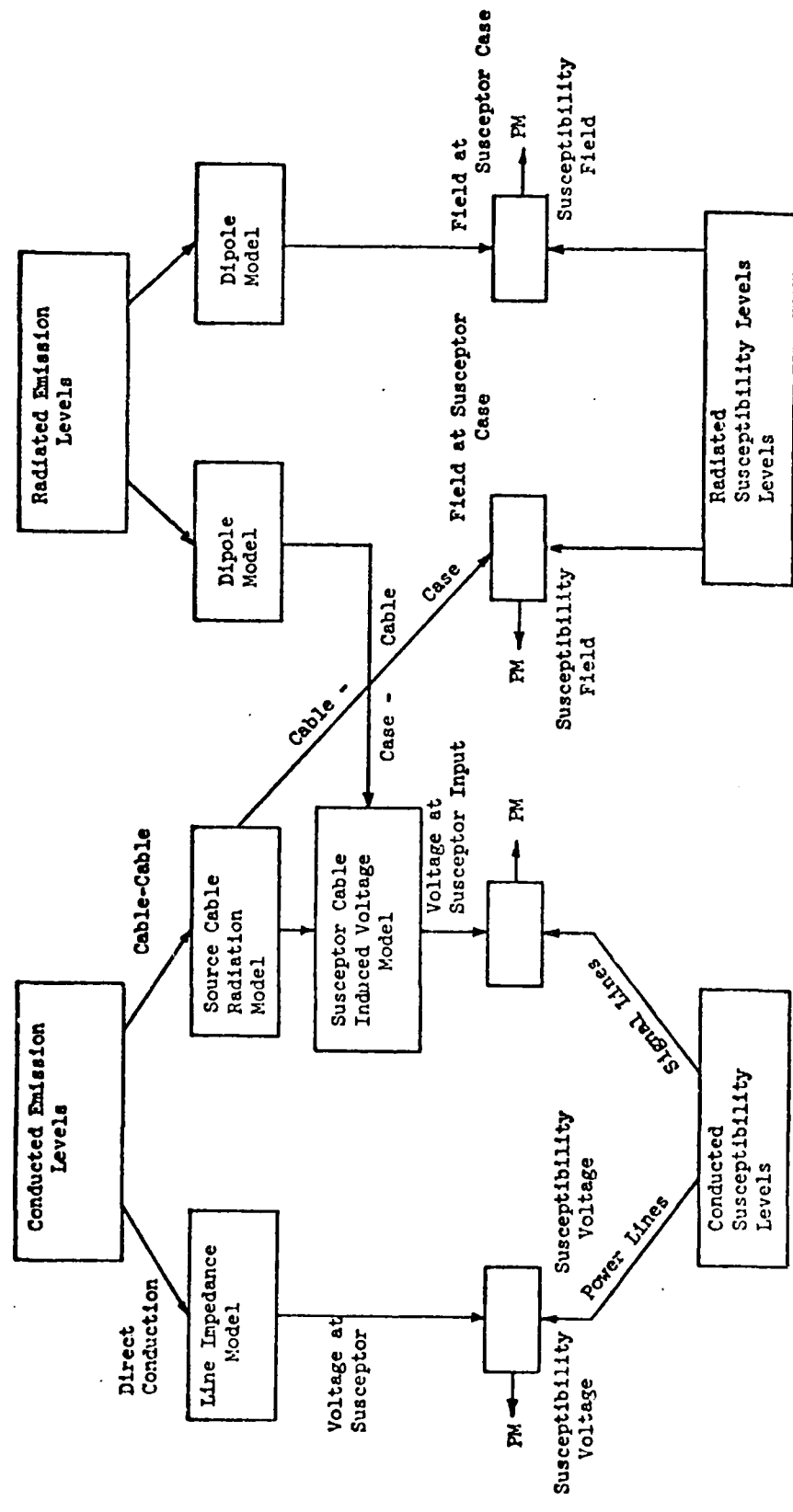


Figure 28 Protection Margin Computation

Figure 29 shows one form of a protection margin chart in which all interactions are considered to occur on a "pair-wise" basis, i.e. the evaluation is made of each interaction as though it occurred between one emitter and one susceptor at a time. Thus, one establishes, for each susceptor, susceptibility levels for conduction in both differential (DM) and common (CM) modes and for radiation both for magnetic and electric fields, and these levels are entered in the four blocks on Fig. 29 immediately below each susceptor listed along the top of the chart. Corresponding levels for each emitter are entered immediately to the right of each emitter listed along the left-hand side. In the four blocks which appear at the intersection of a row corresponding to a particular emitter and a column corresponding to a particular susceptor one can then enter the four values of protection margin for each type of interaction when properly corrected for any isolation, for example, filters in the case of conduction or distance in the case of radiation.

It should be noted that the pair-wise concept is really valid only for "radiation" interactions, i.e. cabinet-to-cabinet, or cable-to-cabinet magnetic and electric field interactions. The reason for this is that generally magnetic field attenuation with distance from the source is quite rapid, and two sources are unlikely to both produce an equally significant interaction on the same susceptor at the same time.

On the other hand, with conduction interactions, especially by means of the ac power cable, the effect of multiple sources in producing, for example, harmonic voltages, is usually cumulative, so that the entire power system configuration must be used to determine the harmonic levels at particular points of connection of susceptible equipments.

The procedures for computation are detailed in section 5 of this report.

### 3.3 Limit Setting Philosophy

By controlling each mechanism of interference with appropriate emission and susceptibility limits, compatibility can be assured if the installation conditions under which the limits were specified are met. These conditions include such factors as maintenance of minimum protection distances between high-level cables and susceptor cases and sensitive cables, proper grounding and shielding techniques, and balanced power lines at low frequencies (i.e., reducing common-mode currents).

To implement this concept one makes use of models for emission, coupling, and susceptance in order to identify appropriate limit levels.

### **4.0 NOMINAL LEVELS**

In the application of the methodology in general, and the calculation of protection margins in particular, it has been found convenient to apply the concept of "nominal" levels of emission and susceptibility. The levels are chosen so as to represent values of voltage, current, or field that might be expected to characterize typical equipments which just meet compatibility

Figure 29 SES INTERACTION CHART

	Suscep-tors →		LFE	Sonar Preamp.	Sonar F/E/C	Power Line Filter	Power Trans-former	DPS Clock Pulse (BB)	Switch-board
Sources ↓	DM	CM							
	H	E	+34	+34	+34				
LFE									
Sonar Preamp.									
Sonar F/E/C									
Power Line Filter	+4.5		0 29.5		0 29.5		0 29.5		
Power Trans-former	+26		0 8		0 8		0 8		
DPS Clock Pulse (BB)	+ 8		0 26		0 26		0 26		
Switch-board	+ 24		0 10		0 10		0 10		
60 Hz Power	0 0		0		0		0		
	0 0		34		34		34		
400 Hz Power	0 0		0		0		0		
	0 0		34		34		34		
2500 V Power Line Pulse(BB)	+84		0		0		0		
	+53		-19		-19		-19		

requirements under specified installation conditions. The nominal level concept is of particular assistance in performing a rapid cull function so as to identify those interactions unlikely to result in negative predicted protection margins. In the following the rationale leading to selected nominal levels is described in each case. In section 5 of this report, their application in protection margin calculations is described.

#### 4.1 Conducted Emissions, Differential Mode

At low frequencies, up to 20 kHz, an important source of interference is the generation of harmonics of the power frequency, in particular by devices such as rectifiers which place a nonlinear load on the power line. These harmonics can be coupled to potentially susceptible devices either by radiation from the line or by direct conduction on the line.

The harmonic levels are not easy to control. The number of harmonics present can be reduced by using multiphase power supplies, which are more complex and costly than a typical 6-phase supply, and filters may be employed. But simple filters that are effective below about 10 kHz may not be available. For these reasons, an attempt is made to accommodate the harmonic levels which are produced.

As discussed in paragraph 2.2.2., rectifier harmonic current levels generally can be expected to be directly proportional to the power frequency current level. Consequently, the "nominal" level of conducted emissions should take the fundamental current into account. Such a tailored or "per ampere" limit has the advantage over a fixed limit in that it is a more realistic interpretation of the actual emissions from a particular device.

The tailored limit\* is equal to the device's load current at the fundamental frequency (60 or 400 Hz) decreasing as  $1/f^n$ ,  $n \geq 1$ , at frequencies  $f$  above the fundamental. In paragraph 2.2.2 it is indicated that a reasonable worst-case value of  $n$  is 1 for a rectifier load with an inductive-input filter.

This  $1/f$  decrement is maintained up to the frequency range at which measured emissions cease to be characterizable as power line harmonics. Available data appear to indicate that this occurs in the 20 kHz to 1 MHz range. In this range, therefore, it seems reasonable that a transition should occur from a tailored limit to an absolute limit, i.e., one that is constant for all devices. The level of this limit could be the level of the present MIL-STD-461 limit at the high frequency end.

A limit curve corresponding to these concepts is shown in Fig. 30.

#### 4.2 Conducted Susceptibility Limit, Differential Mode

A conducted susceptibility limit consistent with the conducted emission limit of Fig. 30 may be derived by calculating harmonic voltage levels expected to appear on typical power networks by utilizing methods described in Ref. 12. In this technique, one essentially assumes that the current at the emission limit flows through the equivalent line impedance,

---

\* The concept of a tailored limit was developed at the Underwater Systems Center, New London, CT, and the limits shown on Fig. 30 were developed there.

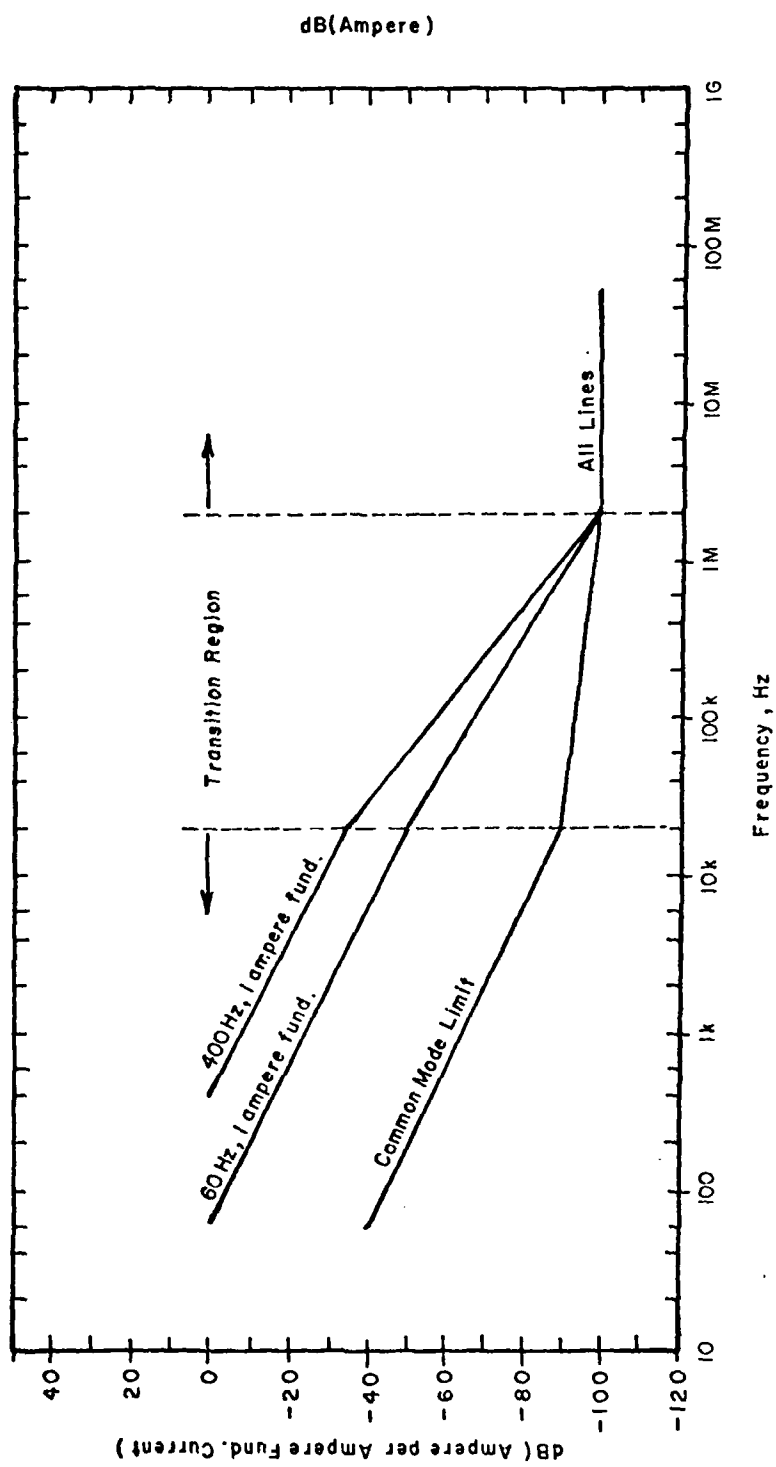


Figure 30 Conducted Emission Limits

generating a voltage which is coupled directly to the susceptor.

$$V_{\text{susc}} = I_{\text{limit}} Z_{\text{line}} \quad (38)$$

The values of harmonic current and equivalent line impedance tend to be reciprocally related. A simplified model for calculating harmonic voltage levels is described in paragraph 2.2.2.1. There it is shown that the harmonic levels may be approximately constant as the harmonic order is increased up to a certain point, and to decrease above that. Calculations on actual systems show that this concept is correct, but that harmonic levels can be as high as 5% of the line voltage. For this reason the "nominal" level is taken as 5 volts out to a frequency of 1 kHz, decreasing to 1 volt at 3 kHz and remaining at 1 volt above that as shown on Fig. 31. Although normally harmonic levels will be less than 1 volt in the 10 kHz to 100 kHz range, experience has shown that it is not difficult to obtain that level of susceptibility.

The radiated field from a cable carrying the limit current of Fig. 30 may be readily calculated once the conductor separation, pitch of twist, and distance from the cable are specified. The voltage induced in a susceptor cable depends on this field, on the effective area of the susceptor cable, and on the frequency.

Taking the above considerations into account, a radiated field limit can be specified as the field at a given distance from a power line of a certain capacity. For a six inch separation from a DSGA-100 twisted cable, carrying 1 ampere per 1000 circular mils or 100 amperes, the limit shown in Fig. 32 results. This field is calculated by assuming differential mode currents flowing at the per-ampere limit of Fig. 30 below 20 kHz.

Below 20 kHz, the limit of Fig. 32 will cause a 40 nV signal to be induced in typical low-level cables such as 2SA, 2SWF, etc., having an effective area of 0.046 in<sup>2</sup>.

For other types of power lines, to produce the same field as that produced by the DSGA-100 cable while carrying the per-ampere limit current of Fig. 30, the distance at which the Fig. 32 field occurs changes in accordance with the current-carrying capacity of the cable. That is, the distance from the line must be increased with the current capacity of the line in order to maintain the same induced voltage or field strength at the susceptor. The variation of this distance with line capacity is shown in Fig. 33 for DSGA-type power cables. The curve in Fig. 33 labeled "60 Hz lines" is the one corresponding to the limit in Fig. 30 for 60 Hz lines, while that labeled "400 Hz" corresponds to the limit in Fig. 30 for 400 Hz lines. Protection distance must be increased for 400 Hz lines due to the fact that the 400 Hz current limit (Fig. 30) is more relaxed than that for 60 Hz lines.

#### 4.3 Application to Cabinet Emissions and Susceptibility

The limit on magnetic flux density shown in Fig. 32 is also applied to radiated emissions from cabinets. Also, the same protection distance

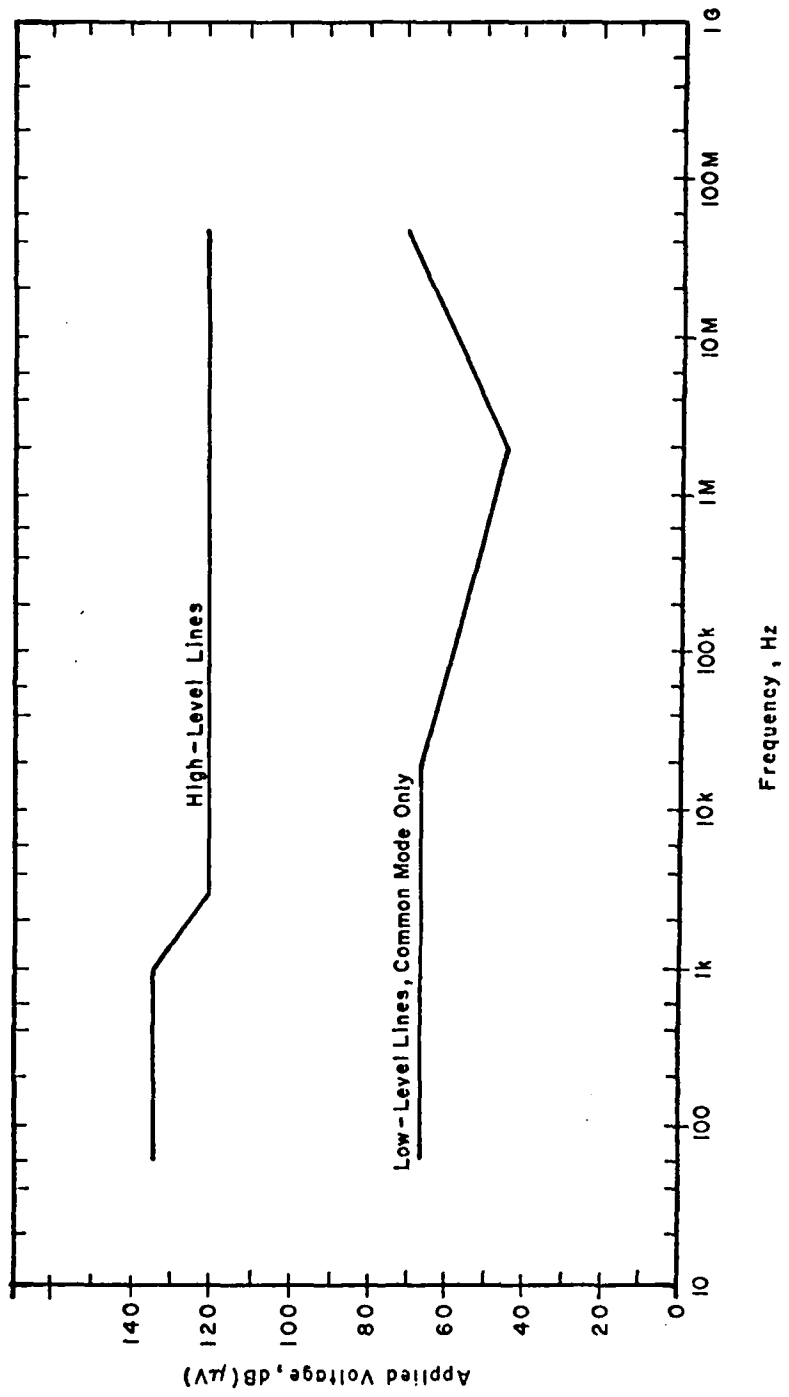
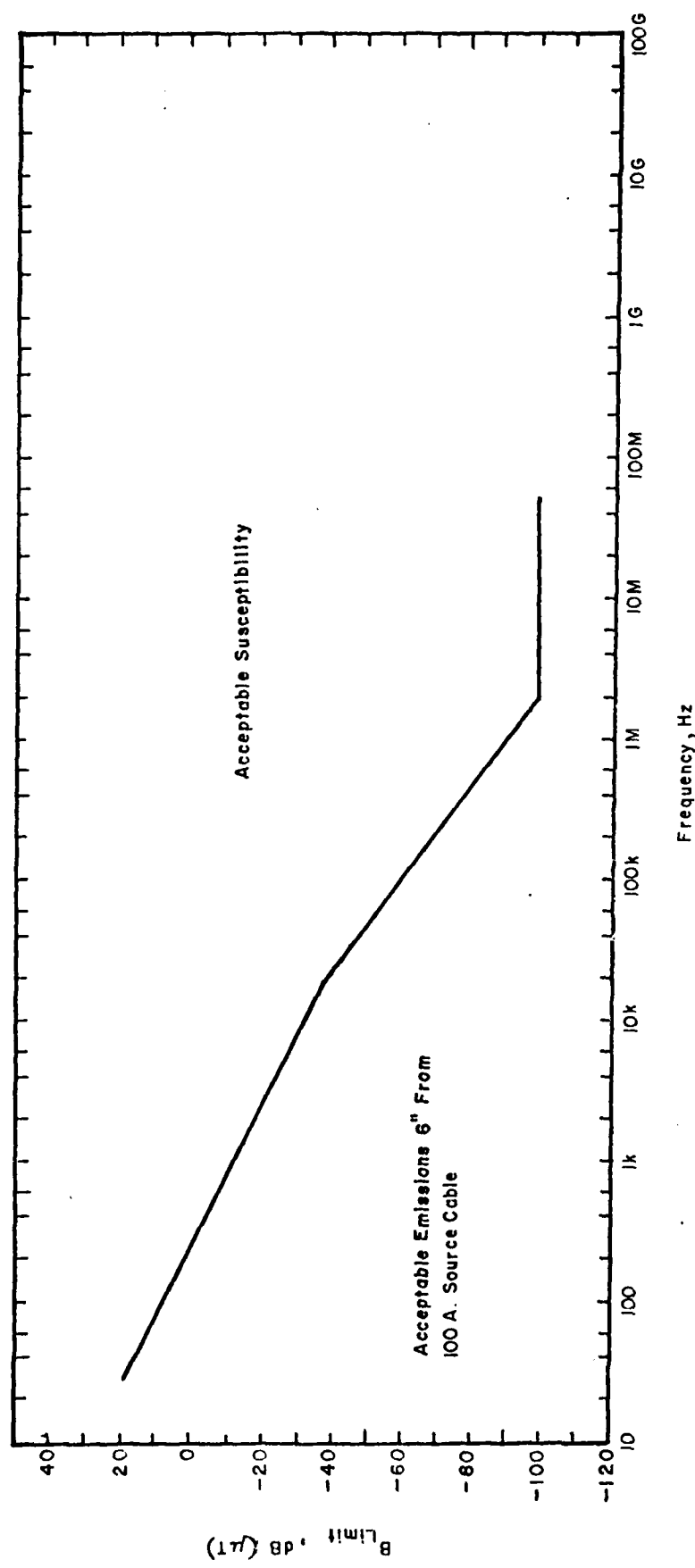


Figure 31 Conducted Susceptibility Limits



**Figure 32 Magnetic Field Limits**

applies to cabinet emissions as applies to the power line supplying the cabinet. Thus, a source drawing 10 amperes of 60 Hz power would have to produce radiated emissions falling below the limit of Fig. 32 at a distance equal to the protection distance for a 10 ampere line. From Fig. 33 this is seen to be of the order of 2-1/4 inches.

A susceptor which does not experience intolerable performance degradation when subjected to magnetic fields given by the limit of Fig. 32 is then protected from fields from sources down to the minimum protection distances given by Fig. 33.

#### 4.4 Common-Mode Emission

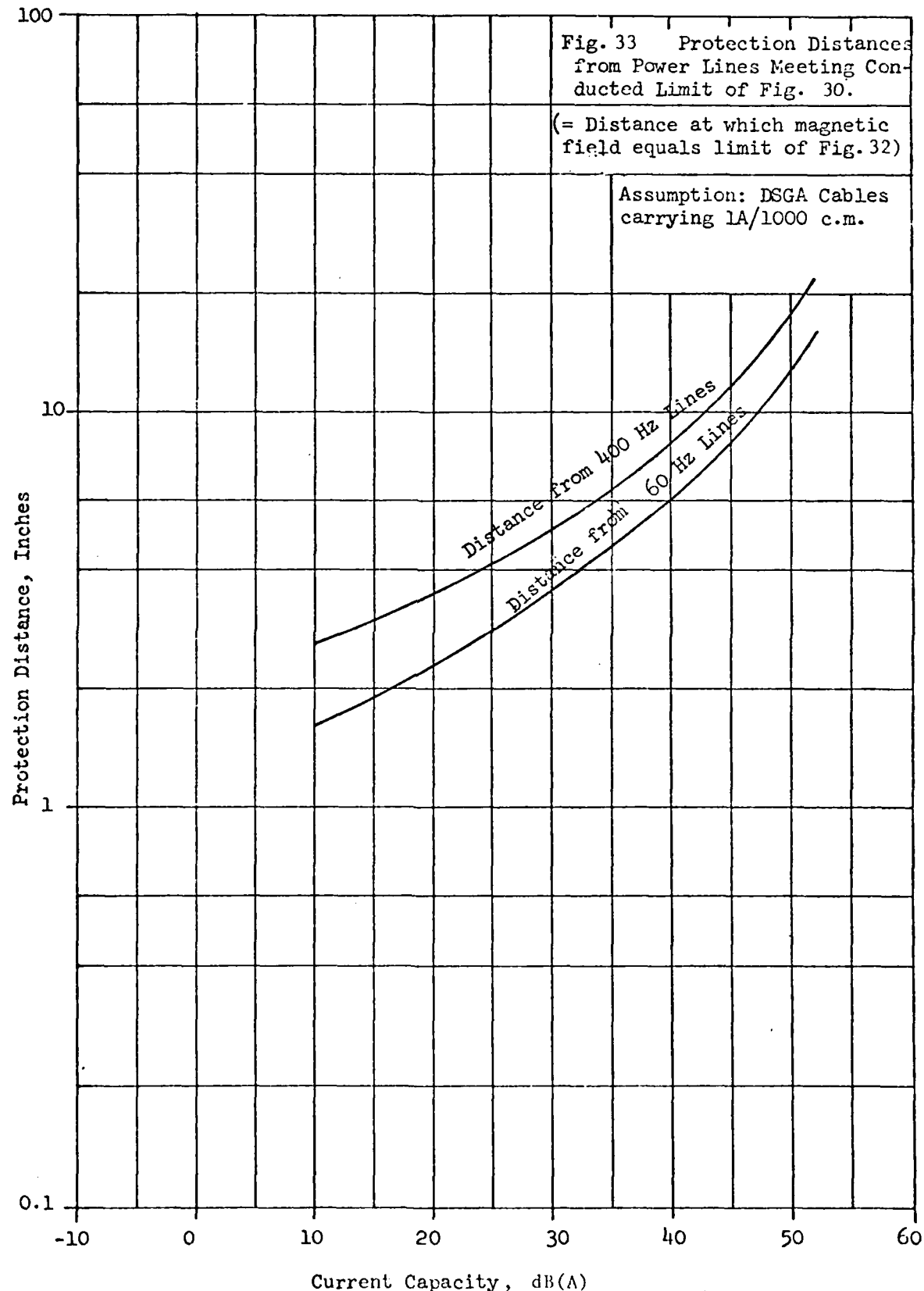
One criterion on common-mode current is related to the magnetic field it produces in the vicinity of a cable carrying it. The objective is to limit that field to the field produced by differential-mode current in the same cable at the protection distance for that cable. Thus, in the frequency range below 20 kHz, the allowed current will decrease as the reciprocal of the frequency. It is found empirically that this condition is fulfilled if the common-mode current in a power cable is limited to about 1% of the permitted differential-mode current. This limit is also shown on Fig. 30. It should be noted that, although the field from the common-mode limit current is the same as that from the differential-mode limit current at the protection distance, it does not fall off with distance beyond the protection distance as rapidly as it does for the differential mode. This effect is shown on Fig. 24.

As is shown in the theory of common-mode current generation, described in paragraph 2.2.3, the common-mode current which is due to line-to-ground capacitors can actually be expected to increase with frequency initially, then level off and finally decrease with frequency. Actually, the conditions on common-mode current may be most difficult to meet at the higher frequencies.

At frequencies of the order of 1 MHz and higher, it is generally not possible to maintain a significant distinction between common-mode and differential-mode current, i.e. there will be substantial differential-mode to common-mode conversion above, say 2 MHz. For this reason, the common-mode limit is merged into the differential-mode limit in the frequency range between 20 kHz and 2 MHz. Above 2 MHz the limits are equal (Fig. 30).

#### 4.5 Common-Mode Susceptibility

The common-mode (or structure) currents are impressed on susceptible devices by either (1) the two conductors of an input power or signal line (usually twisted) or (2) the shields of such lines. In the latter case, the impedance to current flow will be low and the current will be source impedance controlled. In the former case the impedance can be quite high, particularly if the input circuit is balanced. For this reason, two common-mode immunity limits are suggested--one in terms of current, and the other in terms of voltage. The current limit should be the same as the common-mode emission limit. Two models are used in deriving the common-mode voltage limit. In



one the voltage limit is obtained by assuming a source impedance of 50 ohms. Such an impedance is considered representative of power line impedances at frequencies above about 100 kHz and is also representative of many signal line sources. The voltage limit is, then, the current limit multiplied by 50 ohms.

The second model is the voltage induced in a ground loop consisting of a cable above a ground plane. In Fig. 34 are shown the voltages generated in common-mode ground loops of various lengths and heights by the magnetic field limit below 20 kHz.

Thus, for a 10 foot cable run at an average height of 6 in. from the ground plane, a maximum of 62 dB(μV) will be induced. If the differential-mode sensitivity is 1 μV, the sensitivity protected by the environmental magnetic field limits, then the requisite common-mode rejection would be:

$$62 \text{ dB}(\mu\text{V}) - 0 \text{ dB}(\mu\text{V}) = 62 \text{ dB} \quad (40)$$

The limit on common-mode susceptibility for low-level cables may be set by assuming a certain value for run length and height above the ground plane, with the understanding that the required susceptibility threshold will increase proportionally with the increase in the ground loop area over the assumed value. The assumed value is 5 ft<sup>2</sup>, corresponding to a run length of 10 ft and height above the ground plane of 6 inches. The voltage induced in this loop by the magnetic field of Fig. 32 is shown as the limit on common-mode voltage susceptibility on Fig. 31. For other loop areas the voltage induced will be

$$V[\text{dB}(\mu\text{V})] = V_{\text{limit}} [\text{dB}(\mu\text{V})] + 20 \log_{10} \frac{A(\text{ft}^2)}{5} \quad (41)$$

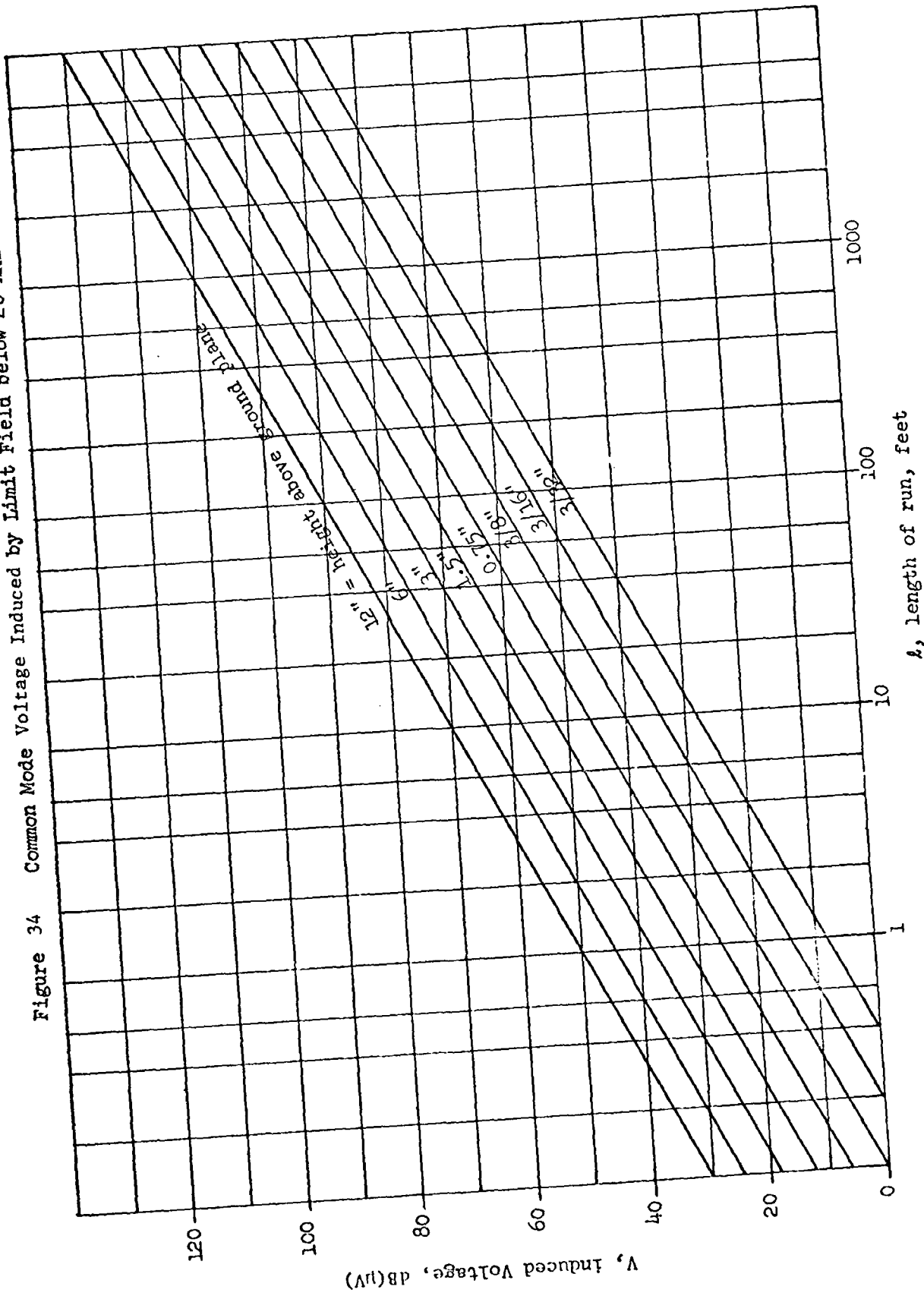
where A = loop area,  $V_{\text{limit}}$  = common-mode voltage susceptibility limit of Fig. 31.

The limit shown in Fig. 31 is considered adequate to cover the model based upon the line impedance since, in fact, in the region where the common-mode current limit is high (at the power line frequency), power line impedance is low. At 2 MHz, where the current limit is 2 μA, a line impedance of 50 Ω will produce 100 μV of common-mode voltage. This is exactly equal to the voltage limit on Fig. 31.

#### 4.6 Electric Field Limits

In the absence of intentionally strong sources (such as transmitter antennas) and intentionally sensitive susceptors (such as receiver antennas) the electric field emission and susceptibility limits may be set in the same manner as the environmental magnetic field limit. That is, emissions a certain distance from the source are limited to a given level and this level is then used to test susceptors. If sources and susceptors meet the limits, they will be compatible if separated by at least the specified distance.

Figure 34 Common Mode Voltage Induced by Limit Field below 20 kHz



The level is chosen to be consistent with the magnetic field limit. The protection distance is chosen to be greater than that for the magnetic field limit, because the effects of the two field types on a susceptor are most likely different. The magnetic field can have a very localized effect on the susceptor while the electric field effect tends to be averaged over the susceptor case or shield. Thus, in setting protection distances for the former, the distance is measured to the nearest point on the susceptor, while in the latter case it is taken to be the average distance of all points on the susceptor.

Thus, while the magnetic field limit protects susceptors from 100 ampere cables and equipment at a distance of 6 inches, the electric field protection distance from such equipment is chosen to be 1 meter.

The electric field emission limits are shown in Fig. 35. The curve limit labeled "Internal E-Field Limit" is consistent with the magnetic field limit arising from the conducted current limit shown as the upper dotted line, converted to electric field units through the free space impedance of 377 ohms. This conversion is valid if the conductor is terminated in its characteristic impedance. In most situations the "effective" conductor will be terminated in an impedance lower than the characteristic impedance (such as by periodic grounding of its shield). Hence, the actual electric field may be well below the theoretical value.

The limit proposed above is consistent with the field level that will protect a receiver antenna 15 feet away at the atmospheric noise level, assuming 20 dB shielding between source and susceptor.

Common-mode voltage can also be induced on cables directly by an electric field. As an estimate, one can take the induced voltage to be the product of the electric field strength and the cable length. The given common-mode limit would be exceeded on a 3 meter length of cable immersed in the limit electric field at all frequencies below 4 MHz. However, it should be noted that since such cables are usually located very close to the ground plane (especially when measured in terms of wavelength), it is unlikely that difficulty will be experienced from this effect. Cables not close to a ground plane would have to be examined more carefully.

#### 4.6.1 Internal and External Limits

If equipment is mounted externally, such that coupling to an antenna is a distinct possibility, then the emission limit must be lowered by the 20 dB shielding factor discussed above. The electric field limit corresponding to this case is shown in Fig. 35 as the lower solid line, labeled "External E-Field Limit."

For exposed equipment which is likely to be nearer than 15" to antennas, the current and magnetic field limits must be reduced even further. Another 20 dB reduction would protect the atmospheric noise level to a distance of about 1.5 ft.

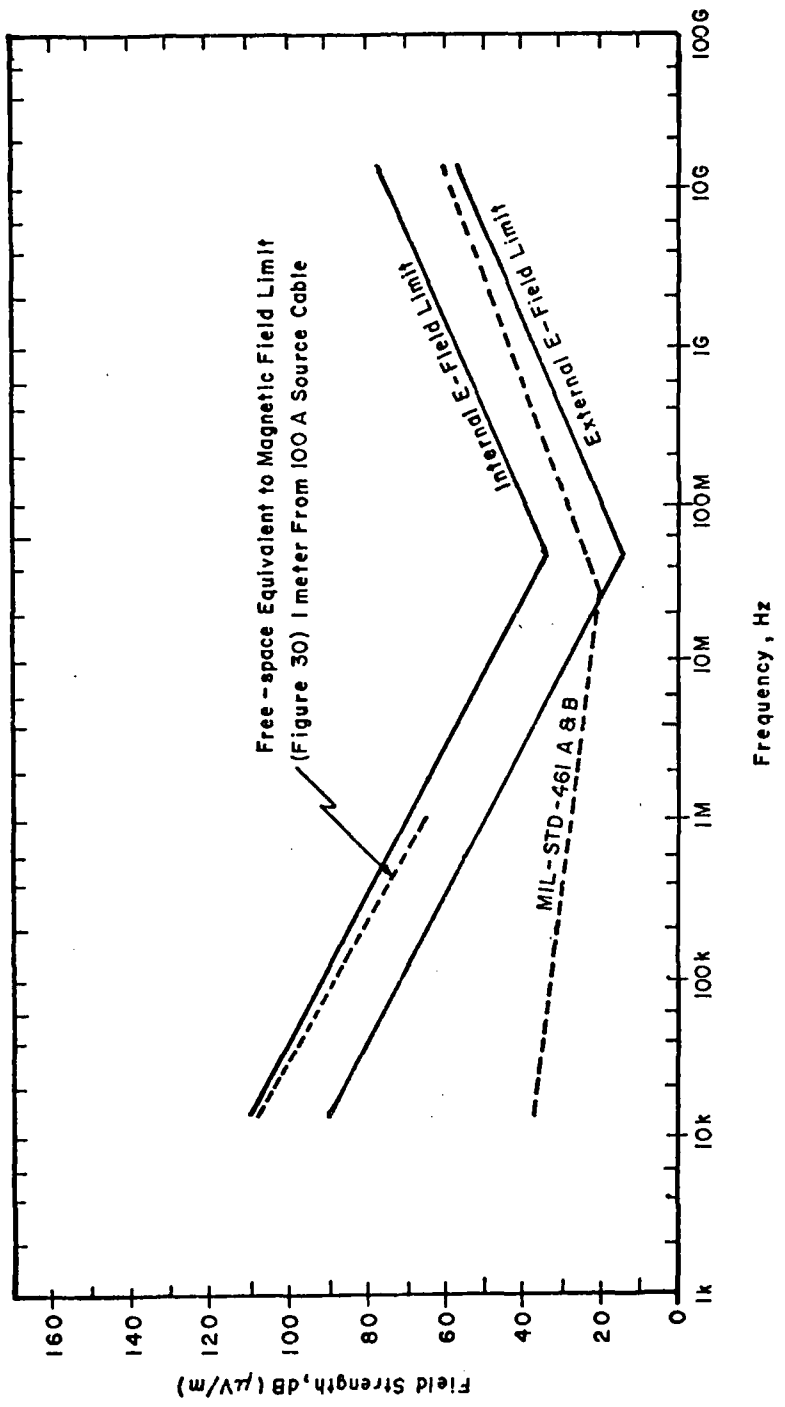


Figure 35 Electric Field Limits, 1 Meter From Source Case

#### 4.7 Broadband Limits

Broadband limits equivalent to the proposed narrow-band limits are found by assuming the peak value of the broadband noise in the susceptor bandwidth to be equal to the narrow-band limit. Thus

$$\text{BB limit} = \frac{\text{NB limit}}{\Delta F_{\text{imp}}} \quad (42)$$

where

$\Delta F_{\text{imp}}$  is the susceptor impulse bandwidth

Assumed susceptor bandwidths as a function of frequency are shown in Fig. 36. Up to 50 MHz, 10 kHz is assumed. Above 50 MHz, this increases gradually to 5 MHz in the range of radar operating frequencies.

### 5.0 PROTECTION MARGIN CALCULATIONS

#### 5.1 Introduction

In calculating protection margins, one should have data as a function of frequency on various characteristics of each equipment. With such data, comparison of emission and susceptibility levels can be made using appropriate coupling factors to account for distances of separation of each emitter-susceptor pair, and any interposed shielding or filtering.

As an alternate procedure and one which must be used when detailed experimental data are not available, protection margins may be estimated based upon certain models. These models will, of course, have limited validity. Generally, they are most useful in providing a basis for eliminating the need to consider detailed evaluation of specific types of interaction where the protection margin is large, and conversely identifying those interactions requiring a detailed analysis to obtain protection margins which are marginal and for which therefore one needs a relatively high degree of confidence. Thus, when used properly, procedures based upon modeled data provide a means of rapidly culling from further analysis configurations for which the protection margin would be found to be quite large if an "exact" analysis were made. Such procedures are identified later in the text.

To carry out the required procedures, the following information may be needed. The ways in which the information is used is described in succeeding paragraphs.

#### Emitters

For each cabinet: Power requirements, V, I, cable type, effective dipole strength and location, shielding effectiveness; H-field at specified cabinet distance.

For each power cable: Type (parallel wire, twisted pair or triple, coax), identification; current carried, both differential and common mode; location.

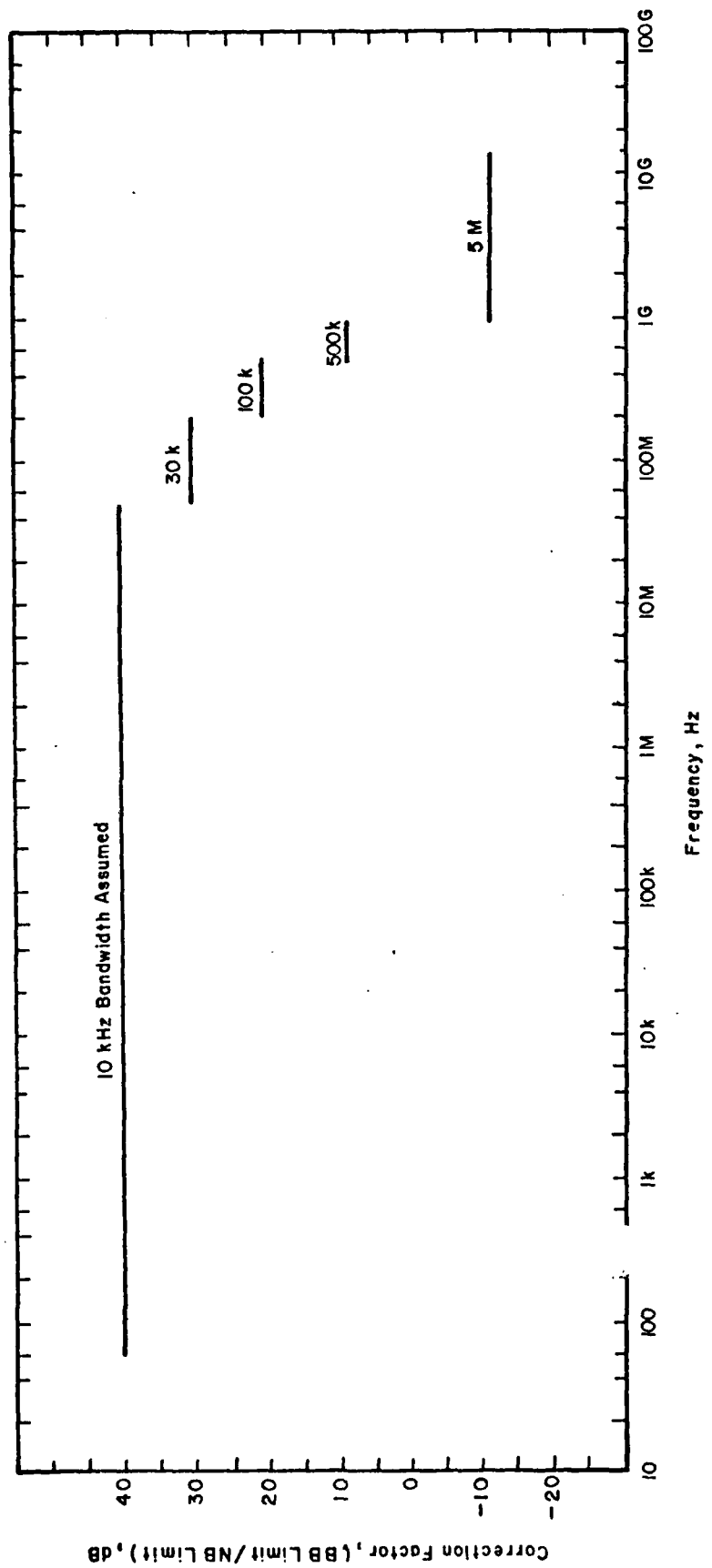


**Figure 36** Narrowband-Broadband Correction Factor (To be Added to Narrowband Limits to Obtain Broadband Limits in dB/unit/MHz)

For each signal cable: Type (parallel wire, twisted pair, coax), location, type and effectiveness of shield and current carried, both differential-and-common-mode.

#### Susceptors

For each cabinet: H-field susceptibility or pickup loop area and shielding effectiveness of cabinet; E-field susceptibility.

For each power cable:  $V_{\text{susc}}^{\text{(DM)}}$ ;  $V_{\text{susc}}^{\text{(CM)}}$

For each signal or control cable:  $V_{\text{sens}}^{\text{(sens)}}$ , type of cable (effective pickup loop area), connector shielding effectiveness;  $V_{\text{susc}}^{\text{(common mode)}}$ .

Ultimately, as illustrated in Fig. 29, there are four basic protection margins that must be evaluated for each cabinet; for each cable connection, those associated with (1) differential mode, and (2) common-mode conduction interactions, and for the cabinet those associated with (3) magnetic field and (4) electric field interactions. The conduction interactions should be evaluated for each cable connection, be it a signal, control or power cable. For the common mode, for a shielded cable, one can consider two interference mechanisms--the first is that due to voltages placed on the "active" conductors, and the second due to current on the shield which usually but not always is connected to the cabinet at the point of cable entry into it. The latter mechanism is similar for all cables and the susceptibility threshold is likely about the same for one cable as for another. In the case of common-mode voltages impressed on "active" conductors the susceptibility threshold may vary widely from one cable to another.

Figure 29 shows that, in concept, in using the protection margin (P.M.) chart, one assigns values pertaining to each of the types of interaction for each equipment as an emitter and also as a susceptor. The protection margin is then calculated for each interaction. The final P.M. for a given pair is then the lowest value of those protection margins.

For cable-to-cable coupling only the magnetic field mechanism is considered. However, the coupling can be of four types, i.e., the source cable can be producing a field because currents appear in the cable in either the differential mode or the common mode. Likewise voltages induced in the susceptor cables can appear in either the differential or common mode.

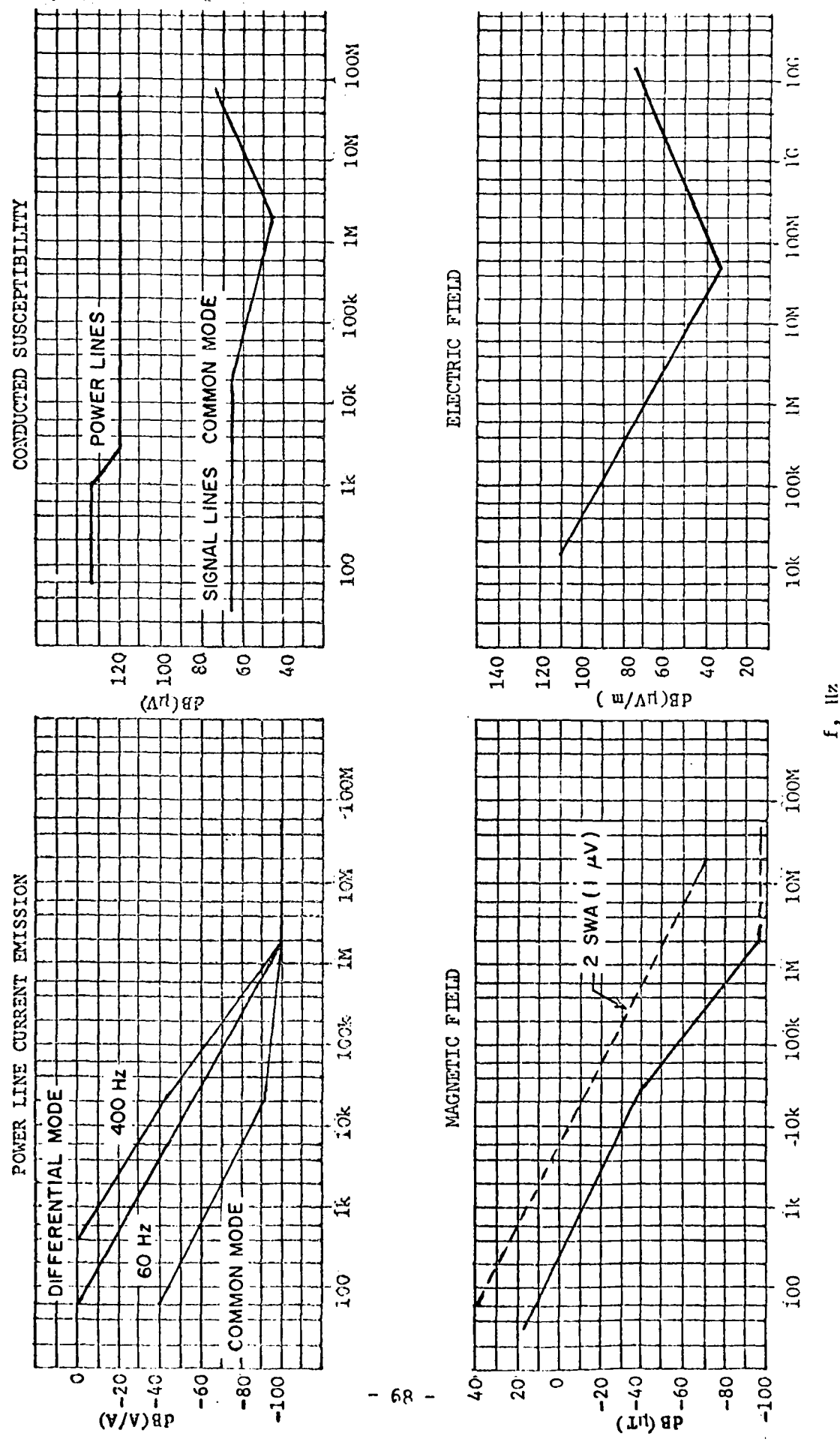
In carrying out the procedures, frequent reference will be made to the nominal levels discussed in Section 4. For convenience, Fig. 37 summarizes these levels.

### 5.2 Magnetic Field Coupling

#### 5.2.1 Cabinet-to-Cabinet Coupling

The general process is illustrated in Fig. 38. One first determines the magnetic flux density at which susceptibility would be observed. As an

Figure 37 PROPOSED ENVIRONMENTAL LIMITS  
(Narrowband)



$S_L$
$E_L$
$\Delta PM$
PM
FPM

$S_L$  = Susceptibility of the susceptor with respect to the appropriate environmental limit (see p. 52, Ref. 11) at the worst case frequency.

$E_L$  = Emissions of the emitter with respect to the appropriate environmental limit at the worst case frequency.

$\Delta PM$  = Distance correction factor

PM =  $S_L - E_L + \Delta PM$

FPM = Final Protection Margin. If PM > 20 dB, then FPM = PM. If PM < 20 dB, then further detailed analysis is performed on this interaction pair, and the resultant protection margin is entered as FPM.

Figure 38 Entries in Protection Margin Calculation

example, the susceptibility of type 2 SWA cable connected to a device having a sensitivity of 1  $\mu$ V occurs at a level of magnetic field 27 dB above the nominal level as shown with the dotted curve on Fig. 37. If the emission level in a given case is equal to the nominal level, and the distance between emitter and susceptor corresponds with the distance at which the emission level was measured, the protection margin would be 27 dB. For a different distance the value of the protection margin would require a distance correction factor as shown on Fig. 38.

If, after making the appropriate correction factor, the P.M. is negative, then a more detailed analysis may be required. For example, if the emitter and susceptor level shown apply only at specific frequencies in each case, then it is still possible that the system may be compatible if the maximum emission and minimum susceptibility frequencies do not coincide. The protection margin which results appears in the block marked FPM (Final Protection Margin).

#### 5.2.1.1 Magnetic Dipole Source

A convenient model for cabinet-to-cabinet coupling calculations is the magnetic dipole-to-loop model. From Eq. 13 we have

$$B = \frac{\mu M}{2\pi r^3} \quad (43)$$

where

$M_n$  is the effective strength of the magnetic source dipole

$r$  is the total distance between the source (measured to its magnetic center) and the susceptible circuit.

Note that in this relation, directional properties of the field and the source are ignored, although  $H$  and  $M_n$  are actually vector quantities. Equation 43 deals only with their magnitudes, and gives the maximum magnetic field strength possible from a source of strength  $M_n$ .

The susceptible device is characterized as having a single turn pickup loop of area A. The voltage induced in such a loop by a magnetic field H at frequency f is, using Eq. 33,

$$v = 2\pi f \mu A H$$

or for a source  $M_n$

$$v = \frac{2\pi f \mu A M_n}{2\pi r^3} \quad (44)$$

This relation is graphed in Fig. 39 for a frequency of 60 Hz and susceptor loop area of 1  $\text{cm}^2$ , and for values of source dipole strength of 1.0, 0.1 and 0.01  $\text{A}\cdot\text{m}^2$ . In utilizing this graph one must correct predicted values of induced voltage in proportion to the ratio of the actual dipole strength, frequency, and susceptor area, to the values labelled on any particular curve,

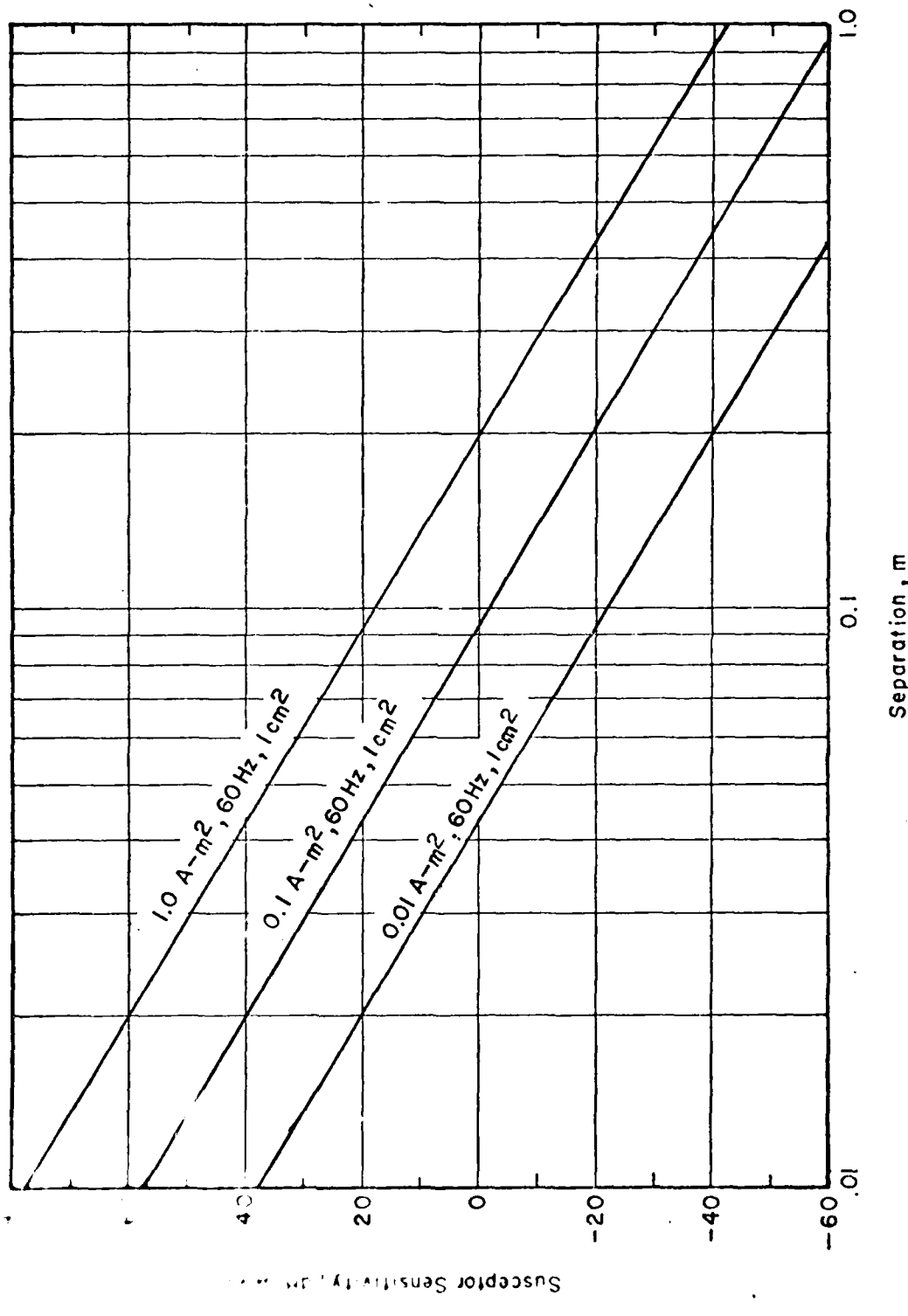


Figure 39 Minimum Spacing of Magnetic Source and Susceptor as Function of Susceptor Sensitivity and Source Strength. Frequency = 60Hz ; Source Strength = 1.0 , 0.1 , 0.01 A-m<sup>2</sup> , Susceptor Area = 1 cm<sup>2</sup>

e.g. for a  $2 \text{ cm}^2$  susceptor area the induced voltage is raised by 6 dB.

The ratio of the induced voltage to the sensitivity of the circuit at that point is the value of the protection margin. For example, if a source of 60 Hz, having an effective dipole strength of  $1.0 \text{ A-m}^2$  is located 10 cms from a susceptor having a sensitivity of  $1 \mu\text{V}$  and an effective area of  $1 \text{ cm}^2$ , the protection margin is 17.5 dB.

In the event the source dipole strength is not known, one can either (1) if it can be approximated as a loop, use Fig. 15 in order to obtain the magnetic flux density at the susceptor; Fig. 26 can then be used to obtain the induced voltage in the susceptor; or (2) estimate the magnetic dipole strength based upon Fig. 17 and Eq. 21 which accompanies it, and then use Fig. 39.

Figure 39 can be used effectively as a cull procedure. The example just given shows a protection margin of 17.5 dB for a spacing of 10 cm (4 in). The dipole strength is perhaps somewhat larger than typical sources (except for "large" electrical transformers, machines and switchboards) and the distance is as small as would usually be expected. Also, the effective area of  $1 \text{ cm}^2$  is about an order of magnitude larger than would be expected in a well-designed system. In other words, unless a system has a sensitivity well below  $1 \mu\text{V}$  or is near a large distribution panel or machine, it is unlikely to experience degradation. Only the most sensitive equipments could experience degradation at a distance of 1 meter. Thus, most cabinet-to-cabinet interactions can be culled quickly. Significant cabinet-to-cable interactions may be more probable, but this depends upon the techniques used in installing cable.

#### 5.2.1.2 Cabinet-to-Cable Calculations

The same model is used as in 5.2.1.1. For differential-mode induced voltages the cable half-loop area is used for  $A$  in Eq. 44 and the shortest distance from the cable to the cabinet is used for  $r$ . The graph of Fig. 39 may be applied.

#### 5.2.1.3 Cable-to-Cabinet Calculations

In this case the procedure used depends upon the type of cable in use. For power cables which are twisted pairs or triples the formulas in section 2.3.3.3 can be applied. Figures 23 and 24 give the fields as a function of distance for TNW and DSGA types. If the area of the susceptor loop is known, the induced voltage can be obtained from Figs. 23 or 26. This voltage, when subtracted from the cabinet equipment sensitivity, will yield the protection margin. Where the effective susceptor loop area is unknown, and where it can be assumed that the circuits contained within the cabinet are well designed from an EMC point of view, a reasonable assumption is that the most susceptible part of the circuit is located in the connector for the input signal cable. The area is assumed to be 10 times the "half loop" area of the connected cable.

For cables which are parallel wires, or for which common-mode currents are the source, one must use the flux density data obtained from Fig. 19 where the wire separation  $d$  is twice the height of the cable above the ground plane.

In the case of coaxial cables the same figure is used but the separation distance  $d$  is obtained from Fig. 20.

#### 5.2.1.4 Cable-to-Cable Calculation

In this case the same procedure is used as for the cable-to-cabinet calculation for the determination of the emission flux density. For the susceptor cable, if it is of the twisted type the "half loop" area is determined and Fig. 26 used to calculate the induced voltage.

When the susceptor configuration consists of parallel lines or the concern is with the common mode, a parallel wire line model should be used. Data on induced voltage can also be obtained from Fig. 26.

### 5.3 Conductive Coupling

Interference voltages appear on the power line due to (1) line frequency harmonic currents originating in nonlinear devices connected to the line; or (2) unintentional coupling of signal oscillators back into the power line.

Methods of modeling the levels of harmonics generated are discussed in paragraph 2.2.2. Methods of modeling a complete power system and of computing levels of harmonic voltages appearing on it are discussed in Ref. 4. These techniques are not further discussed here. However, it should be noted that to estimate common-mode emission levels, the levels of harmonic voltages should be known.

As mentioned in paragraph 2.2.2., for conducted interference the pair-wise interaction concept must be modified, as discussed in the following paragraph.

#### 5.3.1 Differential-Mode Conducted Coupling

Because of the fact that all devices connected to the same power line are "interconnected," they will all be subject to approximately the same harmonic levels. Small differences in these levels will occur because they are connected at different points on the line and voltage differences will appear because of the impedances between the different points of connection. Hence, the differential-mode voltage appearing at a susceptible terminal is not uniquely related to that of a given source. In fact, although it is probably best to characterize the differential mode characteristic of any given source in terms of the current it emits, the susceptance of the susceptor is best characterized in terms of the line voltage. Thus, in making the protection margin calculation for differential-mode voltage, in following the procedure as illustrated in Fig. 38, in the block marked emission level, one inserts the line voltage level actually appearing at the susceptor terminals or, if not available, the level calculated using the model discussed in reference 4.

### 5.3.2 Common-Mode Conducted Coupling

The common mode, or structure currents appearing in a given installation, in general, have a complex pattern which depends upon where line-to-ground capacitors appear in the configuration and also where isolation transformers are used to control such currents.

Where a given cable is used only to interconnect one particular cabinet to another, its emission current level can be directly compared with the susceptibility level of the other cabinet.

However, where more than two cabinets are interconnected, as in the case of the power line, estimates of the levels that may appear must be based upon more complex models. An example of such an estimate is given in paragraph 2.2.3.1.

### 5.4 Isolation Factors

If the source-susceptor separation is different from the distance specified in the limits, then the protection margin will be increased or decreased depending upon whether this distance is greater or less, respectively. The amount of the change in protection margin, or the isolation factor, for each interference mechanism may be computed by the formulas given in this section.

#### 5.4.1 Case-to-Case and Case-to-Cable Coupling

A magnetic dipole model is assumed. The field at a distance  $r$  from the source will be

$$\frac{B}{B_{\text{limit}}} = \left( \frac{r_{\text{limit}}}{r} \right)^3$$

where  $r_{\text{limit}}$  = distance at which the magnetic field limit of Fig. 32 applies. The change in protection margin is thus, for magnetic field coupling

$$\Delta PM(\text{dB}) = 60 \log_{10} \left( \frac{r}{r_{\text{limit}}} \right) = 3(r - r_{\text{limit}}) \text{ (dB)} \quad (45)$$

i.e. the protection margin between susceptibility and emission levels is increased by three times the decibel increase in distance relative to the distance specified in the limit. If  $r_{\text{limit}} = 6$  inches and the source case and susceptor case or cable are separated by 12 inches, then the protection margin obtained by overlaying the emission levels at 6 inches and the susceptibility data is increased by  $3 \times 20 \log_{10} \frac{12}{6} = 3 \times 6 \text{ dB} = 18 \text{ dB}$ .

### 5.4.2 Cable-to-Cable and Cable-to-Case Coupling

#### 5.4.2.1 Differential Mode

The differential mode emission model is that of a twisted-pair cable of pitch  $p$  and conductor separation  $d$ . The field from DSGA-type cables carrying the current of Fig. 30 at the distance of Fig. 33 is equal to the magnetic field limit of Fig. 32. For other types of cables, for other currents and for other distances, the change in magnetic field above or below the limit shown in Fig. 32 may be computed by the use of Fig. 40.

To use Fig. 40 to find the field at distance  $r$  from the line, first the ratio  $r/p$  is calculated. The reference distance  $r_{ref}$  is found from the plot. The change in magnetic field is then found from the formula:

$$(B - B_{limit}) dB = (I - I_{ref}) dB + (d - d_{ref}) - 2(r - r_{ref}) \quad (46)$$

where

$I$  = current actually flowing in the line, dB(A)

$I_{ref}$  = "60 Hz line" limit of Fig. 30 for 100 ampere cable

= 100 A at 60 Hz falling as  $1/f = 40 - 20 \log_{10} f/60$  dB(A)

$d$  = conductor separation

$d_{ref}$  =  $d$  for DSGA 100

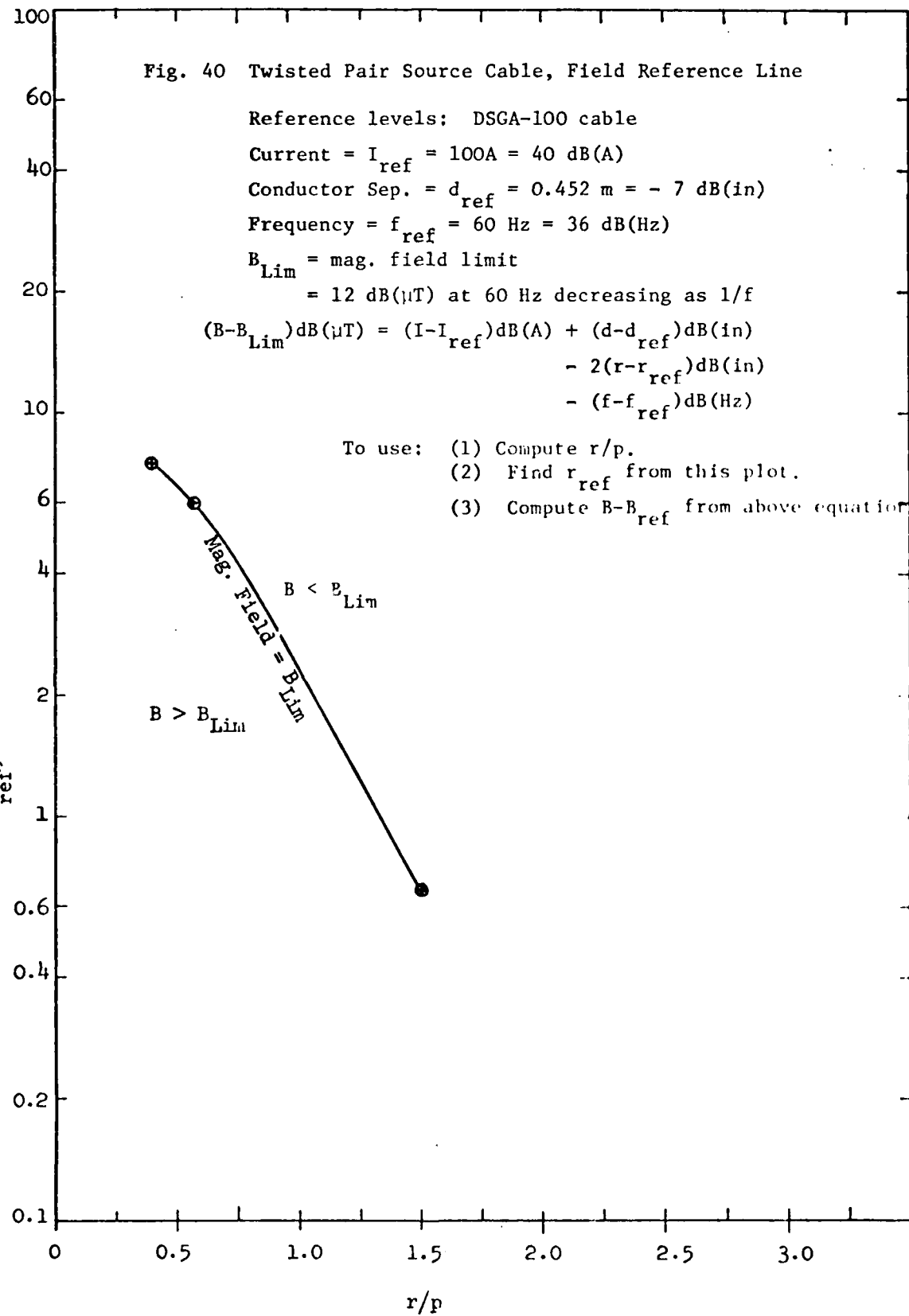
$B_{limit}$  = magnetic field limit of Fig. 32.

The change in protection margin from that obtained by overlaying the source levels at the specified distances of Fig. 33 and the susceptibility data is the negative of the dB increase in magnetic field or

$$PM = PM_o - (B - B_{limit}) \quad (dB) \quad (47)$$

The susceptibility levels are expressed either in terms of the magnetic field at the susceptor case or the voltage on the susceptor cable. In either case, an increase in the magnetic field from the source will decrease the protection margin and vice versa.

As an example, consider the field at a distance of 6 inches from DSGA-50 cable (six inches is the distance specified for 100 ampere cable), carrying 100 amperes at 60 Hz.  $r/p = 6 \text{ inch}/8.0 = 0.75$ .  $r_{ref}$  from the plot of Fig. 40 is 4.2 in.  $d = 0.334 \text{ in.} = -9.5 \text{ dB(in.)}$   $I_{lim} = 50 \text{ amperes}$  for DSGA-50 cable.



$$I - I_{ref} = 40 - 40 = 0 \text{ dB}$$

$$d - d_{ref} = 9.5 - (-7) = -2.5 \text{ dB}$$

$$r - r_{ref} = 20 \log_{10} \frac{6}{4.2} = 3.1 \text{ dB}$$

$$\text{and } B - B_{limit} = 2.5 - 2(3.1) = -2.5 - 6.2 = -8.7 \text{ dB}$$

$$\Delta PM = -(-8.7) = +8.7 \text{ dB}$$

i.e., due to the increase in p and d, the field has been reduced by 8.7 dB from that produced by DSGA-100 cable, increasing the protection margin by the same amount. This result indicates the advisability, generally, of utilizing the maximum capacity of power cables, from an electromagnetic compatibility standpoint, rather than choosing cable sizes larger than necessary to carry a certain load current.

#### 5.4.2.2 Common-Mode Source Cable

The field from a common-mode source varies as  $1/r$  or  $1/r^2$  (where  $r$  = distance from the source cable) depending upon whether  $r$  is smaller or larger than the distance of the cable from the ground plane.

The common-mode field above 2 MHz shown in Fig. 32 is computed for a distance of 6 in. from the line, and assumes that the distance to the ground plane,  $d$ , is greater than this.

To recompute the field for other values of  $r$  and  $d$ , Fig. 41 may be used. First,  $r/d$  is computed and  $r_{ref}$  found from the plot of Fig. 41. The change in the magnetic field level due to the change in  $r$  and  $d$  is then given by

$$(B - B_{limit})_{r,d} = -(r - r_{ref}) \text{ dB}$$

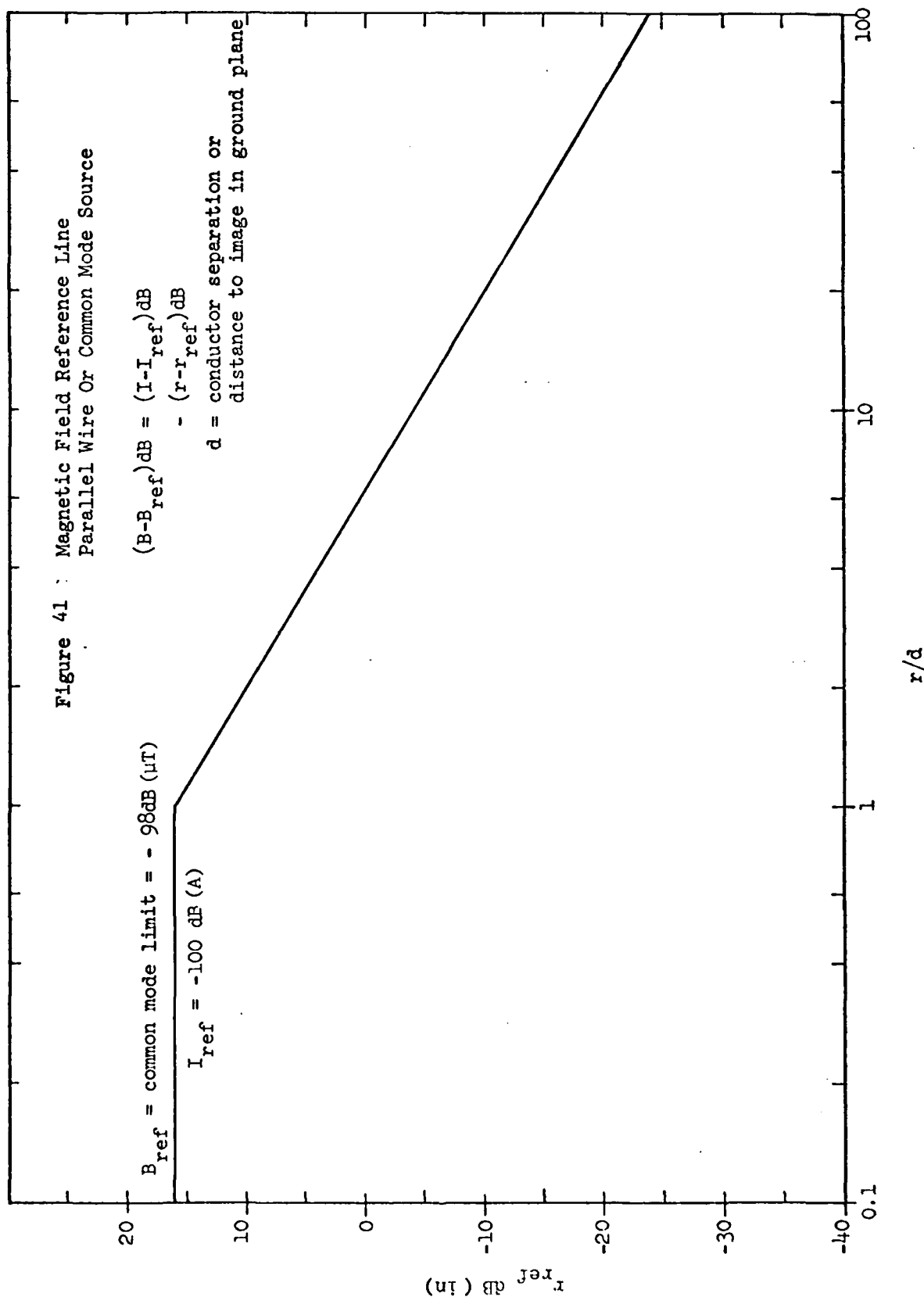
where  $B_{limit}$  = magnetic field limit above 2 MHz = -98 dB( $\mu$ T). To this must be added the dB change in common-mode current level from the common-mode limit of 20 dB( $\mu$ A):

$$(B - B_{limit}) = [I - 20 \text{ dB}(\mu\text{A})] - (r - r_{ref}) \text{ dB} \quad (48)$$

Protection margins calculated on the basis of the magnetic field given in Fig. 32 must be reduced by this change in the field:

$$PM = PM_0 - (B - B_{limit}) \quad (49)$$

Figure 41 : Magnetic Field Reference Line  
Parallel Wire Or Common Mode Source



It should be noted that in metal compartments, the field at any point is affected by images of the cables in walls other than the nearest wall which is considered to be the ground plane. The  $1/r^2$  variation should therefore be used with caution at larger distances from the line, say for  $r > 1/3$  compartment dimension. In such cases the field may actually be constant as  $r$  varies. Prediction of these fields is a matter open for further study; in most cases of practical significance  $r$  may be small enough that the above relationships are adequate.

#### 5.4.3 Common-Mode Susceptor Cable

The voltage induced on the shield of a cable, as discussed earlier in the report, is a function of the area of the ground loop, if any, of which the shield is a part.

In arriving at the voltage susceptibility limit of Fig. 31, a 5 ft<sup>2</sup> ground loop area, corresponding to a 10 ft run and a 6 in. height above the ground plane, was assumed.

For other run lengths ( $\ell$ ) and heights ( $d$ ) that voltage should be corrected by

$$V[dB(V)] = V_{\text{limit}}[dB(V)] + 20 \log_{10} \frac{\ell(\text{ft})}{5} + 20 \log_{10} \frac{d(\text{in})}{6} \quad (50)$$

where  $V_{\text{limit}}$  = common-mode susceptibility limit (Fig. 31).

The protection margin obtained by assuming the common-mode voltage induced is equal to  $V_{\text{limit}}$  should be reduced by the increase in voltage:

$$PM = PM_o - (V - V_{\text{limit}})dB \quad (51)$$

#### 5.4.4 Summary

The coupling models are summarized in Table II. The table is applicable to both broadband and narrow-band interference. For narrow-band interference, the signal quantities ( $B$ ,  $V$ , and  $I$ ) are understood to be amplitudes of sinusoids at the interference frequency  $f$ . For broadband interference, they are understood to be spectral densities at the frequency  $f$ . These are multiplied by the susceptor impulse bandwidth to obtain peak signal in the susceptor bandwidth.

### 5.5 Broadband Interactions

A general approach to the calculation of protection margins in the case of broadband interactions has as yet not been completely formulated. One of the reasons for this is that there is available, at this time, insufficient data on the characteristics of typical broadband emissions. Work is presently going forward on measuring such emissions.

TABLE II - LOW FREQUENCY MAGNETIC COUPLING MODELS

Mechanism	Source Parameters*	Source to Field Coupling	Field to Susceptor Coupling	Measured Susceptor parameters	Compatibility Margin
Case-to-Case	$M_m$ or $B_S$ at $R_S$ $M_m$ = effective magnetic dipole strength $B_S$ = flux density at a distance from source case (Sec. 2.3.2)	$B = \frac{\mu_0 M}{2r}^3$ or $B = B_S \left( \frac{r_3}{r} \right)^3$ ( $r$ measured to dipole location within case), or $B = B_S \left( \frac{r_S}{r} \right)^2 + 6$ dB ( $r$ measured to cabinet) $B$ = flux density at susceptor case (Sec. 2.3.2)	$B$ = Flux density at susceptor case $V = \omega AB$ (Fig. 26) $V$ = induced voltage susceptor loop $A$ = effective area of susceptor loop $\omega = 2\pi f$ = radian frequency	$B_{susc} =$ flux density applied to susceptor to cause intolerable degradation $V_{susc}$ = voltage to cause intolerable performance degradation of susceptor ( $\chi = V_{Sens}$ ) $V_{Sens}$ = equipment sensitivity	$\frac{B_{susc}}{B}$
Case-to-Cable	As above	As above	As above except $A$ = effective cable pickup area	As above	As above
Cable-to-cable Differential mode; Parallel wire or coaxial cable on source	$I_D$ source current on cable (Sec. 2.3.3)	$\frac{B}{I_D} = \frac{\mu_0 d}{2\pi r(r+d)}$ (See Fig. 19) $d$ = separation of parallel-wire conductor or eccentricity of coaxial cable (Fig. 20) $r$ = distance to susceptor cable (Sec. 2.3.3)	Same as above	Same as above	$\frac{V_{susc}}{V}$

\* Preferably should be known as function of frequency

continued

TABLE II - CONTINUED

Mechanism	Source Parameters	Source to Field Coupling	Field to Susceptor Coupling	Measured Susceptor parameters	Compatibility Margin
Cable-to-Cable Common Mode	$I_L$ , common mode current on source model	Same as above $d = 2 \times$ height of source cable above ground plane	Same as above	Same as above	$\frac{V_{susc}}{V}$
Cable-to-cable Differential Mode, Twisted Pair Cable on Source	$I_L$ , diff. mode Current on source cable Sec. 2.2.2	$r < \frac{P}{3}$ $\frac{B}{I_L} = \frac{\mu_0 d}{2\pi r(r+d)}$	Same as above	Same as above	$\frac{V_{susc}}{V}$
Cable-to-Case Differential Mode, Twisted Pair Cable on Source		$r > \frac{P}{3}$ $\frac{B}{I_L} = \frac{\mu_0}{\sqrt{pr}} \left( \frac{2\pi d}{P} \right) I_o \left( \frac{2\pi d}{P} \right)$	$B =$ flux density at susceptor case $e^{-2\pi r/p}$	$B_{susc}$ Flux density applied to susceptor case to cause intolerable performance degradation.	$\frac{B_{susc}}{B}$

See Fig. 22,  
Sec. 2.3.3.3  
 $P$  = pitch of twist  
 $d$  = separation of conductors  
 $r$  = distance to susc. cable

continued

TABLE II - CONTINUED

Mechanism	Source Parameters	Source to Field Coupling	Field to Susceptor Coupling	Measured Susceptor Parameters	Compatibility Margin
Cable-to-Case Differential Mode, Parallel wire or coaxial cable on source	Same as above	$\frac{B}{I_L} = \frac{\mu_0 d}{2\pi r(r+d)}$ r = distance to susceptor d = separation of parallel wire conductors or eccentricity of coaxial cable	Same as above	Same as above	$\frac{B_{susc}}{B}$
Cable-to-Case Common Mode	$I_L$ , common mode current on source cable	Same as above d = $2 \times$ height of source cable	Same as above	Same as above	$\frac{B_{susc}}{B}$

- Application to broadband interference:

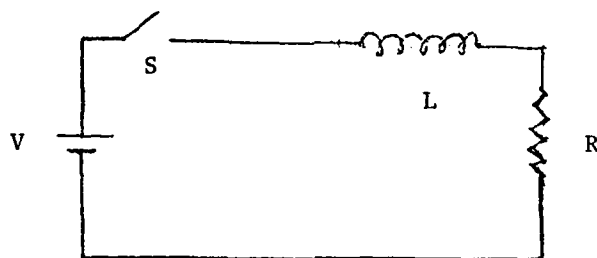
1)  $B_S$ ,  $I_D$ ,  $I_c$  are source spectral densities,  $\mu\text{T}/\text{MHz}$  and  $\mu\text{A}/\text{MHz}$  respectively, for example.2) Coupling equations are used to compute  $B$  and  $V$ , spectral densities at susceptor.3) Compatibility margins are given by:  $\frac{B_{susc} f_o / b_{susc}}{B}$  and  $\frac{V_{susc} f_o / b_{susc}}{V}$ , where $B_{susc} f_o$  = narrow-band susceptibility at center frequency of susceptor (= sensitivity of susceptor) $b_{susc}$  = susceptor bandwidth4) If  $b_{susc} > b_{SIG}$  (broadband susceptor) compatibility margins are given by  $\frac{B_{susc}}{B_{pk}}$  and  $\frac{V_{susc}}{V_{pk}}$ , where  $B_{pk}$  and  $V_{pk}$  are peak values of source signal at susceptor (see Sec. 2.4.1 and 5.5).

5) See Figs. 2 and 3 for additional pulse spectra information.

Accordingly, particular attention has been devoted to one particular type of transient, namely a voltage step applied to an inductive load. It, and the possible coupling of it into other circuits, is discussed in the following paragraphs.

### 5.5.1 Circuit Model

Assume a transient magnetic field arises from closing a switch on an inductive load. The equivalent circuit for the source of the magnetic field is then



The value of L is assumed in the  $\mu\text{H}$  range, say 5  $\mu\text{H}$ .

The value of R is assumed to be equal to the equivalent power load resistance, i.e.

$$P = \frac{V^2}{R}$$

or  $P = \frac{V^2}{P} = \frac{13.7}{P(\text{kW})}$  for 117 V line.

The transient current is then

$$I = I_o \left( 1 - e^{-\frac{R}{L}t} \right) \quad (52)$$

where

$$I_o = \frac{P}{V} = \frac{P(\text{kW})}{0.117}$$

### 5.5.2 Loop Coupling Model

The coupling is modeled as that between two loops of areas  $A_1$ ,  $A_2$  spaced a distance  $r$ .

The flux density at distance  $r$  is given by Eq. 11.

$$B = \mu H_\theta = \frac{\mu M_m}{4\pi r^3} \quad (53)$$

$$M_m = IA_1 \text{ (assumed 1 turn)}$$

The voltage induced in the suscepter loop (assumed 1 turn) is

$$\begin{aligned} v &= \frac{d}{dt} \phi = \frac{d}{dt} (BA_2) \\ &= \frac{d}{dt} \left( \frac{\mu IA_1 A_2}{4\pi r^3} \right) = \frac{\mu I_o A_1 A_2}{4\pi r^3} \frac{R_e}{L} t \\ V_{max} &= \frac{4\pi \times 10^{-7} A_1 A_2 V}{4\pi r^3 L} = 2.3 \frac{A_1 A_2}{r^3} \end{aligned} \quad (54)$$

For case-to-case coupling, assume

$$A_1 = A_2 = (0.3 \text{ m})^2 \text{ (approx. } 1 \text{ ft}^2)$$

$$r = 0.3 \text{ m}$$

$$\text{Then } V_{max} \approx 8V$$

Note that this is independent of the size (power rating) of source equipment, varies inversely as the cube of the distance and is, of course, proportional to both source and suscepter areas. It is also dependent on the effective acceptance bandwidth of the suscepter, here assumed to be completely broadband.

If a finite bandwidth can be defined for the suscepter, the voltage induced can be reduced by the ratio of the acceptance bandwidth to the spectral width of the source field. If the spectrum is assumed flat to the cutoff frequency

$$\frac{R_e}{L} = \frac{13.7}{P(\text{kW}) \times 5 \times 10^{-6}} = \frac{2.7}{P(\text{kW})} \cdot 10^6 \text{ Hz} \quad (55)$$

Thus the induced voltage in a bandwidth of  $\Delta F$  MHz is

AD-A100 402 MOORE SCHOOL OF ELECTRICAL ENGINEERING PHILADELPHIA P=ETC F/B 20/3  
METHODOLOGY FOR EMC EVALUATION.(U)  
DEC 80  
MS-EES-TR-80-1

N00140-79-C-6628

ML

UNCLASSIFIED

2 of 2  
AD A  
100-402

END  
DATE FILMED  
7-81  
DTC

$$\frac{2.3 A_1 A_2}{r^3} \frac{\Delta F \times 10^{+6}}{2.7 \times 10^6} P(\text{kW})$$

$$\frac{2.3 A_1 A_2}{r^3} 0.39 \Delta F(\text{MHz}) P(\text{kW}) \quad (56)$$

Thus, for the above parameters of  $A_1$ ,  $A_2$ , and  $r$ , for

$$\Delta F = 0.01 \text{ and } P = 1 \text{ kW}$$

$$V_{\max} = 8 \times 0.0039 = 0.0312 \text{ volts} \quad (57)$$

For the wide-band case and  $A_1 = A_2 = 1 \text{ sq. ft.}$  and  $r = 1 \text{ ft}$ , the 8 V induced is above the 1 V susceptibility level specified in MIL-STD-461 for power circuits. Considerations that can be used to justify lower induced voltage are the following:

1. If spacing is increased, an inverse cube relation applies, e.g. for a spacing 2 ft, the induced voltage is 1 volt, equal to the MIL-STD limit.
2. Careful wiring of power leads can reduce sharply the effective areas  $A_1$  and  $A_2$  (wires to on-off and other switches should be twisted or closely spaced parallel pairs).
3. Continuous steel or aluminum cabinets will provide significant shielding against magnetic fields, especially at frequencies above 10 kHz.
4. The induced voltage in signal and control cables will be reduced by the factor of the effective intercept area, e.g.

$$\begin{aligned} \text{for 2 SWA cable} \quad A &= 4.6 \times 10^{-2} \text{ m}^2 \\ &= 3.2 \times 10^{-4} \text{ ft}^2 \end{aligned}$$

Thus, without shielding, and for  $A_1 = 1 \text{ sq. ft}$  and  $r = 1 \text{ ft}$

$$V_{\max} = 25.6 \times 10^{-4} = 2.56 \text{ mV} \quad (58)$$

This is not likely to cause difficulty in digital circuits, and in analog circuits usually will be reduced by an effective bandwidth correction factor.

5. Cabinet-to-cable couplings can be estimated in terms of equivalent area of the susceptible cable, either differential mode (in terms of cable construction) or common mode, in terms of height above ground plane and effective field intercept length.

### 5.5.3 Common-Mode Cable Coupling

In this case assume two parallel wires of heights  $h_1, h_2$  above a ground plane spaced by  $r$ . From Table II

$$B = \frac{2\mu_0 h_1 I_{CM}}{2\pi r(r + 2h_1)}$$

At the susceptor cable, common-mode induced voltage per unit length can be calculated as follows:

$$v = \frac{d\phi_2}{dt} = \frac{d}{dt} \left[ \frac{2h_1 h_2 \mu_0 I_{CM}}{2\pi r(r + 2h_1)} \right] \quad (59)$$

The form of the common-mode current is important. As a worst case it can be assumed to be a fixed portion of the differential-mode current (say 0.1). Actually, it can be expected to increase with frequency because imbalance leading to common mode is due to capacitance (either distributed or lumped in filters). Furthermore, the rise time may be lower than for differential mode, because the common-mode inductance will be substantially larger, say 50-100  $\mu H$ .

Using  $I_{CM} = pI$

$$\begin{aligned} v_{max} &= \frac{2h_1 h_2 \mu_0 p I_0}{2\pi r(r + 2h_1)} \frac{R}{L} \\ &= \frac{2h_1 h_2 4\pi \times 10^{-7} p V}{2\pi r(r + 2h_1) L} \\ &= \frac{4 \times 10^{-7} h_1 h_2 117 p}{r(r + 2h_1) 50 \times 10^{-6}} \\ &\approx \frac{p h_1 h_2}{r(r + 2h_1)} \text{ volts} \end{aligned} \quad (60)$$

For  $p = 0.1$ ,  $h_1 = h_2 = r = 6$  inches.

$$V = 0.033 \text{ volts/meter}$$

#### 5.5.4 Calculation of Protection Margins

The spectrum amplitude per ampere ( $I_0 = 1$ ) for the current given by Eq. 52 is shown on Fig. 42. It should be noted that the spectrum amplitude follows a  $1/f$  variation with a magnitude  $1/\pi f$  out to a cutoff frequency which is approximately equal to  $1/\pi\tau$  where  $\tau$  is the rise time of the switched current pulse, given by the quantity  $L/R$ . Beyond this frequency, the spectrum drops off inversely as the square of the frequency. The cutoff frequency shown on Fig. 42 is 0.747 MHz,  $I = 1$  ampere ( $R = 117$  ohms), and  $L = 50 \times 10^{-6}$  H.

Figure 43, obtained using Fig. 15, shows at "A" the value of the flux density produced by such a switching transient for a source loop area equal to 1 square meter at a distance of 7 cm. In this figure it is assumed that the source loop has a sufficient number of turns and correspondingly small enough diameter that the field drops off inversely with the cube of the distance at the 7 cm distance. If the source area is larger than permitted with this assumption, the field at 7 cm would have to be corrected accordingly (see Fig. 15), or in accordance with more exact calculations.

Figure 43 also shows at "B" the susceptibility of a 1 square cm loop sensitive to 1  $\mu$ V when subjected to a broadband magnetic field. This is derived and interpreted as follows. From Eq. 54 it can be seen that the maximum voltage is inversely proportional to the inductance  $L$ . Furthermore, since the cutoff frequency on the spectrum amplitude is also inversely proportional to the inductance  $L$ , one can infer that equal portions of the spectrum below the cutoff frequency have an equal importance in generating peak voltage even though their spectrum amplitude levels are different. For example, neglecting the contribution of the portion of the spectrum above the cutoff frequency, the portion of the spectrum from 0 to 20 kHz produces, according to Eq. 54, just twice the voltage that would be produced by the portion from 0 to 10 kHz. But according to Eq. 52, the spectrum level at 20 kHz is just  $1/2$  of the spectrum level at 10 kHz.

The induced voltage per hertz can be obtained by dividing Eq. 54 by the cutoff frequency, and thereby obtain

$$\begin{aligned} V_{\max}/\text{Hz} &= \frac{\pi 10^{-7} A_1 A_2}{r^3} I \\ &= \frac{\pi 10^{-7} A_2 M_m}{r^3} \end{aligned} \quad (61)$$

where  $M_m$  is the magnetic dipole strength of the source loop equal to the area times the steady state current in the circuit. For a pickup loop area  $A_2$ , of 1 sq cm ( $10^{-4}\text{m}^2$ ) and a distance from the source of 7 cm (0.07 m) and a bandwidth of 10 kHz, one obtains a maximum induced voltage per 10 kHz bandwidth of  $0.915 \times 10^{-3}$  volts. For a 1  $\mu$ V susceptibility the permitted source strength (or magnetic field level) would be 59 dB less than that corresponding to the 1  $\text{A}\cdot\text{m}^2$  curve, as shown at "B". This curve is interpreted

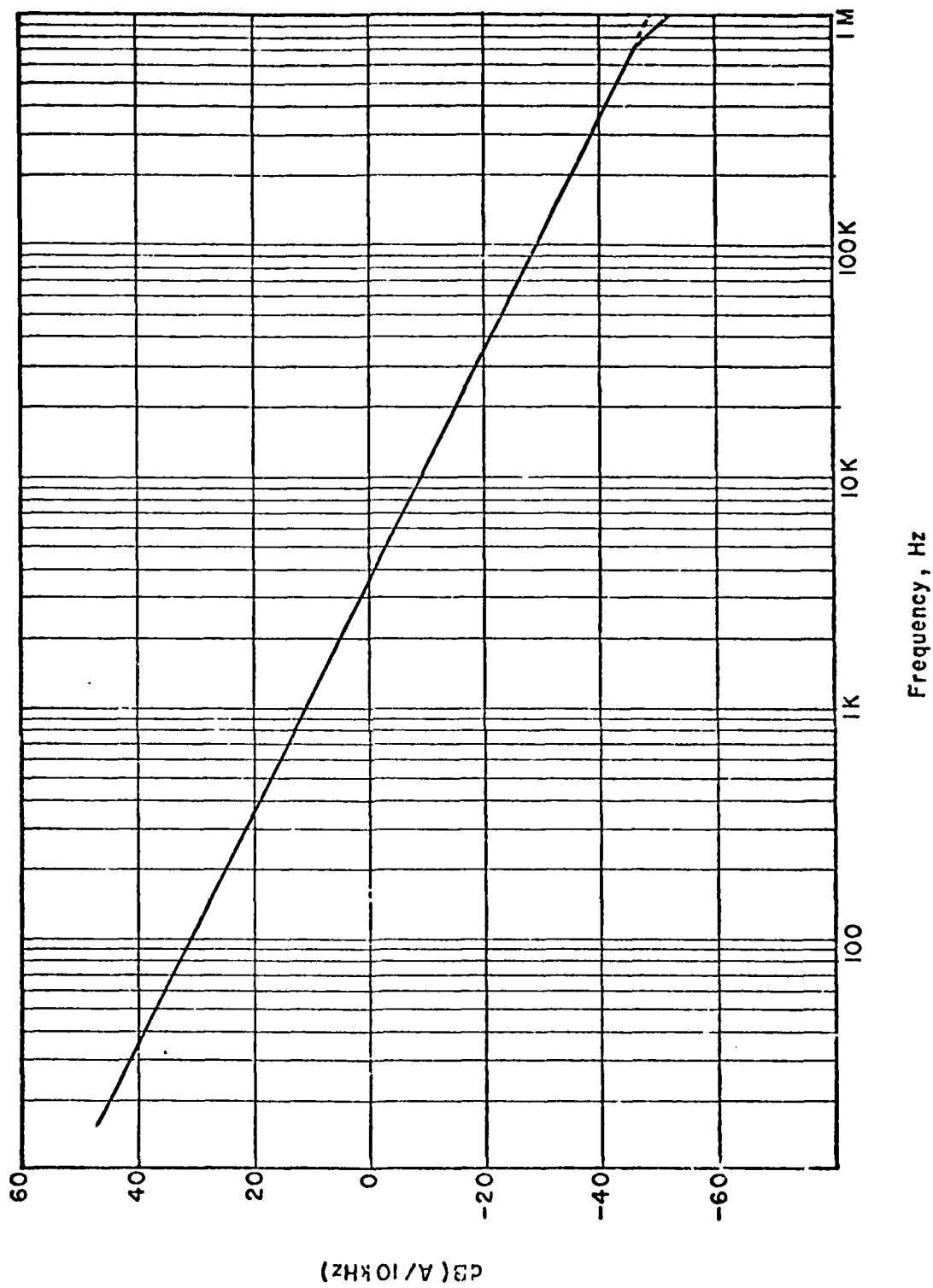


Figure 42 Spectrum of Current Step of 1 Ampere

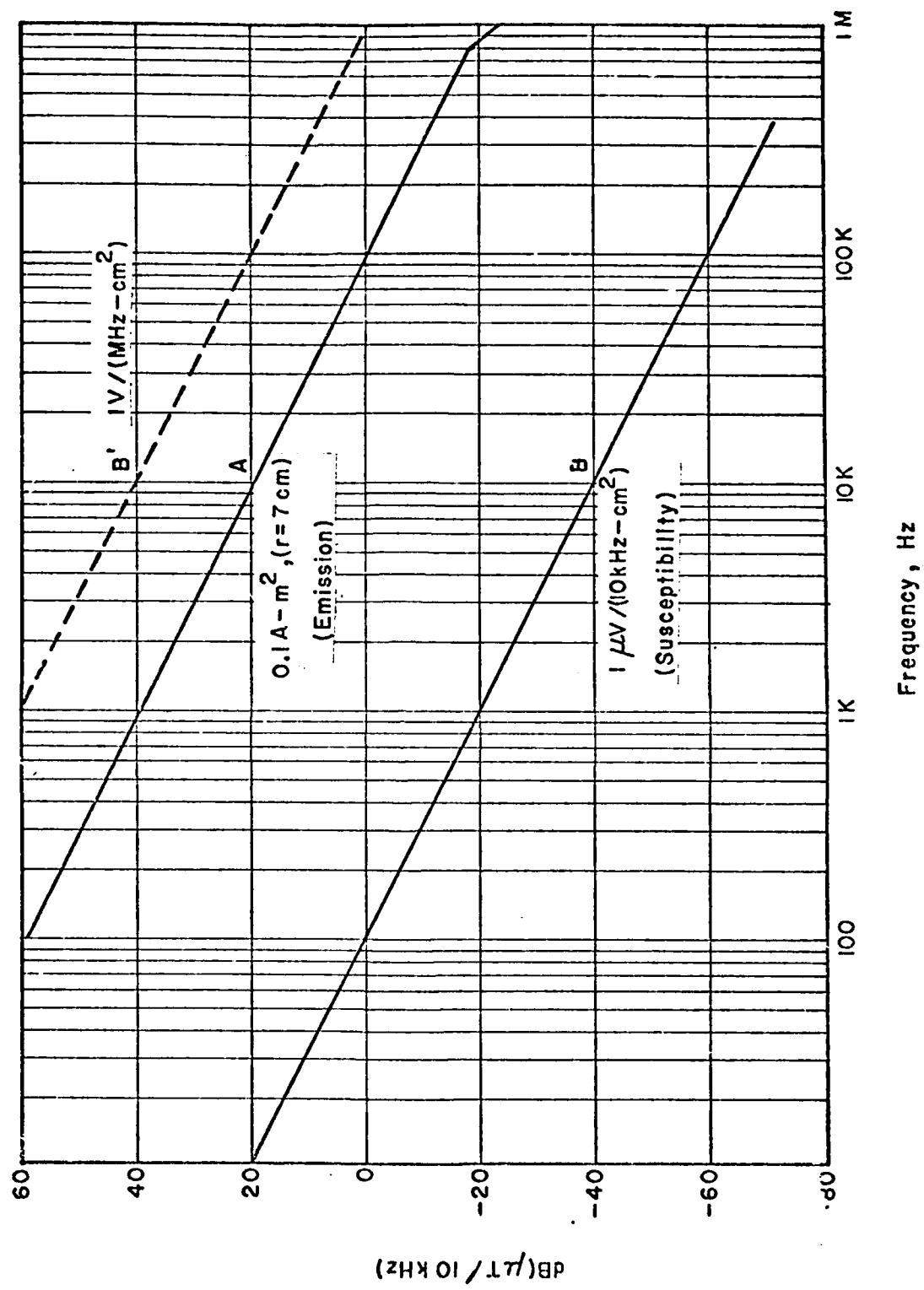


Figure 43 Broad-Band Magnetic Field Emission Spectrum

as follows. It shows the level of flux density spectrum amplitude which over any 10 kHz portion will generate 1  $\mu$ V in a 1  $\text{cm}^2$  loop. The portion may be that from 0 to 10 kHz, 10 kHz to 20 kHz, 25 kHz to 35 kHz, etc. If the susceptible device has a wider bandwidth or different voltage susceptibility level, the "B" curve must be adjusted accordingly. For example, for a 1 : susceptibility in a 1 MHz bandwidth the curve is drawn as at "B'" (120 dB - 40 dB = 80 dB correction).

In applying this technique in practice, one adjusts the level of the emitter for magnitude of current, area of current loop, bandwidth of the susceptor, shielding effectiveness and spacing, and the level of the susceptor for bandwidth, effective pickup area, and susceptibility voltage. Then, as a first estimate, the protection margin is given by the spacing between the susceptibility and emission curves in the frequency range corresponding to the receiver (susceptor) passband. If the apparent protection margin is poorer (lower) outside this frequency range, an estimate of the protection margin requires taking into consideration the receiver rejection of frequencies outside the passband. Also, if the emission and susceptibility curves are not parallel, a visual averaging technique must be used to get a reasonably accurate estimate.

#### 5.5.5 Application to Fields Produced by Power Supplies

For the purpose of making rough estimates, the magnetic field algorithm for power supplies indicates fields at 60 Hz ranging from 20 to 30 dB ( $\mu$ T) for volt-amperes ranging from  $10^3$  to  $10^5$  at a distance of 7 cms from the edge of the device.

Assume the field generating device can be represented as a dipole centered 5 cms from its edge making the distance 12 cms from the dipole to the point of measurement. By using Fig. III.1, p. 53 of Ref. 5, one obtains the relation

$$\frac{H}{M} = 30 \quad (62)$$

where

H is the magnetic field strength in amperes/meter

M is the dipole strength in amperes-meters<sup>2</sup>

To relate the magnetic flux density to the magnetic field strength, we use

$$B[\text{dB}(\mu\text{T})] = H[\text{dB}(A/\text{m})] + 2 \text{ dB} \quad (63)$$

Writing Eq. 62 in dB and using Eq. 63

$$M[\text{dB}(A\text{-m}^2)] = B[\text{dB}(\mu\text{T})] - 32 \text{ dB} \quad (64)$$

Hence, the dipole strengths range between -12 and -2 dB(A-m<sup>2</sup>) for typical sources (at 60 Hz). From Fig. 43 such sources will produce between -12 and -2 dB below 1 V/(MHz-cm<sup>2</sup>).

If for digital circuits it is assumed the susceptibility is 1 volt, and the bandwidth is 1 MHz, a circuit with an effective area of one square cm would be just below the susceptibility level (-12 to -2 dB depending on source strength).

For an analog circuit a more realistic bandwidth is 10 kHz. The induced voltage would be 40 dB less in this case. Whether such a circuit would be susceptible to the sharp impulse generated is uncertain.

It should be noted that as distance increases the induced voltage is correspondingly decreased (according to either a  $1/r^2$  or  $1/r^3$  law).

In addition to power supplies (containing magnetic windings such as with transformers) loops can produce magnetic fields. In the differential mode such loops are likely to be quite small, say 10 sq cms at the most. For a 100 ampere load, one would have a strength of  $100 \times 10^{-3} = 0.1$ (A-m<sup>2</sup>).

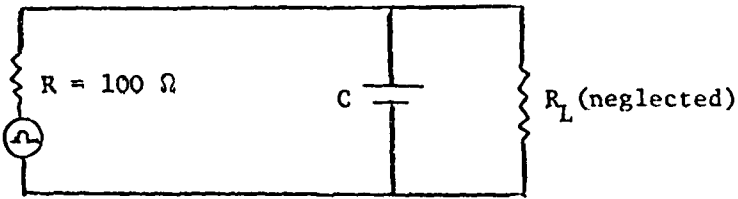
Twisted power cables are likely to be of the same or lower effectiveness as sources.

A more significant model for interference to digital systems is one in which the source arises from common-mode currents. Unbalanced switching transients might occur at the higher frequencies above, say, 50 kHz because of capacitances of as little as tenths of microfarads used from line to ground. The importance of this model has not yet been evaluated.

#### 5.5.6 Conducted Broadband Susceptibility

In the case of power line conduction, coupling can occur in both the differential and common modes. In both cases the length of the line between the source of the transient and the susceptible device may be of consequence in the effectiveness of the pulse. If the length is short (compared with the wavelength for the highest frequency of interest), an accurate calculation depends upon the effective impedance of the transient generator. At the present time, little is known about this. For this reason a long line assumption is made (although invalid) in order to get some sort of estimate.

We assume the transient is propagated on the line and that at the susceptible device it appears to have an internal impedance corresponding to the impedance of the line. In the differential mode this impedance is assumed to be 100 ohms. The susceptor equivalent circuit is assumed to be a capacitor which absorbs the transient and the equivalent circuit as shown below. For a 500 volt transient lasting 2.5  $\mu$ s



the charge  $Q$  flowing into the capacitor is

$$Q = \int i dt = \frac{500}{100} 12.5 \times 10^{-6} \text{ coulombs}$$

and the resulting voltage is  $V = \frac{Q}{C}$ .

For a 1  $\mu\text{F}$  capacitor

$$V = \frac{12.5 \times 10^{-6}}{10^{-6}} = 12.5 \text{ volts} \quad (65)$$

In a typical circuit the suscepter is a power supply with a transformer, rectifier and filter. It is not likely that the full transient will be transferred through the power transformer but even if it were, the filter would reduce the transient to a level which would not cause equipment degradation.

In the common mode the impedance of the power line is probably higher, say 200 ohms. This would result in one-half the voltage as given above, but the voltage would also be reduced somewhat because only the upper frequency components are likely to appear in the common mode. With a line-to-ground capacitance of 0.01  $\mu\text{F}$ , and only 10% of the charge effective in the common mode, the estimate is 12.5 volts line to ground. Since this is coupled to the secondary only through the interwinding capacitance which is quite small (less than 0.001  $\mu\text{F}$ ), it is unlikely to appear on the secondary side with any significant magnitude unless the secondary is not grounded. In that case, unless large line-to-ground filter capacitors are used, significant common-mode voltages could occur. This is possible but considered unlikely.

For signal lines coupling can occur magnetically and electrically. For magnetic coupling with a common-mode source conductor and an adjacent two-wire cable (spaced 2 mm from it), the estimated induced voltage in the differential mode is 0.18 volts. For the suscepter cable in the common mode, computation may be made using Eq. 60. For  $h_1 = h_2 = 2$  inches, spacing = 2 mm and  $p = 0.1$

$$V_{\max} = \frac{0.1 \times 2 \times 2}{\frac{2}{25.4} \left( \frac{2}{25.4} + 4 \right)} \approx 1.2 \text{ volts/meter} \quad (66)$$

An apparently significant means of coupling results from the common impedance of the ground plane. Paragraph 5.5.7 shows that ground plane potential differences of the order of volts can be expected in the vicinity of the point of grounding a pulse-carrying circuit. If a shield of a two-wire line is grounded in that vicinity, that voltage will appear at the input of a susceptible device in the common mode. With a balanced input a digital device should be unaffected by the transient. If the input is not balanced, then signal errors are quite possible.

#### 5.5.7 Experimental Tests

Majewski (Ref. 13) has examined the effect of power line transients in a single-wire conductor on a nearby shielded twisted pair and noted, in passing, that grounding the shield at the end of the cable furthest from the receiver had the same effect on the induced voltages as floating the shield, while grounding at the opposite end reduced the magnitude of the induced voltage. The work described below was performed in an effort to investigate that effect and to determine whether the voltage appearing on the twisted pair was due primarily to magnetic or capacitive induction.

##### 5.5.7.1 Equipment

The wires were supported parallel to each other about 2 inches above the ground plane and closely spaced (about 2 mm). The source wire was a single #12TW insulated copper wire grounded to the copper table top through a  $51 \Omega$  resistor at one end, and connected to the pulse generator with coaxial cable at the other. The susceptor wire was a length of insulated shielded twisted pair, and the  $100 \Omega$  resistor connecting the two wires of the twisted pair was enclosed in a metal box insulated from the cable shielding. Each lead of the other end of the twisted pair was connected to one channel of the oscilloscope, while the sheath was connected to the scope ground. The pulse generator produced  $5 \mu\text{s}$  50 V pulses with a rise time of about 20 ns at a rate of about 400 pps.

##### 5.5.7.2 Procedure and Results

It was initially assumed that the magnetic field generated by the pulse in the source cable could be described by the model proposed in section 5.5.1, and that somewhere along the parallel lengths of cable the magnetic field would pass through a loop the size of one twist of the twisted pair. Calculations indicated that the induced voltage would be of the order of 0.1 V. If such a magnetically induced voltage were a component of the voltage across the two leads of the twisted pair, it would be reasonable to expect the measured voltage to fluctuate as the twisted pair (and therefore any loop within the twisted pair) was rotated along its axis. But even when an unshielded twisted pair was supported close to the source wire and rotated, no fluctuation of the induced voltage was observed.

With the shielded twisted pair as close to the source wire as possible and with the shield ungrounded, common-mode induced voltages exceed 1.5 V. If the receiver is balanced, differential voltages are small (under 0.1 volt), but if one side of the twisted pair is grounded at the receiver the common-mode voltage appears as a differential voltage.

But the voltage induced in the susceptor is not entirely due to current flowing through the single wire. A common-mode voltage of over 0.05 V also appears when the susceptor cable is lying on the ground plane 20 or 30 cm from the emitter; a common-mode voltage will also appear if the pulse generator is completely disconnected from the single wire, the leads connected through a  $50 \Omega$  resistor and the ground lead side of the resistor touched to a remote corner of the copper ground plane. Thus, there are currents flowing through the ground plane, and potential differences along it.

This observation then can explain the results observed when the shield is grounded. Connecting the shield to a point of relatively high potential along the "ground" raises at least a portion of the shield to that potential as well. This, in effect, puts the high potential surface closer to the twisted pair and in some cases leads to an increase in the induced voltage.

This effect has been observed: with the twisted pair lying on the table top, "grounding" the shield at an injudiciously chosen spot can increase the common-mode voltage to almost 0.2 V. Thus, although Ref. 13 notes that grounding the shield at the point most remote from the receiver is equivalent to floating the ground, the important fact is not which end of the line is "grounded," but rather the potential of the surface to which it is grounded.

#### 5.5.8 Summary

A 50 V pulse in the source cable could produce well over 1 V in a shielded twisted susceptor if the ground is floating. Potential differences exist along the ground plane, and grounding the shielding at a point where the ground potential is high can sometimes increase the voltage induced into the susceptor cable. Grounding the shield at either end--the end closest to or farthest from the receiver--can cause such an increase. Moreover, the author of Ref. 13 is somewhat misleading when he claims that the "most likely" transient voltage is 400-600 V, since his source document (Ref. 14) shows nearly as many transients in the 800-1000 V range, and few as high as 1600 V.

## REFERENCES

1. Papoulis, THE FOURIER INTEGRAL AND ITS APPLICATIONS, N.Y., McGraw-Hill, 1962.
2. "Command and Control System Engineering and Integration (CCS E&I) TRIDENT Submarine," EMC Control Plan, Vol. II, 10 November 1972, IBM, Gaithersburg, Md. (C).
3. "Conducted Emissions from a 43 kW Motor Generator Set," USNUSC Tech. Memo., TM EA33-120-72, 22 June 1972.
4. R. M. Showers and C. P. Kocher, "Modeling of Harmonics on Power Systems," Report 77-3, May 1977, University of Pennsylvania, Moore School of Electrical Engineering, May 1977, Contract N00024-75-C-7130, AD B018735L.
5. R. M. Showers and S. Huling, "Systems Electromagnetic Compatibility Effectiveness Evaluation," Report 75-06, March 1975, University of Pennsylvania, Moore School of Electrical Engineering, Contract N00024-72-C-1413, AD B003 090L.
6. R. M. Showers, "Leakage and Coupling of Transmission Lines," Technical Report No. 29, Moore School Report No. 71-27, 15 June 1971, University of Pennsylvania, Contract N00039-71-C-0103.
7. S. C. Moorthy, "Coupling between Coaxial Cables at VLF," Technical Report #17, University of Pennsylvania, Moore School of Electrical Engineering, September 25, 1965, Contract NObsr 85170.
8. J. R. Moser and R. F. Spencer, "Predicting the Magnetic Fields from a Twisted-Pair Cable," IEEE Transactions on EMC, Vol. EMC-10, No. 3, Sept. 1968, p. 324.
9. F. Haber, "The Magnetic Field in the Vicinity of Parallel and Twisted Three-Wire Cable Carrying Balanced Three-Phase Current," IEEE Trans. on Electromagnetic Compatibility, Vol. EMC-16, May 1974, pp 76-82.
10. R. M. Showers, "Modeling of Fields Produced by Currents on Power Supply Wiring," IEEE Trans. on Electromagnetic Compatibility, Vol. EMC-13, No. 4, Nov. 1971, pp. 6-17.
11. R. M. Showers, K. H. Dolle and T. Conrad, "System Electromagnetic Compatibility Evaluation," Moore School Report 74-03, University of Pennsylvania, 31 August 1973, AD 913 996L.
12. R. M. Showers, "Improved Techniques for Electromagnetic Compatibility Evaluation," Moore School Report MS-EES-79-1, University of Pennsylvania, December 31, 1978, AD BO 34303L.
13. G.J. Majewski, "Power Line Transient Effects on Digital Lines," TM No. EA 33-139-75, Underwater Systems Center, New London, CT, 1975.
14. S. F. Cannova, "Short-Time Voltage Transients in Shipboard Electrical Systems," IEEE Transactions on Industry Applications, Vol. IA-9 #5, Sept-Oct 1973, p. 533-538.

## APPENDIX

### COMPARISON OF ERRORS INCURRED IN EXTRAPOLATING MAGNETIC FIELD STRENGTH AT VARIOUS DISTANCES

In the application of the prediction methodology, a method is necessary for extrapolating the value of the field measured at a given distance (from an equipment cabinet) to the field to be expected at a different distance. Experiments have shown that typical magnetic sources have fields varying inversely as the cube of the distance from the location of the effective center of the equivalent dipole generating the field. Since the equivalent dipole is usually located inside a cabinet, it is not always possible to know exactly where the dipole center is located. Furthermore, RE01 requires measurement of the magnetic field at a distance of 7 cms from the cabinet itself.

Two methods of extrapolation that have been proposed are: (1) use an inverse distance squared law where the distance is measured to the perimeter of the cabinet, or (2) use an inverse cube law but estimate the position of the dipole in the cabinet.

#### A.1 Mathematical Analysis

Figure A.1 shows the geometrical arrangement. The reference point is the location of the cabinet boundary.  $r_m$  is the distance from the point at which the measurement has been made to the reference point (7 cms for RE01).  $r$  is the distance from the point at which the field magnitude is desired to the reference point.  $r_t$  is the distance from the point at which the true equivalent dipole source is located within the cabinet from the cabinet boundary (reference point), and correspondingly  $r_a$  is the distance from an assumed location of the source to the reference point.

In terms of these distances, the true field at the location defined by  $r$  is given in terms of the equivalent dipole strength of the source  $M_n$  by

$$H_\theta(r) = \frac{M_n}{4\pi(r+r_t)^3} \quad (A-1)$$

and the true field, the point at which the measurement is made (defined by distance  $r_m$ ) is given by

$$H_\theta(r_m) = \frac{M_n}{4\pi(r_t + r_m)^3} \quad (A-2)$$

Now, if it is assumed that  $r_t$  is equal to zero and the field varies as  $1/r^2$  (case 1 above), the predicted field at  $r$  is given by

$$H_\theta(r)|_{p2} = \frac{M_n}{4\pi(r_t + r_m)^3} \frac{r_m^2}{r^2} \quad (A-3)$$

then the ratio of the predicted field to the true field is given by Eq. A-3 divided by Eq. A-1

$$\frac{H_\theta(r)|_{p2}}{H_\theta(r)} = \frac{(r + r_t)^3}{(r_t + r_m)^3} \frac{r_m^2}{r^2} \quad (A-4)$$

To deal with Eq. A-2 above, one must assume a value for  $r_t$ , namely  $r_a$  and use the  $1/r^3$  variation dependence. Then the predicted field at  $r$  is given by

$$H_\theta(r)|_{p3} = \frac{M_n}{4\pi(r_t + r_m)^3} \frac{(r_m + r_a)^3}{(r + r_a)^3} \quad (A-5)$$

utilizing Eq. A-2 and applying an inverse cubed correction. The ratio of the predicted field to the true field is given by the ratio of Eqs. A-5 and A-2, resulting in

$$\begin{aligned} \frac{H_\theta(r)|_{p3}}{H_\theta(r)} &= \frac{(r_m + r_a)^3}{(r + r_a)^3} \frac{(r + r_t)^3}{(r_t + r_m)^3} \\ &= \left( \frac{r_m + r_a}{r_m + r_t} \right)^3 \frac{(r + r_t)^3}{(r + r_a)^3} \\ &= \left( \frac{r_m + r_a}{r_m + r_t} \quad \frac{r + r_t}{r + r_a} \right) \end{aligned} \quad (A-6)$$

Figure A.2 is a plot of Eq. A-4 expressed in dB as a function of the extrapolated distance location. Note that it has been assumed that a true value has been measured at a distance of 7 cms. Of course, the ratio will depend on the true location of the dipole source and this is plotted as a parameter. Note that the maximum error for these parameters is approximately 14 dB with the predicted value being too small in most cases.

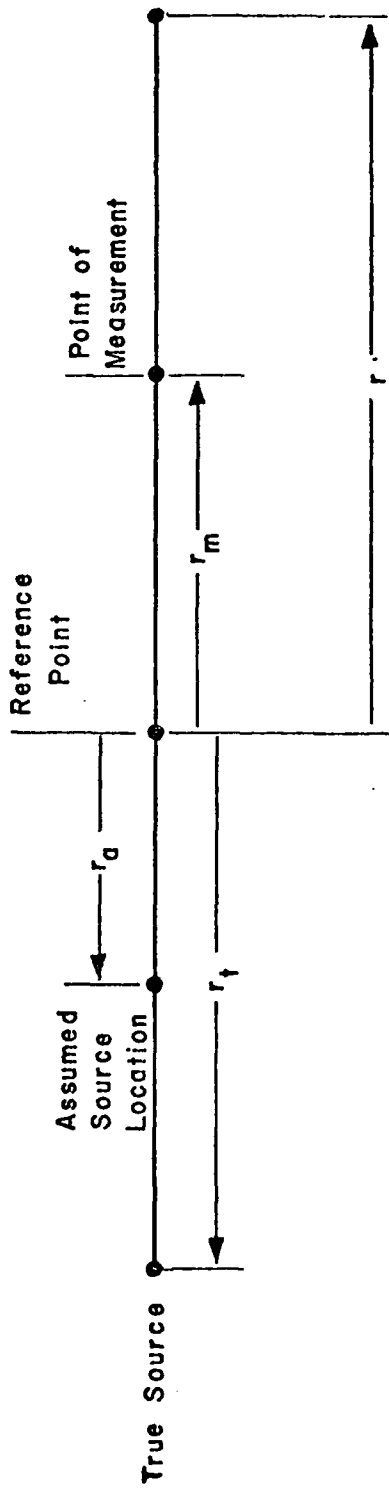


Figure A.1 Geometrical Arrangement

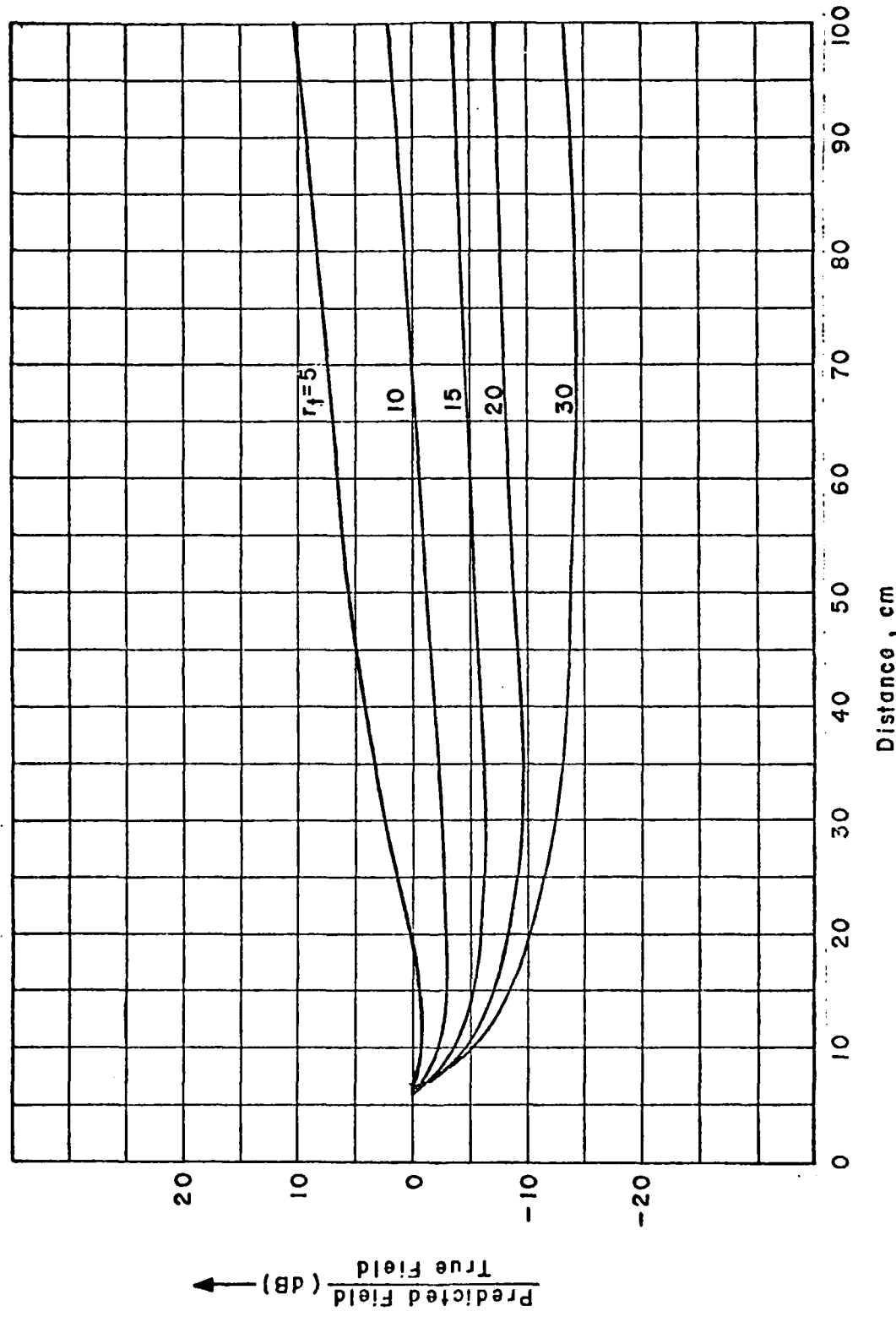


Figure A-2  $\frac{\text{Predicted Field}}{\text{True Field}}$  vs Distance ( $\frac{1}{r^2}$  Assumed,  $r_m = 7 \text{ cms}$ )

Equation A-6 is plotted on Fig. A.3 in terms of the ratio of the assumed distance to the true distance of the dipole source within the cabinet. If the assumed and true distances are the same, there is no error at any distance. If the assumed and true distances are off by a factor of 2 to 1 there is an error of about 6 or 7 dB out to a distance of 50 cms and 10 to 12 dB out to a distance of 100 cms. Within a distance of about 25 cms (10 inches) errors in the true and assumed distances up to 5 to 1 produce errors in estimated field strength up to approximately 10 dB.

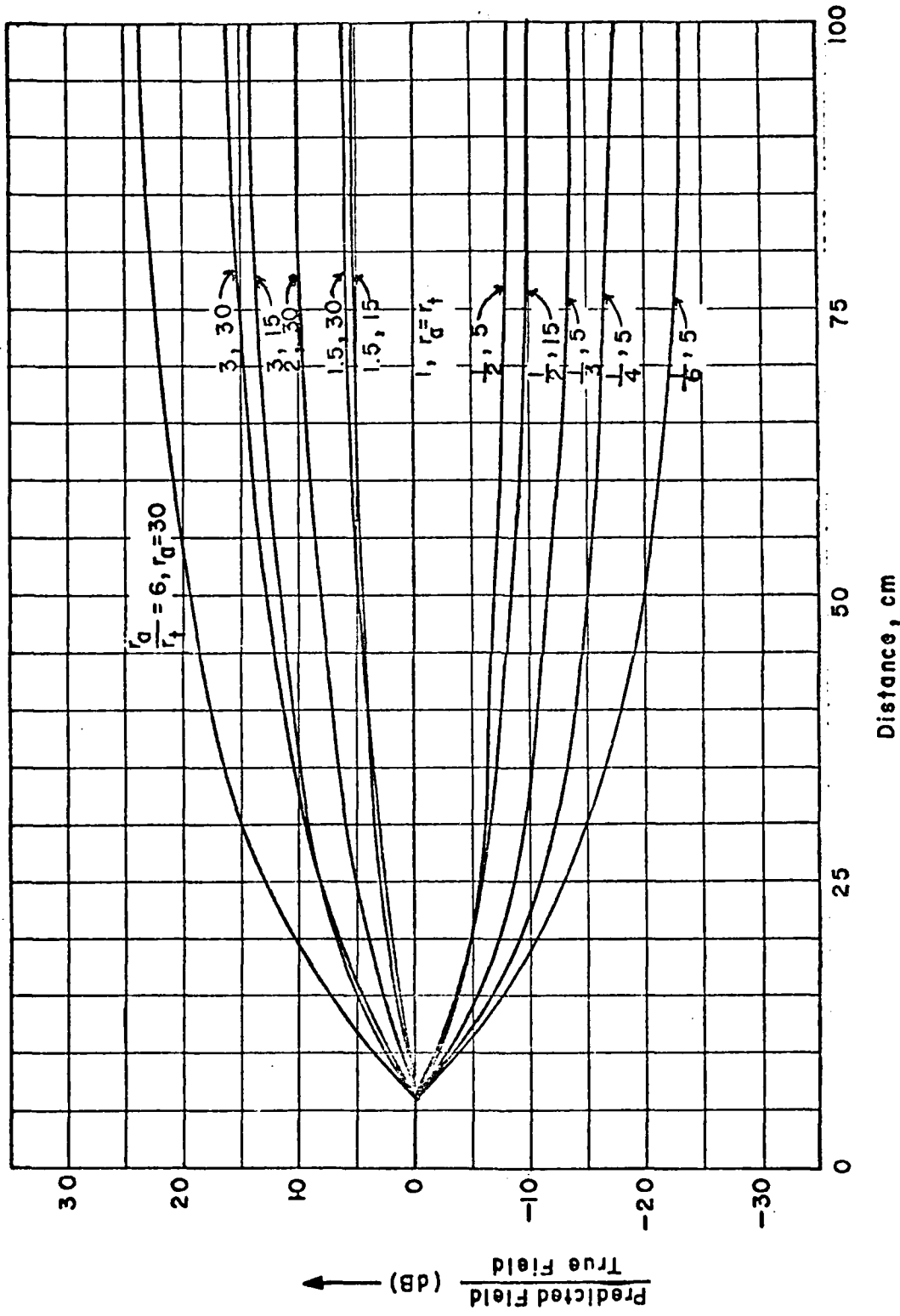
#### A.2 Discussion

If one uses the inverse square relationship, for an equivalent dipole source located in the center of a cabinet which is approximately one foot in dimension, a value of  $r_t = 15$  cms (6 inches) applies. In this case, errors of the order of 6 dB on the low side in the estimated field level are likely to be experienced. One can reduce the risk of underestimating the field by adding a factor of 6 dB to the field predicted on the basis of the inverse square law. For such a size cabinet the use of the inverse cube law with the assumption that the source lies at the center of the cabinet will probably produce more accuracy in the predicted field level than the inverse square law without the correction factor. However, with suitable care either technique can be used with the provision that in the case of marginally satisfactory results some investigation should be made of the true location of the dipole source.

#### A.3 Recommendation

In the absence of detailed information on source location, it is recommended that an inverse distance squared plus 6 dB law be used in estimating magnetic field levels from equipment cabinets. Where reasonably accurate location information is available, the inverse cube law should be used for greater accuracy.

Figure A.3  $\frac{\text{Predicted Field}}{\text{True Field}}$  vs Distance ( $\frac{1}{r^3}$  Assumed,  $r_m = 7 \text{ cms}$ )



DAT  
ILM